1st May 2020

Replies to the Interactive comment on "Ice injected into the tropopause by deep convection – Part 2: Over the Maritime Continent" by Iris-Amata Dion et al.

We would like to thanks Dr Michelle Santee and the Anonymous Referee #2 for their review on the revised manuscript. In the present document we answer Anonymous Referee #2 first and then Dr Michelle Santee. Comments from the reviewers are in blue, our replies are in black. Deleted sentences are crossed out and added words or sentences are in bold.

Replies to Anonymous Referee #2:

Dion and colleagues have substantially improved the manuscript by taking into account both referees' comments. Most of them have been carefully addressed and clarifications were brought whenever comments were not relevant. The overall text is clearer and straightforward. Thus, I recommend the paper to be accepted to ACP. However, I have few remarks/questions before the paper can be published.
Wu et al. (2008) is not in the corrected reference list.
We added Wu et al. (2008) in the corrected reference list.

(1) About the 100% MSL IWC accuracy cited from Wu et al. (2008): what such a large number means for the present analysis?
(1) The accuracy here means the uncertainty for values less than 10 mg m^{-3}. However, according to Wu et al., (2008) : «Most of the inhomogeneity-induced uncertainties can be reduced through averaging (e.g., in monthly maps) because of randomness of the inhomogeneity.". Thus, in our study, the accuracy in IWC is reduced considering the study zones and the long study period used.
We clarify into the manuscript L 101 as follow:
"The precision of the measurement is 0.10 mg m^{-3} at 146 hPa and 0.25 to 0.35 mg m^{-3} at 100 hPa. **While the accuracy is 100 % for values less than 10 mg m^{-3} at both levels, it is strongly reduce by averaging over the long study period and over the study zones.** The valid range is 0.1-50.0 mg m^{-3} at 146 hPa and 0.02-50.0 mg m^{-3} at 100 hPa (Wu et al., 2008)."

(2) How does the accuracy compared with other satellite-borne estimations?
(2) This accuracy is large compared with other satellite-borne. For instance:
- the SMILES instrument measuring IWC from October 2009 to April 2010 present Systematic Errors in the IWC measurement between 54 and 77 % (from 180 to 80 hPa) (source : https://mls.jpl.nasa.gov/data/smiles.php).
- WV from MLS have accuracy between 9 and 20 % between 146 and 80 hPa (source: https://mls.jpl.nasa.gov/data/v4-2_data_quality_document.pdf, page 75).
However, as specified in Wu et al., 2008 and in the previous answer, this accuracy is, in the present paper, largely reduced through the averaging over the study zone and the study period.

(3) Through the corrected version of the paper, there are a lot of references or figure numbers missing, flagged with a question mark. Please reedit carefully the LaTeX version. This has overcomplicated reading.
(3) Sorry for this mistake, we carefully reedited the re-revised LaTeX version.

Replies to Dr Michelle Santee:

Abstract :

(5) L17-18: Where do the values (4−29%, 55−78%) quoted in these lines come from? They appear nowhere else in the manuscript. In particular, they do not match any of the numbers given in the relevant discussion in Section 7.2 or 7.3.

(5) The values have been changed consistently with the values recalculated and given in section 7.2 as follow:

« The reanalysis ΔIWC range between ΔIWC^{ERA5} and $<\Delta IWC^{ERA5}>$ has been also found to be small in the UT **(9 to 33 %)** but large in the TL **(32 to 139 %)**, ... »

(6) L19-21: See point #7 in the comments on Section 7.2 about the phrase "xx% of variability per study zone", which is used four times in these lines.

(6) In the abstract we decided to not show the percentage that does not have strong importance in the results. (Furthermore, the abstract is long enough). We changed the sentence into:

"**Combining observational and reanalysis ΔIWC ranges, the total ΔIWC range is estimated, in the UT, between 4.2 and 10.0 mg m^{-3}, over land and between 0.3 and 4.4 mg m^{-3} over sea, and, in the TL, between 0.5 and 3.7 mg m^{-3} over land and between 0.1 and 0.7 mg m^{-3} over sea."**

(7) L21: See point #4 in the comments on Section 7.3 about these values (0.6 and 3.9 mg m^{-3}).

(7) We updated the values (see point #4 of Section 7.3).

(9) L22-25: It is stated that ΔIWC over land is larger than ΔIWC over sea "with a limit at 4.0 mg m^{-3} in the UT". What does "limit" mean in this context? Where does the value of 4.0 mg m^{-3} come from? In Section 7.1, the minimum ΔIWC over land is given as 4.9 mg m^{-3} and the maximum over sea as 4.4 mg m-3, leading to a maximum difference of only 0.5 mg m^{-3}.

(9) We changed (L23) the sentence by:

« 1) ΔIWC over land has been found to be larger than ΔIWC over sea with a limit around 4.4-4.9 mg m^{-3} in the UT (the limit being defined as the minimum of ΔIWC estimated over land and the maximum of ΔIWC estimated over sea), ... »

(11) L25: It is stated that Java sees the largest ΔIWC in the UT ("7.7 – 9.5 mg m-3 daily mean"). Again, these numbers are not drawn from the main text. Indeed, in Section 7.1, it is stated that "In the UT ... over Java, ΔIWC reaches 7.9–8.7 mg m^{-3}".

(11) In this sentence we are talking about the total ΔIWC range. However, we decided in the abstract to name it only "ΔIWC" instead of " total ΔIWC range" in order to make easier the understanding at this stage. The sentence in the abstract has been changed as follow:

« 2) small islands with high topography present the **largest ΔIWC such as the Java Island (with ΔIWC between 7.7 and 9.5 mg m^{-3} in the UT).** »

And a sentence in the Section 7.3 L472) has been added has follow (see the answer Section 7.1 (6) to understand the definition of $r^{Total)}$:

"Java island presents the highest observational and reanalysis ΔIWC range in the UT (between 7.7 and 9.5 mg m^{-3} daily mean, r^{Total} = 21%)."

(+) Note that to be clearer in the abstract we decided to change some sentences in the new manuscript version as follow (see Section 7.1 point (6) to understand why we change the percentage values):

"... Our study shows that, while the diurnal cycles of Prec and Flash are consistent to each other in timing and phase over land but different over offshore and coastal areas of the MariCont, the observational ΔIWC range between ΔIWC^{Prec} and ΔIWC^{Flash}**, interpreted as the uncertainty of our model to estimate the ice injected,** is small (they agree to within 6 to 22 % over land and to within 6 to 71 % over ocean) in the UT and TL. The reanalysis ΔIWC range between ΔIWC^{ERA5} and $<\Delta IWC^{ERA5}>$ has been also found to be small in the UT (9 to 33 %) but large in the TL (32 to 139 %), **highlighting the larger uncertainty in the TL than in the UT due to the vertical resolution of MLS observations.** Considering estimates **of ΔIWC from all methods**, ΔIWC is estimated in the UT between 4.2 and 10.0 mg $m^{-3,}$ over land, and between 0.3 and 4.4 mg m^{-3} over sea, and, in the TL, between 0.5 and 3.7 mg m^{-3} over land and between 0.1 and 0.7 mg m^{-3} over sea. Finally, from IWC^{ERA5}, Prec and Flash, this study highlights 1) ΔIWC over land has been found t**o be larger than ΔIWC over sea (ΔIWC over land and ocean regions being larger and smaller**

than 4 mg m^{-3}, respectively), and 2) small islands with high topography present the **largest ΔIWC such as the Java Island (with ΔIWC between 7.7 and 9.5 mg m^{-3} in the UT). ”**

Introduction :

(1) to (6) has been corrected.

2.1 MLS :

(8) The sentence in L95-96 (“The horizontal resolution of IWC$_{MLS}$ measurements is ~300 and 7 km along and across the track, respectively.”) is fully redundant with information given below and can be deleted.

(8) We deleted this sentence :

« ~~The horizontal resolution of IWC^{MLS} measurements is ~300 and 7 km along and across the track, respectively.~~ »

2.2 TRMM 3B42 :

(2) L111-112: First, “composing” is not the right word in L111. Second, these two sentences seem to be contradictory. The first states that TRMM-3B42 is “a multi-satellite precipitation analysis” but then mentions only GPM. The second states that it is “computed from the various precipitation-relevant satellite passive Microwave (PMW) sensors” and then lists several, not including GPM. These two sentences should be combined and clarified. Third, why is “Microwave” capitalized? It’s part of the acronym, but so is “passive”.

(2) We changed the previous sentence by the following one:

“ ~~TRMM-3B42 is a multi-satellite precipitation analysis composing a Global Precipitation Measurement (GPM) Mission. TRMM-3B42 is computed from the various precipitation-relevant satellite passive Microwave (PMW) sensors using GPROF2017 computed at the Precipitation Processing System (PPS) (e.g., GMI, DPR, Ku, Ka, Special Sensor Microwave Imager/Sounder [SSMIS], etc.) and including TRMM measurements from 1997 to 2015 (Huffman et al., 2007, 2010; and Huffman and Bolvin, 2018).~~ “

« TRMM-3B42 is a multi-satellite precipitation **analysis. The analysis merges microwave and infrared space borne observations and included TRMM measurements from 1997 to 2015 (Huffman et al., 2007, 2010; and Huffman and Bolvin, 2018).** »

(4) L121-122: I am still confused by the description of how 1-hour precipitation data are obtained. As I said in my previous review, I am under the impression (based on Huffman et al. (2007) and other sources) that the TRMM-3B42 product contains gridded merged precipitation estimates with a 3-hour temporal resolution. I had thought that only by taking advantage of the precessing orbit of TRMM and the long study period (13 years) are the authors able to bin the data in 1-hour bins. Perhaps that is what they are getting at with these two sentences, but it is not clear. “The granule temporal coverage of TRMM-3B42 data is 3 hours, but the temporal resolution of individual measurements is 1 minute. Thus, it is statistically possible to degrade the resolution to 1 hour.” seems to be saying that the 1-minute resolution of the individual measurements is somehow preserved in the 3-hourly averaged TRMM-3B42 data. In addition, since they are starting from data with a 3-hour granularity, it is confusing to talk about “degrading” the resolution to 1 hour.

(4) In order to be clearer and to delete all confusing sentences, we modified the sentence as follow:

« ~~The granule temporal coverage of TRMM-3B42 data is 3 hours, but the temporal resolution of individual measurements is 1 minute. Thus, it is statistically possible to degrade the resolution to 1 hour.~~»

« The TRMM-3B42 data has been averaged over a 1-hour interval from 0 to 24 hours. »

Section 2.3 :

(5) First it is stated (L130-131) that the “instrument detects lightning with storm-scale resolution of 3−6 km (3 km at nadir, 6 km at limb) over a large region (550−550 km) of the Earth’s surface”. I have no idea what “over a large region (550−550 km) of the Earth’s surface” means. Then in the next sentence (L131) it is stated that “LIS horizontal resolution is provided at 0.25°×0.25°.” Are these two sentences consistent? Finally, it is stated several lines below (L138-139) that “The observation range of the sensor is between 38N and 38S.” The latitudinal coverage and spatial resolution of the LIS data should be described together in sentences that logically flow from one to the next.

(5) : We changed L126:

« ~~over a large region (550−550 km) of the Earth's surface »~~
by
« over a large region (550x550 km) of the Earth's surface »

And we moved sentences in the text as follow:
« The observation range of the sensor is between 38ºN and 38ºS.The instrument detects lightning with storm-scale resolution of 3-6 km (3 km at nadir, 6 km at limb) over a large region (550x550 km) of the Earth's surface. **The LIS horizontal resolution is provided** at 0.25º x0.25º. »

(8) First it is stated (L133-134) that "the weak lightning signals that occur during the day are hard to detect because of background illumination". Then it is stated (L134-135) that processing to remove the background signal allows the instrument to "detect weak lightning and achieve a 90% detection efficiency during the day". The next line (L136) states that the "TRMM LIS detection efficiency ranges from 69% near noon to 88% at night", appearing to contradict the previous sentence. Does the detection efficiency during the day really reach as high as 90%, higher than at night?
(8) : The previous sentences were confusing. To be clearer, we changed the paragraph as follow:
"~~A RTEP removes the background signal to enable the system to detect weak lightning and **achieve a 90\%** detection efficiency during the day. LIS is thus able to provide the number of flashes (Flash) measured. The TRMM LIS detection efficiency ranges from 69\% near noon to 88\% at night.~~"

« A RTEP removes the background signal to enable the system to detect weak lightning and **improves the** detection efficiency during the day. LIS is thus able to provide the number of flashes (Flash) measured. The TRMM LIS detection efficiency ranges from 69% near noon to 88% at night. »

Section 2.4
(6) 169: I'm not sure what information "unitary" is meant to convey here, or why this word is needed. In any case, "an unitary" should be "a unitary".
(6) : The term « unitary » has been deleted in the sentence L165:
« a ~~**unitary**~~ box function »

Section 4.3 :
(2) In L242, the amount of IWC injected over seas is stated to be < 10 mg m-3. In L244, the largest amount of IWC injected over seas is stated to be 7−15 mg m^{-3}, contradicting the first statement.
(2) : We changed in the sentence L242, as follow:
« ~~than over seas (< 10 mg m^{-3}). »~~
« than over seas (< **15** mg m^{-3}). »

(10) L267: It is stated that "For pixels with large values of ΔIWC, IWC observed by MLS is between 4.5 and 5.7 mg m-3 over North Australia Sea, South Sumatra and New Guinea". Fig. 5b shows North Australia, not the North Australia Sea. (11) As I pointed out in the original review, the above statement applies only to New Guinea point #1. It is not true for New Guinea point #2, for which the IWC value is much lower.
(10) and (11) : We changed the sentence as follow:
« For pixels with large values of ΔIWC, IWC observed by MLS is between 4.5 and 5.7 mg m^{3} over North Australia, South Sumatra and New Guinea 1. »

(12) For the pixels with low ΔIWC, the IWCMLS ranges from 1.9 to 4.7 mg m-3. Thus the highest IWC for these points is larger than the bottom of the range of the high-ΔIWC points. I note that the revised summary in this section (L269-270) mentions the length of the growing phase of deep convection and the amplitude of the diurnal cycle in Prec as factors associated with large ΔIWC values, but not the magnitude of the IWC values themselves, even though the summary immediately follows discussion of the MLS IWC values. I appreciate that such a statement has been removed in revision. I agree with that deletion and I am NOT suggesting that it be put back in. However, it might strike readers as odd to spend several sentences (L266-269) talking about the MLS IWC values and then end that paragraph with a summary that completely ignores them. The authors should consider adding a sentence or two noting that the IWCMLS ranges overlap for the high and low ΔIWC pixels, and thus no definitive conclusion about the relationship between IWC and

ΔIWC can be drawn.
(12) The sentences of synthesis have been changed as follow :
« To summarize, large values of ΔIWC are observed over land in combination to i) longer growing phase of deep convection (> 9 hours) and/or ii) large diurnal amplitude of Prec (> 0.5 mm h^{-1}). **However, as IWC^{MLS} ranges overlap for the high and low ΔIWC, no definitive conclusion about the relationship between IWC and ΔIWC can be drawn.** »

(13) Furthermore, language linking high-ΔIWC points to high (> 4.5 mg m^{-3}) IWC values has not been removed from the Conclusions section (L539-540).
(13) The sentence has been removed.

(14) In my original review, I suggested that it would be easier to read values off of Fig. 5 if the y-axis for Prec had 4 (not 3) minor tickmarks, as the IWC axis does. I still feel that way.
(14) The number of tickmarks have been changed.

Section 5.1
(4) L285: It is stated that "over NewGuinea where the number of Flash is relatively low (~10-2 – 10-3 flashes day-1)", but I think there are several inland areas of New Guinea where Flash exceeds 10-2 flashes day-1.
(4) We changed the sentence as follow :
« Differences between Flash and Prec distributions are found over North Australia Sea, with relatively large number of Flash (>10^{-2} flashes day^{-1}) compared to low Prec (4 – 10 mm day^{-1}) (Fig. 2c), and over **several inland areas of New Guinea** where the number of Flash is relatively low (~10^{-2}- 10^{-3} flashes day^{-1}) ... »

Section 5.2
(3) L300-302: These sentences ("In that case, we can easily discriminate between land and coastlines or sea and coastlines by applying the land/ocean/coastlines filters. Consequently, this particular pixel will be flagged both as land and coastlines or sea and coastlines") are awkwardly worded, hard to follow, and appear to contradict previous statements. I understand that pixels can straddle land/coastline and sea/coastline boundaries. I believe that this description is saying that a pixel containing both land and coastline information will be "bookkept" in both the MariCont_L and MariCont_C categories. However, as noted above, in L298 offshore pixels are defined in such a manner as to exclude the 10 pixels nearest land, so I do not see how in this context there could be any sea/coastline confusion. The areas within 5 pixels from land are put in the MariCont_C category, and those more than 10 pixels away are put in the MariCont_O category; presumably the areas stretching between 5 and 10 pixels from land are omitted from this part of the analysis.
(3) You are right, it is a mistake to say that pixel in the coastline and in the sea can be mixed. We changed the sentence as follow:
« ~~A given 0.25◦×0.25◦pixel can contain information from different origins : land/coastlines or sea/coastlines. In that case, we can easily discriminate between land and coastlines or sea and coastlines by applying the land/ocean/coastlines filters. Consequently, this particular pixel will be flagged both as land and coastlines or sea and coastlines »~~

« At the border between the land and the coast areas, a given 0.25◦×0.25◦ pixel can contain information from both land and coastlines. In that case, we can easily discriminate between land and coastlines by applying the land/coastlines filters. Consequently, this particular pixel will be flagged both as land and coastlines. »

(4) The Flash lines in Fig. 7 are described in the caption as being "dashed", but in actuality they are dotted. This causes confusion when the reader gets to Figs. 8 and 9 and expects the similar Flash curves to also be dotted. However, in those plots Flash lines are dashed and IWCERA5 lines are dotted. For consistency, it would be better to depict Flash data in Fig. 7 with dashed lines.
(5) As I mentioned in my previous review, it would be very helpful to have more minor tickmarks on both the x- and y-axes in Fig. 7 (as well as Figs. 8 and 9).
(4) and (5) Figures have been improved: dashed lines have been added into Fig. 7 and minor tickmarks have been added in Figs. 7, 8 and 9.

(8) It is stated (L310-311) that "Prec minimum is around 18:00 LT". It is then asserted (L312- 314) that "These results are consistent with Mori et al. (2004) showing ... a diurnal minimum of precipitation around 11:00 LT". To me, 18:00 LT is not consistent with 11:00 LT.
(8) Indeed, we corrected the description of the Figure 2 in Mori et al. (2004). We changed the sentence as follow L311:
"These results are consistent **with the work of** Mori et al. (2004) showing a diurnal maximum of precipitation in the early morning between 02:00 **and** 03:00 LT and a diurnal minimum of precipitation **between** 11:00 **and 21:00 LT**, over coastal zones of Sumatra."

Section 6 :
(1) Both referees questioned whether, given that $IWC^{ERA}5$ is itself unvalidated at this point, ΔIWC^{ERA5} can really be used to validate the observationally derived values, or might this study rather in some sense serve to use the ΔIWC^{Prec} and ΔIWC^{Flas}h to validate the new ERA5 values. The authors responded in their reply letter that they are not using $\Delta IWC^{ERA}5$ to validate ΔIWC^{Prec} and ΔIWC^{Flash} but to "assess the amounts estimated by our model", and they have added to the manuscript (L384-386) the sentence "The diurnal cycle of IWC over the MariCont from ERA5 will be used to calculate ΔIWC from ERA5 in order to assess the horizontal distribution and the amount of ice injected in the UT and the TL deduced from our model combining MLS ice and TRMM Prec or MLS ice and LIS flash." To me, there is no difference between "assessing the distribution and amount of" the ΔIWC deduced from their model and "validating" it. I still feel that it would be appropriate to acknowledge that ERA5 IWC data cannot be considered "truth", their quality has not yet been fully evaluated, and the consistency or lack thereof found in the comparisons between ΔIWC^{ERA5} and both ΔIWC^{Prec} and ΔIWC^{Flash} may have implications for both their methodology and ERA5.
(1) : As you were suggesting, we decided to add the following sentence L386 :
« The ERA5 reanalyses provide hourly IWC at 150 and 100 hPa (IWC^{ERA5}). The diurnal cycle of IWC over the MariCont from ERA5 will be used to calculate ΔIWC from ERA5 in order to **support** the horizontal distribution and the amount of ice injected in the UT and the TL deduced from our model combining MLS ice and TRMM Prec or MLS ice and LIS flash. **Since IWC^{ERA5} data quality has not yet been fully evaluated, this may impact on the consistency or lack thereof found in the comparisons between ΔIWC^{ERA5} and both ΔIWC^{Prec} and ΔIWC^{Flash} may have implications for both our methodology and ERA5.** »

(3) In both L389 and L390, the maximum value reached by IWC^{ERA5} in the UT is stated to be 6.4 mg m-3. But I wonder where the authors are getting that number from. Clearly there are values larger than 6.4 mg m-3 in Fig. 10a (as evidenced by the white patches in the middle of the reddish colors).
(3) We changed « reaching » by « exceeding ».

(7) L408: it is stated that the differences in the timing of the maximum of the diurnal cycle of Prec, Flash and IWC^{ERA5} "do not impact on the calculation of the ΔIWC^{Prec}, ΔIWC^{Flash} or ΔIWC^{ERA5}." Is the timing unimportant because only the magnitude of the diurnal cycle (max- min) matters for the ΔIWC calculation? There is also a pervasive lack of superscripting in this sentence.
(7) We changed the sentence as follow exactly as you were suggesting:
"However, these differences do not impact on the calculation of the ΔIWC^{Prec}, ΔIWC^{Flash} or ΔIWC^{ERA5}, **because only the magnitude of the diurnal cycle (max-min) matters for the ΔIWC calculation."**

Section 7.1
(1) It is stated (L418) that over Java, ΔIWC "reaches 7.9−8.7 mg m^{-3}". This sentence pertains to only two values; thus, I presume that ΔIWC^{Prec}=8.7 and ΔIWC^{Flash}=7.9 mg m^{-3}. In that case, $\Delta IWC^{Flash}-\Delta IWC^{Prec}$=0.8 mg m^{-3}.
(1) We corrected the sentence as follow:
« ~~ΔIWC^{Flash} is generally greater than ΔIWC^{Prec} by less than 1.0 mg m^{-3}~~ »
« ΔIWC^{Flash} is generally greater than ΔIWC^{Prec} by less than **0.8** mg m^{-3} »

(2) The sentence in L419-420 is not complete: "except for Java where is larger than ΔIWC^{Flash} by 0.7 mg m^{-3} (−8%)".

(2) We completed the sentence as follow:
« ... except for Java where **ΔIWC^{Prec}** is larger than ΔIWC^{Flash} by 0.7 mg m^{-3}. »

(3) Assuming that the above sentence should read "except for Java where ΔIWC^{Prec} is larger than ΔIWC^{Flash}", then the difference is 0.8 mg m^{-3}, not 0.7 as stated.
(3) It has been changed to 0.8 mg m^{-3}

(4) Since no sign is attached to the raw difference in L420, why is the percent difference negative? It doesn't make sense to say that "ΔIWC^{Prec} is larger than ΔIWCFlash by −8%".
(4) The sign has been deleted L425.

(5) Furthermore, the percent difference as defined here should be 0.8/7.9=10%, not 8% as stated (L420).
(5) It has been corrected to 10%.

(6) More fundamentally, why did the authors choose to use ΔIWC^{Flash} in the denominator for the percent differences? ΔIWC^{Flash} is no more "correct" than ΔIWC^{Prec}. Thus, a perhaps less arbitrary approach would have been to use the average of the two ΔIWC estimates in the denominator rather than picking one of them.
(6) As you were suggesting we recalculate all the percentage values, and renamed its as follow:

→ Equation has been added L421 in the new manuscript version :
$r^{Prec\text{-}Flash} = ((\Delta IWC^{Prec} - \Delta IWC^{Flash})/((\Delta IWC^{Prec} + \Delta IWC^{Flash})/2)\times 100$

→ L449:
$r^{ERA5-\langle \Delta IWCERA5 \rangle} = ((\Delta IWC^{ERA5} - \langle \Delta IWC^{ERA5} \rangle/((\Delta IWC^{ERA5} + \langle \Delta IWC^{ERA5} \rangle)/2)\times 100,$

→ L466: " The consistency between observational and reanalysis ΔIWC range is calculated as the difference between the minimal value of the largest range minus the maximum value of the lowest range divided by the mean of these two values. In the UT, over land, observational and reanalysis ΔIWC are found consistent to within 0 to 25% while over sea they are inconsistent (to within 62 to 96%) in the UT."

" In the following we will consider rTotal as the relative differences between the minimal value of the lower range minus the maximum value of the largest range divided by the mean of these two values. The range between observational and reanalysis ranges is named the total IWC range, and is estimated in the UT between 4.2 and 10.0 mg m^{-3} (r^{Total} from 8 to 59%) over land ..."

(7) L422: "ΔIWC^{Flash} is almost twice as large as than ΔIWC^{Prec} (53%)" – to me it looks like ΔIWC^{Flash} is ~4.3 mg m^{-3}, whereas ΔIWCPrec is ~2 mg m^{-3} (which does work out to ~53% by the percent difference definition used here), so that ΔIWC^{Flash} is more than twice as large as ΔIWC^{Prec}, not almost twice as large. Also note: large as than --> large as.
(7) It was a mistake in the sentence. The sentence has been changed as suggested and the percentage value has been recalculated as a function of the comments Section 7.2 point #(7). We changed the sentence as follow (L518 of the new manuscript):
"Additionally, Fig. 11 shows that the strongest differences between ΔIWC^{Prec} and ΔIWC^{Flash} are found over the North Australia Sea, with ΔIWC^{Flash} **greater than ΔIWC^{Prec} by 2.3 mg m^{-3} in the UT ($r^{Prec-Flash}$ = ~71%) and by 0.4 mg m^{-3} in the TL ($r^{Prec-Flash}$ = - 75%)."**

(8) The lack of any tickmarks whatsoever on the right-hand y-axes of Fig. 11 makes it quite difficult for readers to judge any of the values quoted in the text for themselves.
(8) The figure has been completed as suggested.

Section 7.2
(5) L439: The first sentence on this line ("Consistently ... respectively.") is redundant and unnecessary. It should be deleted.
(5) We deleted the sentence.

(7) L444: The phrase “xx% of variability per study zone”, used here and in eight other places in Sections 7.2 and 7.3 as well as four times in the Abstract, makes no sense to me. I believe that the authors wish to quantify the range of the relative differences between ΔIWC^{ERA5} and $\langle \Delta IWC^{ERA5} \rangle$ in the various study zones (that is, the smallest and the largest difference between the convolved and unconvolved ΔIWC estimates from the 5 islands for the island zone and similarly from the 5 seas for the sea zone), but “xx% of variability” means something else and is not the way to convey that information. If my understanding of what the authors are intending is correct, then perhaps something like this would work: “with relative differences between ΔIWC^{ERA5} and $\langle \Delta IWC^{ERA5} \rangle$ of ~19-22% over the island study zone”.
(7) We changed the phrase “xx% of variability per study zone” in the section 7.2, 7.3 and 9 in order to be clearer on what has been considered in the percentages. Our answer here, details also the answer to the question Section 7.1 point #(6). (Differences between the previous manuscript version and the new version are also clearly highlighted in the Supplement document provided.)

- In the Section 7.1, from L417:
  « Thus, the observational ΔIWC range calculated between ΔIWC^{Prec} and ΔIWC^{Flash} provides an upper and lower bound of ΔIWC calculated from observational datasets. In the following, we will consider the relative difference between ΔIWC^{Prec} and ΔIWC^{Flash} as:
  $r^{Prec-Flash}\ \Delta IWC^{Prec} - \Delta IWC^{Flash} = 100 \times (\Delta IWC^{Prec} + \Delta IWC^{Flash}) \times 0.5$ (4)
  In the UT (Fig. 11a), over islands, ΔIWC calculated over Sumatra, Borneo, Sulawesi and New Guinea varies from 4.9 to 6.9 mg m^{-3} whereas, over Java, ΔIWC reaches 7.9–8.7 mg $m^{-}3$. ΔIWC^{Flash} is generally greater than ΔIWC^{Prec} by 0.8 mg m^{-3} (with $r^{Prec-Flash}$ ranges from - 6 to - 22% over the study zone) for all the islands, except for Java where ΔIWC^{Prec} is larger than ΔIWC^{Flash} by 0.8 mg m^{-3} ($r^{Prec-Flash}$ = 7.1%). Over sea, ΔIWC varies from 1.2 to 4.4 mg m^{-3}. ΔIWC^{Flash} is greater than ΔIWC^{Prec} by 0.6 to 2.1 mg m−3 ($r^{Prec-Flash}$ = - 35 to - 71%), except for Java Sea, where ΔIWC^{Prec} is … »

- In the Section 7.2 , from L. 444 :
  « The ice injected from ERA5 at z = 146 and 100 hPa with degraded vertical resolution ($\langle \Delta IWC^{ERA5}_{z0} \rangle$) is thus calculated from $\langle IWC^{ERA5}_{z0} \rangle$. In the following we can consider the difference $r^{ERA5-\langle ERA5 \rangle}$ between ΔIWC^{ERA5} and $\langle \Delta IWC^{ERA5} \rangle$ as:

  $r^{ERA5-\langle ERA5 \rangle}\ \Delta IWC^{ERA5} - \langle \Delta IWC^{ERA5} \rangle = 100 \times (\Delta IWC^{ERA5} + \langle \Delta IWC^{ERA5} \rangle) \times 0.5$ (5)

  Figure 11 shows ΔIWC^{ERA5} and $\langle \Delta IWC^{ERA5} \rangle$ at z = 150 and 100 hPa, over the island and the sea study zones. In the UT (Fig. 11a), over islands, ΔIWC^{ERA5} and $\langle \Delta IWC^{ERA5} \rangle$ calculated over Sumatra and Borneo vary from 4.9 to 7.0 mg 150 150 m^{-3} ($r^{ERA5-\langle ERA5 \rangle}$ ranges from 20 to 22 %) whilst ΔIWC^{ERA5} and $\langle \Delta IWC^{ERA5} \rangle$ over Java, Sulawesi and New Guinea reach 7.5–10.0 mg m^{-3} ($r^{ERA5-\langle ERA5 \rangle}$ = 21 to 24 %). Over sea, ΔIWC^{ERA5} and $\langle \Delta IWC^{ERA5} \rangle$ vary from 0.35 to 1.1 mg 150 150 m^{-3} ($r^{ERA5-\langle ERA5 \rangle}$ = 9 to 33 %). ... »

- In the Section 7.3 – Synthesis :
  The comparison between the observational ΔIWC range and the reanalysis ΔIWC range is presented in Fig. 11. In the UT, over land, observation and reanalysis ΔIWC ranges agree to within 0.1 to 1.0 mg m^{-3}, which highlights the robustness of our model over land, except over Sulawesi and New Guinea, where the observational and the reanalysis ΔIWC range differ by at least 1.7 and 0.7 mg m^{-3}, respectively. Over sea, the observational ΔIWC range is systematically greater than the reanalysis by ~ 1.0 – 2.2 mg m^{-3}, showing a systematic larger estimate derived from observation than derived from reanalysis. The consistency between observational and reanalysis ΔIWC range is calculated as the difference between the minimal value of the largest range minus the maximum value of the lowest range divided by the mean of these two values. In the UT, over land, observational and reanalysis ΔIWC are found consistent to within 0 to 25% while over sea they are inconsistent (to within 62 to 96%) in the UT. In the TL, observational and reanalysis ΔIWC ranges are consistent to within 0 to 49% over land and to within 0 to 28% over sea. In the following we will consider r^{Total} as the relative differences between the minimal value of the lower range minus the maximum value of the largest range divided by the mean of these two values. The range between observational and reanalysis ranges is named the total IWC range, and is estimated in the UT between 4.2 and 10.0 mg m−3 (r^{Total} from 8 to 59%) over land and between 0.3 and 4.4 mg m^{-3} (r^{Total} from 104 to 149%) over sea and, in the TL, between 0.5 and 3.7 mg m^{-3} (r^{Total} = 85 to 127%) over land, and between 0.1 and 0.7 mg m^{-3} (r^{Total} = 142 to 160%) over sea. Amounts of ice injected deduced from observations and reanalysis are consistent to each other over land in the UT and over land and sea in the TL (to within 0 to 49%) but inconsistent over sea in the UT (up to 96%).

However, the impact of the vertical resolution on the estimation of ΔIWC is much larger in the UT than in the TL (r^{Total} is larger in the TL than in the UT). At both levels, observational and reanalyses ΔIWC estimated over land is more than twice as large as ΔIWC estimated over sea. Java island presents the highest observational and reanalysis ΔIWC range in the UT (between 7.7 and 9.5 mg m^{-3} daily mean, r^{Total} = 21%). However, whatever the level considered, although Java has shown particularly high values in the observational ΔIWC range compared to other study zones, the reanalysis ΔIWC range shows that Sulawesi and New Guinea would also be able to reach similar high values of ΔIWC as Java (assuming that ERA5 IWC data have not yet been evaluated).

- In Section 8.3 L508: See Section 7.1 point #(7).

- In the Section 9 – Conclusion :
  « ...The largest ΔIWC^{Prec} has been found over areas where the convective activity is the deepest. ΔIWC^{Prec} and ΔIWC^{Flash} depart from -6 to -22 % over land and to -6 to -71 % over sea. The largest differences between ΔIWC^{Prec} and ΔIWC^{Flash} over sea might be due to the combination of the presence of stratiform precipitation included in Prec and the very low values of Flash over seas ($<10^{-2}$ flashes day^{-1}). The diurnal cycle of IWC^{ERA5} at 150 hPa is more consistent with that of Prec and Flash over land than over ocean. Finally, ΔIWC estimated from observations has been shown to be consistent with ΔIWC estimated from reanalysis to within 25% over land in the UT, to within 48 % over land in the TL and to within 28 % over sea in the TL, but inconsistent to within 96 % over sea in the UT. Thus, thanks to the combination of the observational and reanalysis ΔIWC ranges, the total ΔIWC range has been found in the UT to be between 4.2 and 10.0 mg m^{-3} over land and between 0.3 and 4.4 mg m^{-3} over sea and, in the TL, between 0.5 and 3.7 mg m^{-3} over land and between 0.1 and 0.7 mg m^{-3} over sea. The impact of the vertical resolution on the estimation of ΔIWC has been found higher in the TL than in the UT. ... »

(9) L449: Again, without tickmarks on the right-hand axis it is hard to tell, but the value for New Guinea looks higher than 3.7 mg m^{-3} to me, more like 3.9. (10) L449: same comment as above for "xx% of variability per study zone".
(9) It was a mistake. The percentage does not change. We corrected the sentence as follow:
"In the TL, over land, ΔIWC^{ERA5}_{100} and $<\Delta IWC^{ERA5}_{100}>$ vary from 0.5 to **3.9** mg m^{-3} …"

(11) L450: It is stated that $\langle \Delta IWC^{ERA5} \rangle$ is larger than ΔIWC^{ERA5} "by less than 2.1 mg m^{-3}". To me the difference between the two estimates looks more like 2.4 mg m^{-3} for Sulawesi and 2.5 mg m^{-3} for Java. Thus the statement "by as much as 2.5 mg m^{-3}" would be more accurate. (12) L451: same comment as above for "xx% of variability per study zone".
(11) We changed the value by 2.11 in the sentence as follow:
« ...being larger than ΔIWC^{ERA5} by less than **2.5** mg m^{-3}. »

(13) L451-452: Again, the value of 0.2 mg m^{-3} should be checked here, as it looks as though it might be larger than that for the Java and North Australia seas, and "by as much as" would be better than "by less than".
(13) We have changed as suggested:
« Over sea, ΔIWC^{ERA5} and $<\Delta IWC^{ERA5}>$ vary from 0.05 to 0.4 mg m^{-3} (r^{ERA5} = ~71 %) with ΔIWC^{ERA5} lower than $<\Delta IWC^{ERA5}>$ by **as much as** 0.2 mg m^{-3}. »

Section 7.3
(4) L462: I note that the authors' response letter indicates that the values 0.6 and 3.9 mg m^{-3} in this line have been changed to 0.5 and 3.7 mg m^{-3}. However, such changes have not actually been made in the revised text.
(4) It was a mistake. We corrected by the true values of 0.5 and 3.7 mg m^{-3}

(9) L466: It is stated that significant differences are found over all individual offshore study zones "within 0.7 to 2.1 mg m^{-3}". But differences for the sea zone were given as "1.0 – 2.2 mg m^{-3}" on L459. (And again "as much as" would be better than "within".)
(9) All the sentence has been deleted. See answer Section 7.3 #(10).

(10) The previous couple of points lead me to wonder why the information in the sentence in L464-466 is repeated, as these values were already given in the previous paragraph. I think that these two paragraphs could be combined and written more efficiently.
(10) We deleted the sentence L464:
"~~The amounts of ice injected in the UT deduced from observations and reanalysis are consistent to each other over MariCont_L, Sumatra, Borneo and Java, with significant differences over Sulawesi, New Guinea (within 1.7 to 0.7 mg m^{-3}, respectively) and all individual offshore study zones (within 0.7 to 2.1 mg m^{-3}).~~"
and sentences in the Section 7.3 synthesis has been changed. See below the answer Section 7.3 point #(7).

(11) L470-471: Based on the reanalysis ΔIWC range, it is suggested that Sulawesi and New Guinea may also reach high ΔIWC values comparable to those over Java, even though the observationally derived ΔIWC estimates do not indicate such strong injections over those two islands. But might it not also be the case that the reanalysis might be in error in those regions? Perhaps they pose particularly challenging environments for the models to get right. Again, it seems to me that the authors see the comparisons with ERA5 only as a means of validating (or assessing) their model, and not as a two-way street that possibly highlights regions of potential issues in the reanalysis.
(11) : We completed the sentence L477 in order to consider the eventual error from the reanalysis, as follow:
"However, whatever the level considered, although Java has shown particularly high values in the observational ΔIWC range compared to other study zones, the reanalysis ΔIWC range shows that Sulawesi and New Guinea would also be able to reach similar high values of ΔIWC as Java (assuming that ERA5 IWC data have not yet been evaluated). "

Section 8.2
(1) L505-508: There is a pervasive lack of superscripting in these lines.
(1) Yes, we were refering to about Mori et al. (2004). The sentences have been clarified as follow:
« The diurnal cycle of stratiform and convective precipitations over West Sumatra Sea has been studied by Mori et al. (2004) using 3 years of TRMM precipitation radar (PR) datasets, following the 2A23Algorithm (Awaka, 1998). **Mori et al. (2004)** have shown that rainfall over Sumatra is characterized by convective activity with a diurnal maximum between 15:00 and 22:00 LT while ... »

(3) L508: same comment as above for "xx% of variability".
(3) This sentence has been change and detailed in Section 7.1 point #(7) (see L517 in the new manuscript version).

Section 9
(1) L523-525: It struck me that the summary in the Conclusions does not mention that a key assumption in the model is that deep convection is in the growing phase. Since many readers may only skim the paper and focus mostly on the Conclusions, and many may also be unfamiliar with the earlier Dion et al. (2019) paper, the authors should make clear that they are only applying their model during the increasing phase of the diurnal cycle of deep convection.
(1) : The sentences L523-525 have been modified as follow:
« ...troposphere (UT) and the tropopause level (TL) over the MariCont, from the method proposed in a companion paper (Dion et al., 2019). ~~ΔIWC is firstly calculated using the IWC measured by MLS (IWC^{MLS}) in DJF from 2004 to 2017 at the temporal resolution of 2 observations per day and Prec from TRMM-3B42 during the same period, to obtain a 1-hour resolution diurnal cycle. In the model used (Dion et al., 2019), Prec is considered as a proxy of deep convection impacting ice (ΔIWC^{Prec}) in the UT and the TL.~~ While Dion et al. (2019) have... »

« ...troposphere (UT) and the tropopause level (TL) over the MariCont, from the method proposed in a companion paper (Dion et al., 2019). **The study is focused on the austral convective season of DJF from 2004 to 2017. In the model used (Dion et al., 2019), Prec is considered as a proxy of deep convection impacting ice (ΔIWC^{Prec}) in the UT and the TL. ΔIWC^{Prec} is firstly calculated by the correlation between the growing phase of the diurnal cycle of Prec from TRMM (obtained at a 1-hour resolution**

diurnal cycle) and the value of IWC measured by MLS (IWC^{MLS} , provided at the temporal resolution of 2 observations in local time per day) selected among the growing phase of the diurnal cycle of Prec. While Dion et al. (2019) have ... »

(7) L546-547: It is stated that "the observational ΔIWC range has been shown to be consistent with the reanalysis ΔIWC range to within 23 % over land and to within 30−50 % over sea in the UT and to within 49% over land and to within 39% over sea in the TL". It is not clear where these numbers are derived from, as none of them have appeared previously in the manuscript.
(7) These values have been deleted by error. Thus, we added back these values in to the section 7.3 Synthesis, L469 as follow (note that the percentages values have been changed considering the new calculation of the percentage as defined in the sentence):
« The consistency between observational and reanalysis ΔIWC range is calculated as the difference between the minimal value of the largest range minus the maximum value of the lowest range divided by the mean of these two values. In the UT, over land, observational and reanalysis ΔIWC are found consistent to within 0 to 25% while over sea they are inconsistent (to within 62 to 96%) in the UT. In the TL, observational and reanalysis ΔIWC ranges are consistent to within 0 to 49% over land and to within 0 to 28% over sea. »

These values has been changed in the conclusion section 9 as follow:
"Finally, ΔIWC estimated from observations has been shown to be consistent with ΔIWC estimated from reanalysis to within 25% over land in the UT, to within 49 % over land in the TL and to within 28 % over sea in the TL, but inconsistent to within 96 % over sea in the UT."

(11) L551-552: Although the differences between ΔIWC^{ERA5} and $\langle \Delta IWC^{ERA5} \rangle$ at the two levels suggest that the vertical resolution of the observations has a stronger impact in the TL than in the UT, the total ΔIWC variation range being discussed in this sentence does not. Short comings in the methodology, Prec, or Flash could all contribute to the total ΔIWC variation range.
(11) To be clearer the confusing sentence L551-552 has been deleted.
~~The ΔIWC variation range in the TL is larger than that in the UT highlighting the stronger impact of the vertical resolution in the observations in the TL compared to the UT.~~

(12) L554-556: Are the values quoted in these lines (0–0.6, 1.0, 0.3 mg m^{-3}) consistent with the corresponding numbers given in Section 7 (I don't think so)?
(12) Firstly, we corrected the consistencies by adding the following sentence in Section 7.1, (L432 in the new manuscript version):
«To summarize, independently of the proxies used for the calculation of ΔIWC, and at both altitudes, Java island shows the largest injection of ice over the MariCont. **Observational ΔIWC over Java island is larger by about 1.0 mg m^{-3} in the UT and about 0.3 mg m^{-3} in the TL than other land study zones.** Furthermore, it has been shown ...»
Then, we correct the consistencies by correcting the values (L566 in the new manuscript version) in Section 9 as follow:
« The study at small scale over islands and seas of the MariCont has shown that ΔIWC from ERA5, Prec and Flash in the UT agree to within **0.1 – 1.0** mg m^{-3} over MariCont_L, Sumatra, Borneo and Java with the largest values obtained over Java Island. »

(14) Concerning the sentence discussed above, see point #11 in the comments on Section 7.3.
(14) As previously, we changed the text as follow (L555):
" The study at small scale over islands and seas of the MariCont has shown that ΔIWC from ERA5, Prec and Flash in the UT agree to within 0.1 – 1.0 mg m^{-3} over MariCont_L, Sumatra, Borneo and Java with the largest values obtained over Java Island. **Based on observations,** the Java Island presents the largest amount of ice in the UT and the TL (larger by about 1.0 mg m^{-3} in the UT and about 0.3 mg m^{-3} in the TL than other land study zones). **Based on the reanalysis,** New Guinea and Sulawesi reach similar ranges of ice injection in the UT and even larger ranges of values in the TL than the Java Island keeping in mind that ERA5 IWC

data have not yet been evaluated. »

References
We carefully checked all references in the list.

Supplement
All changes in the manuscript have been highlighted below.

Ice injected into the tropopause by deep convection – Part 2: Over the Maritime Continent

Dion Iris-Amata[1], Dallet Cyrille[1], Ricaud Philippe[1], Carminati Fabien[2], Dauhut Thibaut[3], and Haynes Peter[4]

[1]CRNM, Meteo-France - CNRS, Toulouse, 31057, France
[2]Met Office, Exeter, Devon, EX1 3PB, UK
[3]Max Planck Institute for Meteorology, Hamburg, Germany
[4]DAMTP, University of Cambridge, Cambridge, CB3 0WA, UK

Correspondence: iris.dion@umr-cnrm.fr

Abstract. The amount of ice injected up to the tropical tropopause layer has a strong radiative impact on climate. In the tropics, the Maritime Continent (MariCont) region presents the largest injection of ice by deep convection into the upper troposphere (UT) and tropopause level (TL) (from results presented in the companion paper Part 1). This study focuses on the MariCont region and aims to assess the processes, the areas and the diurnal amount and duration of ice injected by deep convection over islands and over seas using a 2° × 2° horizontal resolution during the austral convective season of December, January and February. The model presented in the companion paper is used to estimate the amount of ice injected (ΔIWC) up to the TL by combining ice water content (IWC) measured twice a day in local time in tropical UT and TL by the Microwave Limb Sounder (MLS; Version 4.2) ~~,~~ from 2004 to 2017, and precipitation (Prec) measurement from the Tropical Rainfall Measurement Mission (TRMM; Version 007) averaged at high temporal resolution (1 hour). The horizontal distribution of ΔIWC estimated from Prec (ΔIWC^{Prec}) is presented at 2° × 2° horizontal resolution over the MariCont. ΔIWC is also evaluated by using the number of lightning events (Flash) from the TRMM-LIS instrument (Lightning Imaging Sensor, from 2004 to 2015 at 1-h and 0.25° × 0.25° resolutions). ΔIWC^{Prec} and ΔIWC estimated from Flash (ΔIWC^{Flash}) are compared to ΔIWC estimated from the ERA5 reanalyses (ΔIWC^{ERA5}) ~~degrading~~ with the vertical resolution degraded to that of MLS observations ($\langle \Delta IWC^{ERA5} \rangle$). Our study shows that, while the diurnal cycles of Prec and Flash are consistent ~~to~~ with each other in timing and phase over ~~lands and~~ land but different over offshore and coastal areas of the MariCont, the observational ΔIWC range between ΔIWC^{Prec} and ΔIWC^{Flash} ~~is small~~ , interpreted as the uncertainty of our model to estimate the ice injected, is smaller over land (they agree to within ~~4 – -~~ 6 to - 22 %~~over land and to within 7 – 53%over ocean~~) than over ocean (to within 6 to - 71 %) in the UT and TL. The ~~reanalysis~~ impact of the vertical resolution on the estimation of ΔIWC ~~range~~ is higher in the TL (difference between ΔIWC^{ERA5} and $\langle \Delta IWC^{ERA5} \rangle$ ~~has been also found to be small in the UT (4 – 29 %) but large in the TL (55 – 78 %), highlighting the stronger impact of the vertical resolution on the TL than in the UT. Combining observational and reanalysis~~ of 32 to 139 %) than in the UT (difference of 9 to 33 %). Considering estimates of ΔIWC ~~ranges, the total~~ from all the methods, ΔIWC ~~range~~ is estimated in the UT between 4.2 and 10.0 mg m^{-3} ~~(20 % of variability per study zone) over land~~over land, and between 0.3 and 4.4 mg m^{-3} ~~(30% of variability per study zone)~~ over sea, and, in the TL, between ~~0.6 and 3.9~~ 0.5 and 3.7 mg m^{-3} ~~(70% of variability per study zone)~~ over land and between 0.1 and

0.7 mg m^{-3} ~~(80% of variability per study zone)~~ over sea. Finally, ~~from IWC~~ ^{ERA5}based on IWC from MLS and ERA5, Prec and Flash, this study highlights that 1) ΔIWC over land ($\geq$ 4 mg m^{-3}) has been found to be larger than ΔIWC over sea ~~with a limit at 4.0~~ ($\leq$ 4 mg m^{-3}~~in the UT between minimum of ΔIWC estimated over land and maximum of ΔIWC estimated over sea~~), and 2) small islands with high topography present the ~~strongest amounts of~~ largest ΔIWC such as the Java Island ~~, the area of the largest ΔIWC in the UT~~ (7.7 ~~–~~ to 9.5 mg m^{-3} ~~daily mean~~in the UT).

1 Introduction

In the tropics, water vapour (WV) and ice cirrus clouds near the cold point tropopause (CPT) have a strong radiative effect on climate (**?**) and an indirect impact on stratospheric ozone (**?**). WV and water ice crystals are transported up to the tropopause layer by two main processes: a three-dimensional large-scale slow process (3-m month $^{-1}$), and a ~~small scale~~ small-scale fast convective process (diurnal timescale) (e.g. **??**). Many studies have already shown the impact of convective processes on the hydration of the atmospheric layers from the upper troposphere (UT) to the lower stratosphere (LS) (e.g. **????**). However, the amount of total water (WV and ice) transported by deep convection up to the tropical UT and LS is still not well understood. The vertical distribution of total water in those layers is constrained by thermal conditions of the CPT (**?**). During deep convective events, **?** have shown that air masses transported up to 146 hPa in the UT and up to 100 hPa in the tropopause layer (TL) have ice to total water ratios of more than 50% and 70%, respectively, and that ice in the UT is strongly spatially correlated with the diurnal increases of deep convection, while WV is not. **?** hence focused on the ice phase of total water to estimate the diurnal amount of ice injected into the UT and the TL over convective tropical areas, showing that it is larger over land than over ocean, with maxima over land of the Maritime Continent (MariCont), the region including Indonesian islands. For these reasons, the present study is focusing on the MariCont region in order to better understand small-scale processes impacting the diurnal injection of ice up to the TL.

A method to estimate the amount of ice injected into the UT and up to the TL over convective areas and during convective seasons has been proposed by **?**. This method provides an estimation of the amplitude of the diurnal cycle of ice in those layers using the twice daily in local times Ice Water Content (IWC) measurements from the Microwave Limb Sounder (MLS) instrument and the full diurnal cycle of precipitation (Prec) measured by the Tropical Rainfall Measurement Mission (TRMM) instrument, at one hour resolution. The method first focuses on the increasing phase of the diurnal cycle of Prec (peak to peak from the diurnal Prec minimum to the diurnal Prec maximum) and shows that the increasing phase of Prec is consistent in time and in amplitude with the increasing phase of the diurnal cycle of deep convection, over tropical convective zones and during convective season. The amount of ice (ΔIWC) injected into the UT and the TL is estimated by relating IWC measured by MLS during the growing phase of the deep convection to the increasing phase of the diurnal cycle of Prec. **?** conclude that deep

convection over the MariCont region is the main process impacting the increasing phase of the diurnal cycle of ice in those layers.

The MariCont region is one of the main convective center in the tropics with the wettest troposphere and the coldest and driest tropopause (**???**). **?** have shown that, over the Indonesian area, the phase of the convective activity diurnal cycle drifts from land to coastlines and to offshore areas. Even though those authors have done a comprehensive ~~work around the~~ study of the diurnal cycle of precipitation and convection over the MariCont, the diurnal cycle of ice injected by deep convection up to the TL over this region is still not well understood. **?** have tentatively evaluated the upper tropospheric diurnal cycle of ice from Superconducting Submillimeter-Wave Limb-Emission Sounder (SMILES) measurements over the period 2009-2010 but without differentiating land and sea over the MariCont, which caused their analysis to show little diurnal variation over that region. **?** have 1) highlighted that the MariCont must be considered as two separate areas: the MariCont land (MariCont_L) and the MariCont ocean (MariCont_O), with two distinct diurnal cycles of the Prec and 2) estimated the amount of ice injected in the UT and the TL. Over these two domains, it has also been shown that convective processes are stronger over MariCont_L than over MariCont_O. Consequently, the amount of ice injected in the UT and the TL is greater over MariCont_L than over MariCont_O.

Building upon the results of **?**, the present study aims to improve ~~the methodology of Dion et al. (2019)~~ their methodology by i) studying smaller study zones than in Dion et al. (2019) and by distinguishing island and sea of the MariCont, ii) ~~assessing~~ comparing the sensitivity of our model to different proxies of deep convection and iii) ~~assessing~~ comparing the amount of ice injected in the UT and the TL inferred by our model to that of ERA5 reanalyses. Based on space-borne observations and meteorological reanalyses, ΔIWC is assessed at a horizontal resolution of $2^\circ \times 2^\circ$ over 5 islands (Sumatra, Borneo, Java, Sulawesi and New Guinea) and 5 seas (West Sumatra Sea, Java Sea, China Sea, North Australia Sea, and ~~Bismark~~ Bismarck Sea) of the MariCont during convective season (December, January and February, hereafter DJF) from 2004 to 2017. ΔIWC will be first estimated from Prec measured by TRMM-3B42. A sensitivity study of ΔIWC based on the number of flashes (Flash) detected by the TRMM Lightning Imaging Sensor (TRMM-LIS), an alternative proxy for deep convection as shown by Liu and Zipser (2008), is also proposed. Finally, we will use IWC calculated by the ERA5 reanalyses from 2005 to 2016 to estimate ΔIWC in the UT and the TL over each study zone and compare it to ΔIWC estimated from Prec and Flash.

The observational datasets used in our study are presented in Sect. 2. Method is ~~recalled~~ reviewed in Sect. 3. The amount of ice (ΔIWC) injected up to the TL estimated from Prec is evaluated in Sect. 4. Diurnal cycles of Prec and Flash are compared to each other over different areas of the MariCont in Sect. 5. Results of the estimated ΔIWC injected up to the UT and the TL over five islands and five seas of the MariCont are presented and compared with the ERA5 reanalyses in Sect. 6. Results are discussed in Sect. 7, and conclusions are drawn in Sect. 8. This paper contains many abbreviations and acronyms. To facilitate reading, they are compiled in the Acronyms list.

2 Datasets

This section presents the instruments and the reanalyses used for this study.

2.1 MLS Ice Water Content

The Microwave Limb Sounder (MLS, data processing algorithm version 4.2) instrument on board NASA's Earth Observing System (EOS) Aura platform (**??**) launched in 2004 provides ice water content (IWC^{MLS}, mg m^{-3}) measurements. MLS data processing provides IWC^{MLS} ~~are given~~ at 6 levels in the UTLS (82, 100, 121, 146, 177 and 215 ~~). However, we~~ hPa). Although optimal estimation is used to retrieve almost all other MLS products, a cloud-induced radiance technique is used to derive the IWC^{MLS} (**??**). We have chosen to study only two levels: an upper and a lower level of the TTL. Because the level at 82 hPa does not provide enough significant measurements of IWC to have a good signal-to-noise, we have selected~~2 levels~~: 1) ~~at~~ 100 hPa as the upper level of the TTL (named TL for tropopause level), and 2) ~~at~~ 146 hPa as the lower level of the TTL (named UT for upper ~~tropopshere~~troposphere). MLS follows a sun-synchronous near-polar orbit, completing 233 revolution cycles every 16 days, with daily global coverage every 14 orbits. The instrument ~~is crossing~~ crosses the equator twice a day ~~the equator at fixed time~~at fixed times, measuring IWC^{MLS} at 01:30 local time (LT) and 13:30 LT. The ~~horizontal resolution of IWC^{MLS} measurements is $\sim$ 300 and 7 km along and across the track, respectively. The~~ vertical resolution of IWC^{MLS} is 4 and 5 km at 146 and 100 hPa, respectively. ~~Although optimal estimation is used to retrieve almost all other MLS products, a cloud-induced radiance technique is used to validate the MLS IWC (Wu et al., 2008; Wu et al., 2009).~~ In our study, high horizontal resolution is now possible because we consider 13 years of MLS data, allowing ~~to average~~ the IWC^{MLS} measurements ~~within the~~ to be averaged within bins of horizontal resolution of 2° ×2° ($\sim$ 230 km^2). We select IWC^{MLS} during all austral convective seasons DJF between 2004 and 2017. The IWC measurements were filtered following the recommendations of the MLS team described in **?**. The ~~resolutions~~ resolution of IWC^{MLS} (horizontal along the path, horizontal perpendicular to the path, vertical) measured at 146 and 100 hPa ~~are~~ is 300×7×4 km and 250×7×5 km, respectively. The precision of the measurement is 0.10 mg m^{-3} at 146 hPa and 0.25 to 0.35 mg m^{-3} at 100 hPa. ~~The~~ While the accuracy is 100% for values less than 10 mg m^{-3} at both levels~~and the~~ , it is strongly reduce by averaging on the study period and over the study zones. The valid range is ~~0.02~~0.1-50.0 mg m^{-3} at 146 hPa and ~~0.1~~0.02-50.0 mg m^{-3} at 100 hPa (Wu et al., 2008).

2.2 TRMM-3B42 Precipitation

The Tropical Rainfall Measurement Mission (TRMM) was launched in 1997 and provided measurements of Prec until 2015. TRMM is composed of five instruments, three of them are complementary sensor rainfall suite (PR, TMI, VIRS). TRMM had an almost circular orbit at 350 km altitude ~~height~~ performing a complete revolution in one and a half hour. The 3B42 algorithm product (TRMM-3B42) (version V7) has been created to estimate the precipitation and extend the precipitation product through 2019. TRMM-3B42 is a multi-satellite precipitation analysis~~composing a Global Precipitation Measurement (GPM) Mission. TRMM-3B42 is computed from the various precipitation-relevant satellite passive Microwave (PMW) sensors using GPROF2017 computed at the Precipitation Processing System (PPS) (e.g., GMI, DPR, Ku, Ka, Special Sensor Microwave Imager/Sounder SSMIS, etc.) and including~~ . The analysis merges microwave and infrared space-borne observations and included TRMM measurements from 1997 to 2015 ~~(Huffman et al. , 2007, 2010; and Huffman and Bolvin, 2018).~~ (**???**) . Work is currently underway with NASA funding to develop more appropriate estimators for random error, and to introduce

estimates of bias error (Huffman and Bolvin, 2018). Prec data are provided at a 0.25° × 0.25° (∼ 29.2 km^2) horizontal resolution, extending from 50° S to 50° N (https://pmm.nasa.gov/data-access/downloads/trmm, last access: April 2019). Prec from TRMM-3B42 products ~~depends on input from microwave and IR sensors (?) and~~ does not differentiate between stratiform and convective precipitation. In our study, Prec from TRMM-3B42 is selected over the austral convective seasons (DJF) from 2004 to 2017 and averaged to a horizontal grid of 2° ×2 ° to be compared to IWC^{MLS}. The ~~granule temporal coverage of~~ TRMM-3B42 data ~~is 3 hours, but the temporal resolution of individual measurements is 1 minute. Thus, it is statistically possible to degrade the resolution to 1 hour.~~ have been averaged over a 1-hour interval from 0 to 24 hours. TRMM-3B42 data are provided in Universal Time that we converted into local time (LT). Details of the binning methodology of TRMM-3B42 is provided by Huffman and Bolvin (2018).

2.3 TRMM-LIS number of Flashes

The Lightning Imaging Sensor (LIS) aboard of the TRMM satellite measures several parameters ~~relative~~ related to lightning. According to Christian et al. (2000), LIS used a Real-Time Event Processor (RTEP) that discriminates lightning ~~event~~ events from Earth albedo light. A lightning event corresponds to the detection of a light anomaly on a pixel representing the most fundamental detection of the sensor. After ~~a~~ spatial and temporal processing, the sensor was able to characterize a flash from several detected events. The observation range of the sensor is between 38° N and 38° S. The instrument detects lightning with storm-scale resolution of 3-6 km (3 km at nadir, 6 km at limb) over a large region (~~550-550~~ 550×550 km) of the Earth's surface. The LIS horizontal resolution is provided at 0.25°~~×0.10~~× 0.25°. A significant amount of software filtering has gone into the production of science data to maximize the detection efficiency and confidence level. Thus, each datum is a lightning signal and not noise. Furthermore, the weak lightning signals that occur during the day are hard to detect because of background illumination. A ~~real-tile event processor~~ RTEP removes the background signal to enable the system ~~and~~ to detect weak lightning and ~~achieve a 90%~~ improves the detection efficiency during the day. LIS is thus able to provide the number of flashes (Flash) measured. The TRMM LIS detection efficiency ranges from 69% near noon to 88% at night. The LIS instrument performed measurements between 1 January 1998 and 8 April 2015. To be as consistent as possible to the MLS and TRMM-3B42 period of study, we are using LIS measurements during DJF from 2004 to 2015. ~~The observation range of the sensor is between 38° N and 38° S.~~ As LIS is on the TRMM platform, with an orbit that precesses, Flash from LIS can be averaged to obtain the full 24-h diurnal cycle of Flash over the study period with a 1-h temporal resolution. In our study, Flash measured by LIS is ~~studied~~ binned at 0.25° × 0.25° horizontal resolution to be compared to Prec from TRMM-3B42.

2.4 ERA5 Ice Water Content

The European Centre for Medium-range Weather Forecasts (ECMWF) Reanalysis 5, known as ERA5, replaces the ERA-Interim reanalyses as the fifth generation of the ECMWF reanalysis providing global climate and weather for the past decades (from 1979) (**?**). ERA5 provides hourly estimates for a large number of atmospheric, ocean and land surface quantities and covers the Earth on a 30 km grid with 137 levels from the surface up to a height of 80 km. Reanalyses such as ERA5 provide a physically constrained, continuous, global, and homogeneous representation of the atmosphere through combining a large

number of observations (space-borne, air-borne, and ground-based) with short-range forecasts. Although there is no direct observation of atmospheric ice content in ERA5, the specific cloud ice water content (mass of condensate / mass of moist air) (IWC^{ERA5}) corresponds to the changes in the analysed temperature (and at low levels, humidity) which is mostly driven by the assimilation of temperature-sensitive radiances from satellite instruments (https://cds.climate.copernicus.eu/cdsapp!/dataset/reanalysis-era5-pressure-levels-monthly-means?tab=form, last access: July 2019). IWC^{ERA5} used in our analysis is representative of non-precipitating ice. Precipitating ice, classified as snow water, is also provided by ERA5 but not used in this study in order to focus only on the injected and non-precipitating ice ~~into~~ in the TTL. Furthermore, results from Duncan and Eriksson (2018) have highlighted that ERA5 is able to capture both seasonal and diurnal variability in cloud ice water but the reanalyses exhibit noisier and higher amplitude diurnal variability than borne out by the satellite estimates. The present study uses the IWC^{ERA5} at 100 and 150 hPa averaged over DJF from 2005 to 2016 with one-hour temporal resolution. IWC^{ERA5} is governed by the model microphysics which allows ice supersaturation with respect to ice (100-150% in relative humidity) but not with respect to liquid water. Although microwave radiances at 183 GHz (sensitive to atmospheric scattering induced by ice particles) (Geer et al., 2017) are assimilated, ~~cloud and precipitations are~~ clouds and precipitation are not used as control ~~variable~~ variables in the 4D-Var assimilation system and cannot be adjusted independently in the analysis (Geer et al., 2017). The microwave data have sensitivity to the frozen phase hydrometeors but mainly to larger particles, such as those in the cores of deep convection (Geer et al., 2017), but the sensitivity to cirrus clouds in ERA5 is strongly dependent on microphysical assumptions on the shape and size of the cirrus particles. Indirect feedbacks are also acting on cirrus representation in the model – e.g. changing the intensity of the convection will change the amount of outflow cirrus generated. This is why observations that ~~affects~~ affect the troposphere by changing for example the stability, the humidity, or the synoptic situation can affect the upper level ice cloud indirectly (Geer et al., 2017). IWC^{ERA5} is ~~used to assess~~ compared to the amount of ice injected in the UT and the TL as estimated by the model developed in Dion et al. (2019) and in the present study. IWC^{ERA5} have been degraded along the vertical at 100 and 150 hPa ($\langle \Delta IWC^{ERA5} \rangle$) consistently with the MLS vertical resolution of IWC^{MLS} (5 and 4 km at 100 and 146 hPa, respectively) using ~~an unitary~~ a box function (see section **??**). IWC^{ERA5} and $\langle \Delta IWC^{ERA5} \rangle$ will be both considered in this study. IWC^{ERA5}, initially provided in kg kg^{-1}, has been converted into mg m^{-3} using the temperature provided by ERA5 in order to be compared with ~~MLS IWC~~observationsIWC^{MLS}.

3 Methodology

This section summarizes the method developed by **?** to estimate ΔIWC, the amount of ice injected into the UT and the TL. **?** have presented a model relating Prec (as proxy of deep convection) from TRMM to IWC^{MLS} over tropical convective areas during austral convective season DJF. The IWC^{MLS} value measured by MLS during the growing phase of the convection (at ~~x~~ x = 01:30 LT or 13:30 LT) is compared to the Prec value at the same time ~~x~~ x in order to define the correlation coefficient (C) between Prec and IWC^{MLS}, as follows:

$$C = \frac{IWC_x^{MLS}}{Prec_x} \quad (1)$$

The diurnal cycle of IWC estimated ($IWC^{est}(t)$) can be calculated by using C applied to the diurnal cycle of Prec (~~Prec(t))~~$Prec(t)$), where t is the time, as follows:

$$IWC^{est}(t) = Prec(t) \times C \tag{2}$$

The amount of IWC injected up to the UT or the TL (ΔIWC^{Prec}) is defined by the difference between the maximum of IWC^{est} (IWC$^{est}_{max}$) and its minimum (IWC$^{est}_{min}$).

$$\Delta IWC^{Prec} = C \times (Prec_{max} - Prec_{min}) = IWC^{est}_{max} - IWC^{est}_{min} \tag{3}$$

where $Prec_{max}$ and $Prec_{min}$ are the diurnal maximum and minimum of Prec, respectively. Figure **??** illustrates the relationship between the diurnal cycle of Prec and the two MLS measurements at 01:30 ~~LT~~ and 13:30 LT. The growing phase of the convection is defined as the period of increase in precipitation from $Prec_{min}$ to $Prec_{max}$. The amplitude of the diurnal cycle is defined by the difference between $Prec_{max}$ and $Prec_{min}$. In Fig. 1, because the growing phase of the convection illustrated is happening during the afternoon, only the MLS measurement at 13:30 LT is used in the calculation of ΔIWC. IWC at 01:30 LT is not used in that case.

4 Horizontal distribution of ΔIWC estimated from Prec over the MariCont

4.1 Prec from ~~TRMM~~ TRMM-3B42 related to IWC from MLS

In order to identify the main areas of injection of ice in the TL over the MariCont, Figure **??** presents different parameters associated to this area: a) the name of the main islands and seas over the MariCont, b) the elevation (http://www.soda-pro.com/web-services/altitude/srtm-in-a-tile, last access: June 2019), c) the daily mean of Prec at 0.25° × 0.25° horizontal resolution, d) the hour of the diurnal maxima of Prec at 0.25° × 0.25° horizontal resolution, and e) the daily mean ($I\bar{W}C = (IWC_{01:30} + IWC_{13:30}) \times 0.5$) of IWC^{MLS} at 146 hPa at 2° × 2° horizontal resolution. Several points need to be highlighted. Daily means of Prec over land and coastal parts are higher than over oceans (Fig. **??**c). Areas where the daily mean of Prec is maximum are usually surrounding the highest elevation over land (e.g. over ~~NewGuinea~~) and near coastal areas (North West of Borneo in the China Sea and ~~South of~~ southern Sumatra in the Java Sea) (Fig. **??**b and c). The times of the maxima of Prec are over land during the evening (18:00-00:00 LT), over coast during the night-morning (00:00-06:00 TL) and over sea during the morning-noon and even evening depending ~~of~~ on the sea considered (09:00-12:00 LT and 15:00-00:00 LT). These differences ~~could illustrate~~ may be related to the impact of the land/sea breeze ~~within the~~ over the course of 24 hours. The sea breeze during the day favours the land convection at the end of the day when land ~~temperature surface~~ surface temperature is higher than oceanic ~~temperature surface~~ surface temperature. During the night, the coastline sea surface temperature ~~becomes larger than~~ rises above the land surface temperature, and the land breeze ~~favours systematically the convection development over coast~~systematically favours the development of convection over coasts. These observations are consistent

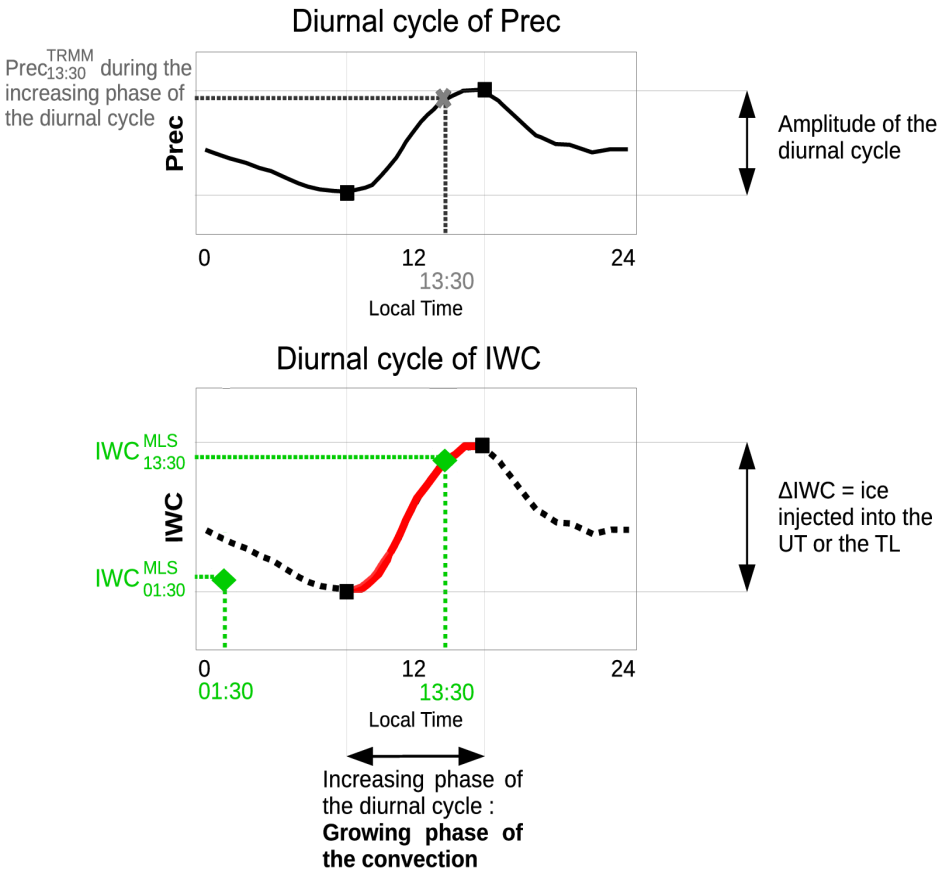

Figure 1. Illustration of the model ~~used~~ developed in **?** to estimate the amount of ice (ΔIWC) injected into the UT or the TL. Diurnal cycle of a proxy of deep convection (Prec) (a), diurnal cycle of ice water content (IWC) estimated from diurnal cycle of the proxy of deep convection (b). In red line, the increasing phase of the diurnal cycle. In black dashed line, the decreasing phase of the diurnal cycle. The green diamonds are the two IWC^{MLS} measurements from MLS. Grey thick cross represents the measurement of Prec during the growing phase of the convection ($Prec_x$), used in the model. Maximum and minimum of the diurnal cycles are represented by black squares. Amplitude of the diurnal cycle is defined by the differences between the maximum and the minimum of the cycle.

215 with results presented ~~in ?, explaining~~ by **?**, who explained that high precipitation is mainly concentrated over land in the MariCont because of the strong sea-breeze convergence, but also because of the combination with the mountain–valley winds and cumulus merging processes. Amplitudes of the diurnal cycles of Prec over the MariCont will be detailed as a function of island and sea in section **??**. The location of the largest concentration of IWC^{MLS} (3.5 – 5.0 mg m^{-3}, Fig. **??**e) is consistent with that of Prec ($\sim$ 12 – 16 mm day^{-1}) over the West Sumatra Sea, and over the South of Sumatra island. However, over

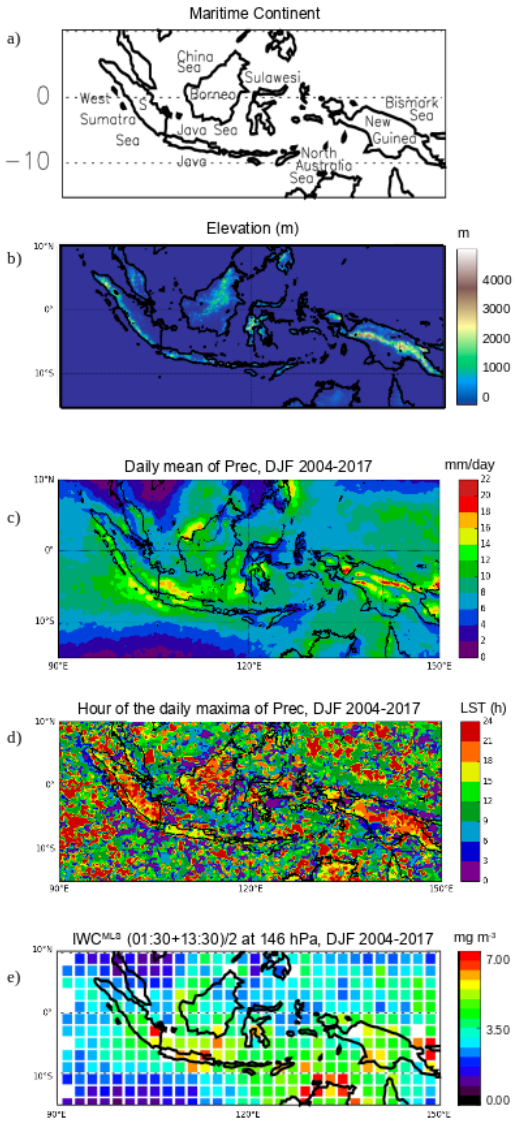

Figure 2. Main islands and seas of the MariCont (S is for Sumatra) (a), elevation from Solar Radiation Data (SoDa) (b); daily mean of Prec ~~measured by~~ obtained from TRMM analysis over the Maritime Continent, averaged over the period of DJF 2004-2017 (c), hour (local solar time (LST)) of the diurnal maxima of Prec over the MariCont (d); daily mean (01:30 LT + 13:30 LT)/2 of IWC^{MLS} at 146 hPa from MLS over the MariCont averaged over the period of DJF 2004-2017 (e). Observations are presented with a horizontal resolution of $0.25^\circ \times 0.25^\circ$ (b, c and d) and $2^\circ \times 2^\circ$ (e).

North Australia seas (including the Timor Sea and the Arafura Sea), we observed large differences between Prec low values (4 – 8 mm day^{-1}) and IWC^{MLS} large concentrations (4 – 7 mg m^{-3}).

4.2 Convective processes compared to IWC measurements

Although TRMM horizontal resolution is 0.25° × 0.25°, we require information at the same resolution as ~~MLS IWC~~IWC^{MLS}. From the diurnal cycle of ~~TRMM Prec measurements~~Prec in TRMM analysis, the duration of the increasing phase of Prec can be known for each 2° × 2° pixel. The duration of the growing phase of the convection can then be defined from Prec over each pixel. Figures ~~??a~~ 3a and b present the anomaly (deviation from the mean) of Prec ~~measured by TRMM–3B42 over the MariCont at 01:30 LT and 13:30 LT, respectively, only over pixels when the convection is in the growing phase. The anomaly of IWC measured by MLS~~ in TRMM-3B42 over the MariCont ~~is shown in Figs. ??c and d, over pixels when the~~ for the pixels where convection is in the growing phase at 01:30 LT and 13:30 LT, respectively. ~~Each pixel of Prec at 01:30 LT or 13:30 LT during the~~ Anomalies are calculated relative to the average computed over the entire MariCont region. Thus, red colors signify regions that are experiencing the growing phase of ~~the convection deviates by the average of the all Prec at~~ convection and whose Prec value is greater than the overall MariCont mean at the respective time (01:30 LT or 13:30 LT), whereas blue colors signify those regions where there is little precipitation compared to the overall MariCont mean during the growing phase of ~~the convectionover the whole MariCont~~convection. The gray color denotes pixels for which convection is not ongoing. ~~Some pixels can be presented on both sets of Prec and IWC panels in Figs. 3~~ Pixels can be represented in the panels for both local times when: 1) the onset of the convection is before 01:30 LT and the end is after 13:30 LT, or 2) the onset of the convection is before 13:30 LT and the end is after 01:30 LT. Similar anomalies of IWC^{MLS} over the MariCont are shown in Figs. 3c and d, over pixels when the convection is in the growing phase at 01:30 LT and 13:30 LT, respectively. Note that, ~~whithin~~ within each 2°~~x2°~~ ° × 2° pixel, at least 60 measurements of Prec or IWC^{MLS} at 13:30 LT or 01:30 LT over the period 2004-2017 have been selected for the average.

The Prec anomaly at 01:30 LT and 13:30 LT varies between -0.15 and +0.15 mm h^{-1}. The IWC^{MLS} anomaly at 13:30 LT and 01:30 LT varies between -3 and +3 mg m^{-3}. At 13:30 LT, the growing phase of the convection ~~over land is mainly at 13:30 LT~~is found mainly over land. At 13:30 LT, over land, the strongest Prec and IWC^{MLS} anomalies (+0.15 mm h^{-1} and +2.50 mg m^{-3}, respectively) are found over the Java island, and ~~north of~~ northern Australia for IWC^{MLS}. At 01:30 LT, the growing phase of the convection is found mainly over sea (while the pixels of the land are mostly gray), with maxima of Prec and IWC^{MLS} anomalies over coastlines and seas close to the coasts such as the Java Sea and the ~~Bismark Sea. The IWC anomaly at 13:30 LT and 01:30 LT varies between -3 and +3 mg m^{-3}.~~ Bismarck Sea. Three types of areas can be distinguished from Fig. **??**: i) area where Prec and IWC^{MLS} anomalies have the same sign (positive or negative either at 01:30 LT or 13:30 LT) (e.g. over Java, Borneo, Sumatra, Java Sea and coast of Borneo or the China Sea); ii) area where Prec anomaly is positive and IWC^{MLS} anomaly is negative (e.g. over West Sumatra Sea); and iii) area where Prec anomaly is negative and IWC^{MLS} anomaly is positive (e.g. over the North Australia Sea at 01:30 LT). Convective processes associated to these three types of areas over islands and seas of the MariCont are discussed in Sect. 6.

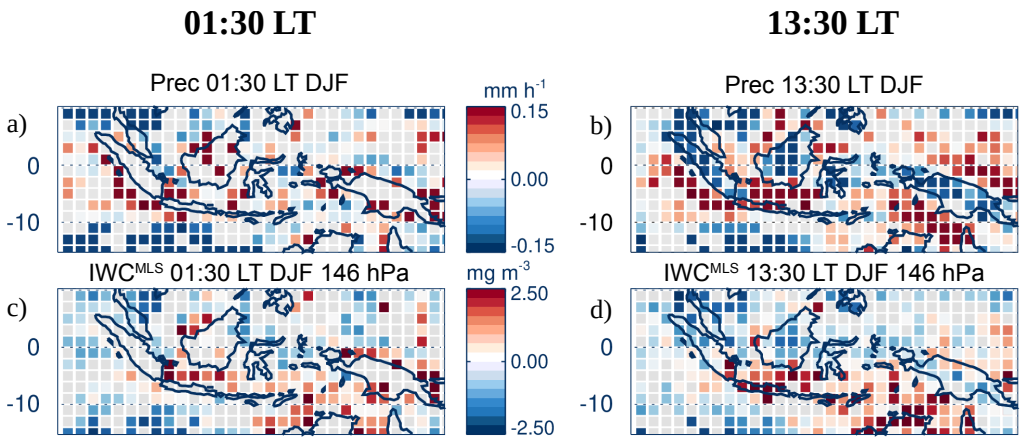

Figure 3. Anomaly (deviation from the mean) of Prec (a-b) and Ice Water Content (IWC^{MLS}) at 146 hPa (c-d), at 01:30 LT (left) and at 13:30 LT (right) over pixels where 01:30 LT and 13:30 LT are during the growing phase of the convection, respectively, averaged over the period of DJF 2004-2017. The gray color denotes pixels for which convection is not ongoing.

4.3 Horizontal distribution of ice injected into the UT and TL estimated from Prec

From the model developed in **?** based on Prec from TRMM–3B42 and IWC from MLS and synthesized in section 2.4, we can calculate the amount of IWC injected (ΔIWC) at 146 hPa (UT, Figure **??**a) and at 100 hPa (TL, Figure **??**b) by deep convection over the MariCont. In the UT, the amount of IWC injected over land is on average larger (> 10 – 20 mg m^{-3}) than over seas (< ~~10~~ 15 mg m^{-3}). ~~South of~~ Southern Sumatra, Sulawesi, ~~North of~~ northern New Guinea and ~~North of~~ northern Australia present the largest amounts of ΔIWC over land (15 – 20 mg m^{-3}). Java Sea, China Sea and ~~Bismark~~ Bismarck Sea present the largest amounts of ΔIWC over seas (7 – 15 mg m^{-3}). West Sumatra Sea and North Australia Sea present low values of ΔIWC (< 2 mg m^{-3}). We can note that the anomalies of Prec and IWC during the growing phase over North Australia Sea at 13:30 LT are positive (> 0.2 ~~mg m^{-3}~~ mm h^{-1}, Fig. **??**~~a and~~ b and > 2.5 mg m^{-3}, Fig. **??**~~c and~~ d, respectively). In the TL, the maxima (up to 3.0 mg m^{-3}) and minima (down to 0.2 – 0.3 mg m^{-3}) of ΔIWC are located within the same pixels as in the UT, although 3 to 6 times lower than in the UT. The decrease of ΔIWC with altitude is larger over land (by a factor 6) than over sea (by a factor 3). We can note that the similar pattern between the two layers ~~come~~ comes from the diurnal cycle of Prec in the calculation of ΔIWC at 146 and 100 hPa. ~~Only the measured value of IWC^{MLS} at 146 and 100 hPa can explain the observed différences in~~ The differences in the magnitudes of the ΔIWC values at ~~these~~ 100 and 146 hPa arise from the different amounts of IWC measured by MLS at those two levels. ~~Thus~~That is, similar ΔIWC patterns are expected between the two levels because, according to the model developed in Dion et al. (2019), ~~the~~ deep convection is the main process transporting ice into the UT and the TL during the growing phase of the convection. Convective processes associated to land and sea are further discussed in Sect. 6.

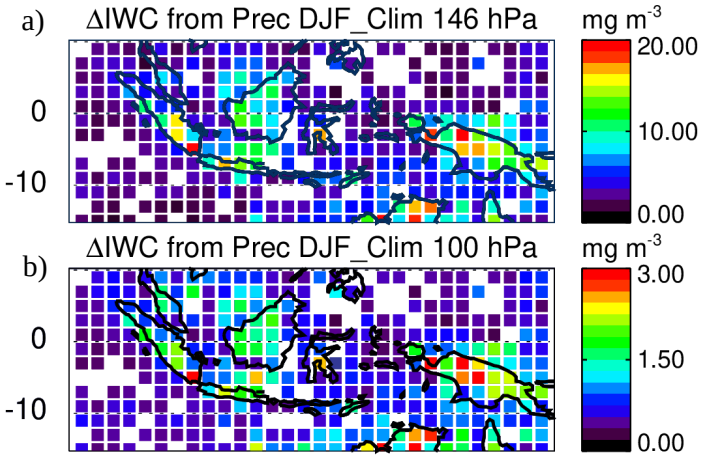

Figure 4. Daily amount of ice injected (ΔIWC) up to the UT (a) and up to the TL (b) estimated from Prec, averaged during DJF 2004-2017.

In order to better understand the impact of deep convection on the strongest ΔIWC injected per pixel up to the TTL, isolated pixels selected in Fig. 4a are presented separately in Figure **??**a and f. This Figure shows the diurnal cycles of Prec in four pixels selected for their large ΔIWC in the UT ($\geq$ 15 mg m^{-3}, Fig. **??**b, c, d, e), and the diurnal cycle of Prec in four pixels selected for their low ΔIWC in the UT (but large enough to observe the diurnal cycles of IWC between 2.0 and 5.0 mg m^{-3}, Fig. **??**g, h, i, j). Pixels with low values of ΔIWC over land (~~Figs~~Fig. **??**g, h and i) present small amplitude of diurnal cycles of Prec ($\sim$ +0.5 mm h^{-1}), with maxima between 15:00 LT and 20:00 LT and minima around 11:00 LT.

The pixel with low value of ΔIWC over sea (Fig. **??**j) presents an almost null amplitude of the diurnal cycle of Prec~~with low value~~, with low values of Prec all day long ($\sim$ 0.25 mm h^{-1}). Pixels with large values of ΔIWC over land (Fig. **??**b, c, d, e) present longer duration of the increasing phase of the diurnal cycle (from $\sim$ 09:00 LT to 20:00 – 00:00 LT) than the increasing phase of Prec diurnal cycle over pixels with low values of ΔIWC (from 10:00 LT to 15:00 – 19:00 LT). More precisely, pixels labeled 1 and 2 over New Guinea (Fig. **??**d and e) and the pixel over ~~South of~~ southern Sumatra (Fig. **??**c) show amplitude of diurnal cycle of Prec reaching 1.0 mm h^{-1}, while the pixel over North Australia (Fig. **??**b) presents lower amplitude of diurnal cycle of Prec (0.5 mm h^{-1}).

~~IWC measured by MLS~~

IWC^{MLS} during the growing phase of deep convection and the diurnal cycle of IWC estimated from Prec are also shown on Fig. **??**. For pixels with large values of ΔIWC, IWC~~observed by MLS~~ ^{MLS} is between 4.5 and 5.7 mg m^{-3} over North Australia~~Sea~~, South Sumatra and New Guinea ~~.~~1. For pixels with low values of ΔIWC, IWC~~observed by MLS~~ ^{MLS} is found between 1.9 and 4.7 mg m^{-3}. To summarize, large values of ΔIWC are observed over land in combination to i) longer growing phase of deep convection (> 9 hours) and/or ii) large diurnal amplitude of Prec (> 0.5 mm h^{-1}). However, as IWC^{MLS} ranges

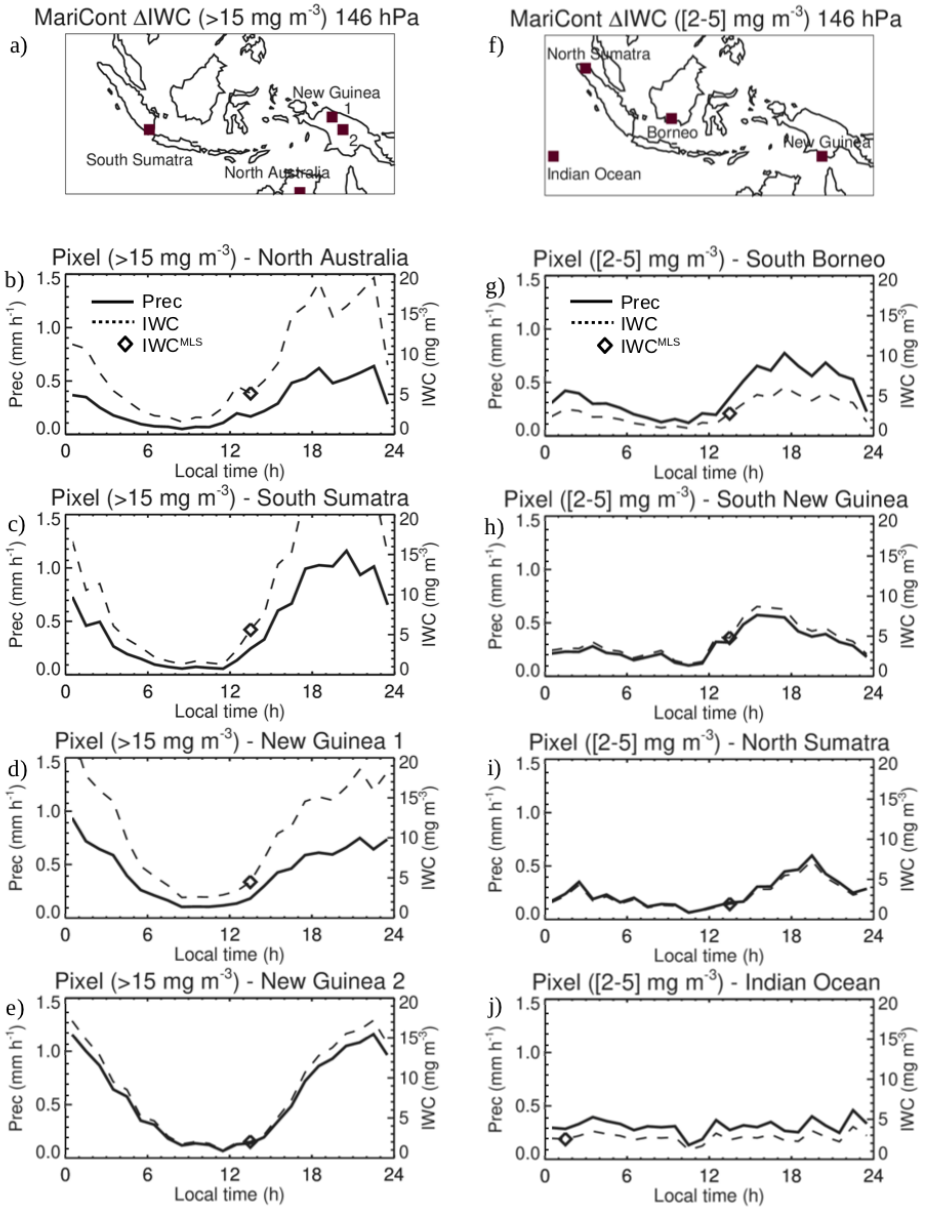

Figure 5. a) and f) Location of 2° × 2° pixels where ΔIWC have been found higher than 15 mg m^{-3} (in Fig. 4) and where ΔIWC have been found between 2 and 5 mg m^{-3} (in Fig. 4), respectively. Diurnal cycle of Prec (solid line): (b, c, d, e) over 4 pixels where ΔIWC have been found higher than 15 mg m^{-3} (in Fig. 4), (g, h, i, j) over 4 pixels where ΔIWC have been found between 2 and 5 mg m^{-3} (in Fig. 4), during DJF 2004-2017. The diamond represents IWC^{MLS} during the increasing phase of the convection. The dashed line is the diurnal cycle of IWC estimated from the diurnal cycle of Prec and from IWC^{MLS}.

overlap for the high and low ΔIWC, no definitive conclusion about the relationship between IWC^{MLS} and ΔIWC can be drawn.

In the next section, we estimate ΔIWC using another proxy of deep convection, namely Flash measurements from LIS.

~~a) and f) location of 2° × 2° pixels where ΔIWC have been found higher than 15 mg m^{-3} (in Fig. 4) and where ΔIWC have been found between 2 and 5 mg m^{-3} (in Fig. 4), respectively. Diurnal cycle of Prec (solid line): (b, c, d, e) over 4 pixels where ΔIWC have been found higher than 15 mg m^{-3} (in Fig. 4), (g, h, i, j) over 4 pixels where ΔIWC have been found between 2 and 5 mg m^{-3} (in Fig. 4), during DJF 2004-2017. The Diamond is IWC^{MLS} measured by MLS during the increasing phase of the convection. The dashed line is the diurnal cycle of IWC estimated from the diurnal cycle of Prec and from IWC^{MLS}.~~

5 Relationship between diurnal cycle of Prec and Flash over MariCont land and sea

Lightning is created ~~into~~ in cumulonimbus clouds when the electric potential energy difference is large between the base and the top of the cloud. Lightning can appear at the advanced stage of the growing phase of the convection and during the mature phase of the convection. For these reasons, in this section, we use Flash measured from LIS during DJF 2004-2015 as another proxy of ~~the~~ deep convection in order to estimate ΔIWC (ΔIWC^{Flash}) and check the consistency with ΔIWC obtained with Prec (ΔIWC^{Prec}).

5.1 Flash distribution over the MariCont

Figure **??**a presents the daily mean of Flash in DJF 2004-2015 at 0.25° × 0.25° horizontal resolution. Over land, Flash can reach a maximum of 10^{-1} flashes day^{-1} per pixel while, over seas, Flash are less frequent ($\sim 10^{-3}$ flashes day^{-1} ~~day~~ per pixel). When compared to the distribution of Prec (Fig. **??**c), maxima of Flash are found over ~~the same~~ similar areas as maxima of Prec (Java, East of Sulawesi coast, Sumatra and ~~North Australialands~~northern Australia). Over Borneo and ~~NewGuinea~~New Guinea, coastlines present more Flash ($\sim 10^{-2}$ flashes day^{-1}) than inland ($\sim 10^{-3}$ flashes day^{-1}). Differences between Flash and Prec distributions are found over North Australia Sea, with relatively large number of Flash (~~~~>10^{-2} flashes day^{-1}) compared to low Prec (4 – 10 mm day^{-1}) (Fig. **??**c), and over ~~NewGuinea~~ several inland areas of New Guinea where the number of Flash is relatively low ($\sim 10^{-2}$~~–~~ 10^{-3} flashes day^{-1}) while Prec is high (~14 – 20 mm day^{-1}). Figure **??**b shows the hour of the Flash maxima. Over land, the maximum of Flash is between 15:00 LT and 19:00 LT, slightly earlier than the maximum of Prec (Fig. **??**d) observed between 16:00 LT and 24:00 LT. Coastal areas present similar hours of maximum of Prec and Flash, i.e between 00:00 LT and 04:00 LT although, over the West Sumatra Coast, diurnal maxima of both Prec and Flash happen 1–4 hours earlier (from 23:00-24:00 LT) than those of other coasts.

5.2 Prec and Flash diurnal cycles over the MariCont

This section compares the diurnal cycle of Flash with the diurnal cycle of Prec in order to assess the potential for Flash to be used as a proxy of deep convection over land and sea of the MariCont. Diurnal cycles of Prec and Flash over the MariCont land, coastline and offshore (MariCont_L, MariCont_C, MariCont_O, respectively) are shown in Figs. **??**a–c, respectively. Within

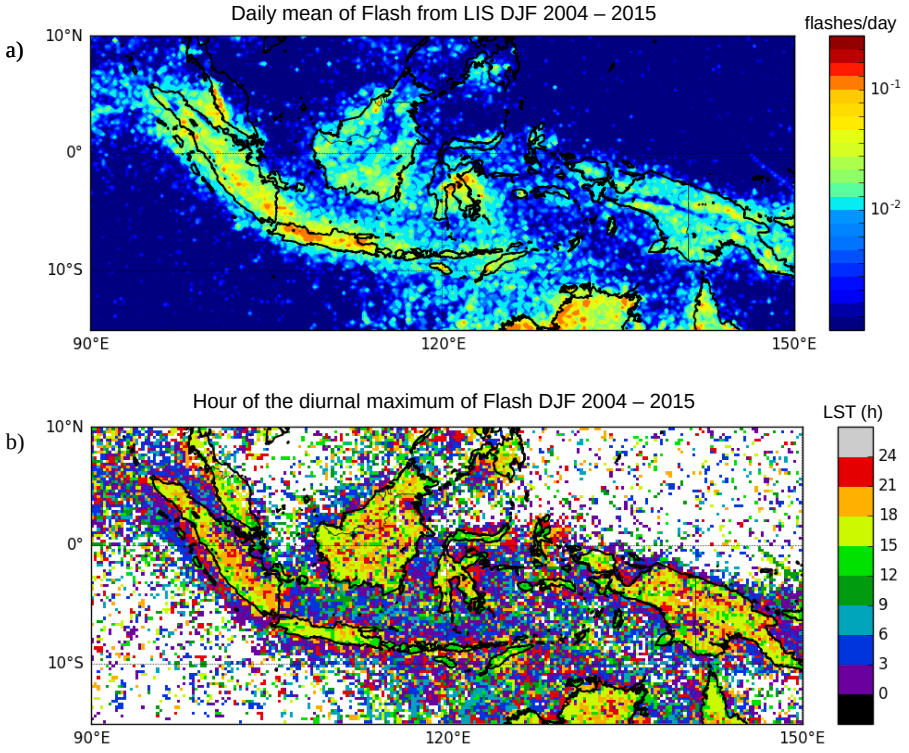

Figure 6. Daily mean of Flash measured by LIS averaged over the period DJF 2004-2015 (a); Hour (local solar time (LST)) of the diurnal maximum of Flash (b).

each 0.25° × 0.25° bin, land/coast/ocean filters were applied from the Solar Radiation Data (SoDa, http://www.soda-pro.com/web-services/altitude/srtm-in-a-tile). MariCont_C is the average of all coastlines defined as 5 pixels extending into the sea from the land limit. This choice of 5 pixels ~~has been taken applying~~ was made after consideration of some sensitivity tests in order to have the best compromise between a high signal-to-noise ratio and a good representation of the coastal region. The MariCont_O is the average of all offshore pixels defined as sea pixels excluding 10 pixels (~~-~~2000 km~~off the land~~) over the sea from the land~~coasts~~, thus coastline pixels are excluded as well as all the coastal influences. MariCont_L is the area of all land pixels. ~~A~~ At the border between the land and the coast areas, a given 0.25°×0.25°pixel can contain information from ~~different origins : land /coastlinesor sea/coastlines~~both land and coastlines. In that case, we can easily discriminate between land and coastlines ~~or sea and coastlines~~ by applying the land/~~ocean/~~coastlines filters. Consequently, this particular pixel will be flagged both as land and coastlines~~or sea and coastlines~~.

Over land, during the growing phase of the convection, Prec and Flash start to increase at the same time (10:00 LT – 12:00 LT) but Flash reaches a maximum earlier (15:00 LT – 16:00 LT) than Prec (17:00 LT – 18:00 LT). This is consistent with the finding of Liu and Zipser (2008) over the whole tropics. Different maximum times could come from the fact that, while the deep convective activity intensity starts to decrease with the number of flashes, Prec is still high during the dissipating stage of

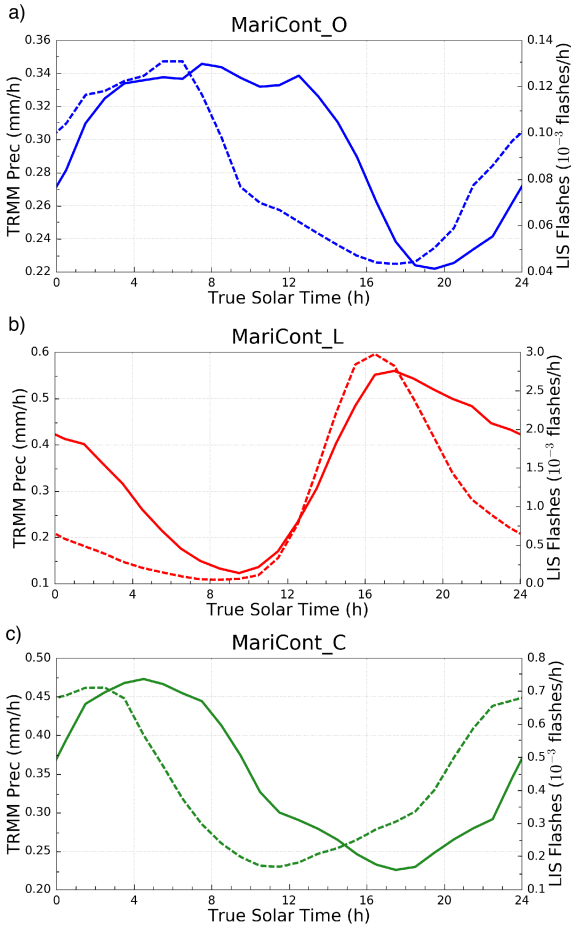

Figure 7. Diurnal cycle of Prec (solid line) and diurnal cycle of Flash (dashed line) over MariCont_L (~~top~~a), MariCont_C (~~middle~~b) and MariCont_O (~~bottom~~c).

the convection and takes longer ~~times~~ to decrease than Flash. Consequently, combining our results with the ones presented in **?**, Flash and Prec can be considered as good proxies of deep convection during the growing phase of the convection over the MariCont_L.

Over coastlines (Fig. **??**~~c~~b), the Prec diurnal cycle is delayed by about +2 to 7 h with respect to the Flash diurnal cycle. Prec minimum is around 18:00 LT while Flash minimum is around 11:30 LT. Maxima of Prec and Flash are found around 04:00 LT and 02:00 LT, respectively. This means that the increasing phase of Flash is 2-3 h longer than that of Prec. These results are consistent with the work of **?** showing a diurnal maximum of precipitation in the early morning between 02:00 LT and 03:00 LT and a diurnal minimum of precipitation ~~around~~ between 11:00 LT and 21:00 LT, over coastal zones of Sumatra. According

to **?** and **?**, coastal zones are areas where precipitation results more from convective activity than from stratiform activity and the amplitude of diurnal maximum of Prec decreases with the distance from the coastline.

Over offshore areas (Fig. **??**~~b~~c), minima of diurnal cycle of Prec and diurnal cycle of Flash are in the late afternoon, between 16:00 LT and 17:00 LT (Flash) and 17:00 LT and 18:00 LT (Prec), whilst maxima of diurnal cycle of Prec and Flash are reached in the early morning, between 06:00 LT and 07:00 LT (Flash) and around 08:00 LT – 09:00 LT (Prec). Results over offshore areas are consistent with diurnal cycle of Flash and Prec calculated by **?** over the whole tropical ocean, showing the increasing phase of the diurnal cycle of Flash starting 1–2 hours before the increasing phase of the diurnal cycle of Prec.

The time of transition from maximum to minimum of Prec is always longer than that of Flash. The period after the maximum of Prec is likely more representative of stratiform rainfall than deep convective rainfall. ~~Consistently~~Consistent with that picture, model results from **?** have shown the suppression of ~~the~~ deep convection over ~~offshore area in West~~ the offshore area west of Sumatra from the early afternoon due to ~~downwelling wavefront highlighted~~ a downwelling wavefront characterized by deep warm anomalies around noon. According to the authors, later in the afternoon, gravity waves are forced by the stratiform heating profile and propagate slowly offshore. They also highlighted that the diurnal cycle of the offshore convection responds strongly to the gravity wave forcing at the horizontal scale of 4 km. To summarize, diurnal cycles of Prec and Flash show that:
i) over land, Flash increases proportionally with Prec during the growing phase of the convection,
ii) over coastlines, Flash increasing phase is ~~advanced by~~ more than 6–7 hours ~~compared to~~ ahead of Prec increasing phase,
iii) over offshore areas, Flash increasing phase is ~~advanced by~~ about 1–2 hours ~~compared to~~ ahead of Prec increasing phase.

In section **??**, we investigate whether this time difference impacts the estimation of ΔIWC over land, coasts, and offshore areas.

5.3 Prec and Flash diurnal cycles and small-scale processes

In this subsection, we study the diurnal cycle of Prec and Flash at $0.25° \times 0.25°$ resolution over areas of deep convective activity over the MariCont. In line with the distribution of large value of Prec (Fig. **??**), IWC^{MLS} (Fig. **??**) and ΔIWC (Fig. **??**), we have selected five islands and five seas over the MariCont. Diurnal cycles of Prec and Flash are presented over land for a) Java, b) Borneo, c) New Guinea, d) Sulawesi and e) Sumatra as shown in Figure **??** and over sea for the a) Java Sea, b) North Australia Sea (NAusSea), c) ~~Bismark~~ Bismarck Sea, d) West Sumatra Sea (WSumSea) and e) China Sea as shown in Figure **??**. Diurnal cycles of IWC from ERA5 (IWC^{ERA5}) are also presented in ~~Fig~~Figs. 8 and 9 and will be discussed in Section 6.

Over land, the amplitude of the diurnal cycle of Prec is the largest over Java (Fig. **??**a), consistent with **?**, with a maximum reaching 1 mm h^{-1}, while, over the other areas, maxima are between 0.4 and 0.6 mm h^{-1}. Furthermore, over Java, the duration of the increasing phase in the diurnal cycle of Prec is ~~6 h~~ 6 h, consistent with that of Flash~~and elsewhere,~~ , whereas elsewhere the duration of the increasing phase is longer in Prec than in Flash by 1–2 h. The particularity of Java is related to the increasing phase of the diurnal cycle of Prec (6 h), ~~that~~ which is faster than over all the other land areas considered in our study (7 – 8 h). The strong and rapid convective growing phase measured over Java might be explained by the fact that the island is narrow with high mountains (up to $\sim$ 2000 m of altitude, as shown in Fig. 2b) reaching the coast. The topography promotes the growth of intense and rapid convective activity. The convection starts around 09:00 LT, rapidly elevating warm air up to the top of

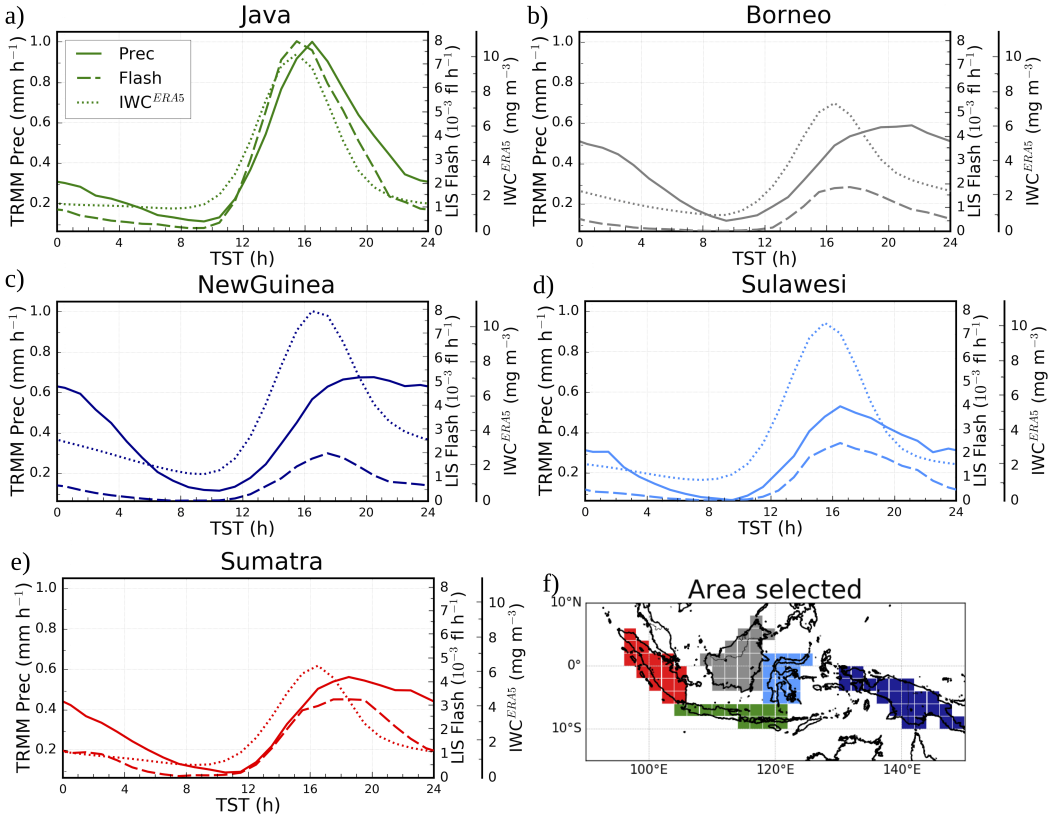

Figure 8. Diurnal cycles of Prec (solid line), Flash (dashed line) and IWC^{ERA5} from ERA5 at 150 hPa (dotted line) over MariCont islands: Java (a), Borneo (b), New Guinea (c), Sulawesi (d) and Sumatra (e) and map of the study zones over land (f).

the mountains. Around 15:00 LT, air masses cooled in altitude are transported to the sea favoring the dissipating stage of the convection. Sulawesi is also a small island with high topography as Java. However, the amplitude of the diurnal cycle of Prec and Flash is not as strong as over Java. Other islands, such as Borneo, New Guinea and Sumatra, have high mountains but also large lowland areas. Mountains promote deep convection at the beginning of the afternoon while lowlands help maintain the convective activity through shallow convection and stratiform rainfall (**??**). Deep and shallow convection are then mixed during the slow dissipating phase of the convection (from $\sim$ 16:00 LT to 08:00 LT). However, because Flash are observed only in deep convective clouds, the decreasing phase of Flash diurnal cycles decreases more rapidly than the decreasing phase of Prec. The diurnal maxima of Prec found separately over the 5 islands of the MariCont (at 0.25° $\times$ 0.25° resolution) are much higher than the diurnal maxima of Prec found over tropical land (South America, South Africa and MariCont_L, at 2° $\times$ 2° resolution) from **?**: $\sim$ 0.6 – 1.0 mm h^{-1} and $\sim$ 0.4 mm h^{-1}, respectively. However, the duration of the increasing phase of the diurnal cycle of Prec is consistent with the one calculated over tropical land by **?**.

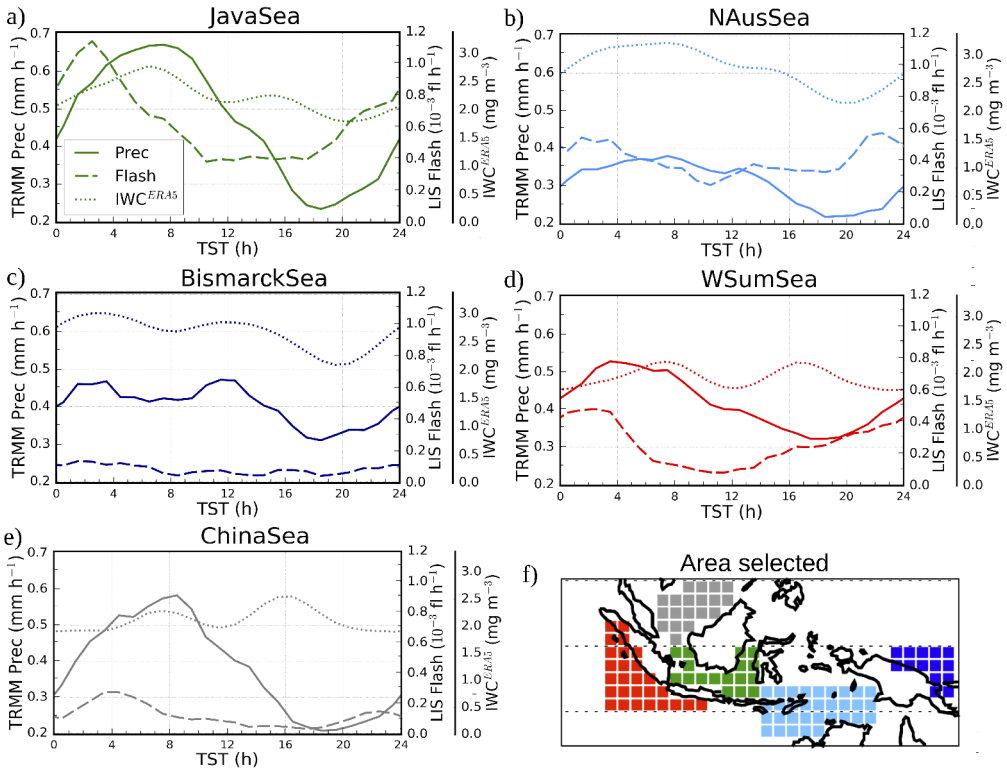

Figure 9. Diurnal cycles of Prec (solid line), Flash (dashed line) and IWC^{ERA5} from ERA5 at 150 hPa (dotted line) over MariCont seas: Java Sea (a), North Australia Sea (NAusSea) (b), ~~Bismark~~ Bismarck Sea (c), West Sumatra Sea (WSumSea) (d), China Sea (e) and map of the study zones over sea (f).

Over sea, the five selected areas (Fig. **??**a–e) show a diurnal cycle of Prec and Flash similar to that of either coastline or offshore areas depending ~~onthe area~~on the region considered. The diurnal cycle of Prec and Flash over Java Sea is similar to the one over coastlines (Fig. **??**~~e~~b). Java Sea (Fig. **??**a), an area mainly surrounded by coasts, shows the largest diurnal maximum of Prec ($\sim$ 0.7 mm h^{-1}) and Flash ($\sim$ 1.1 10^{-3} flashes h^{-1}) with the longest growing phase. In this area, land and sea breezes observed in coastal areas impact the diurnal cycle of the convection (**?**). During the night, land breeze develops from a temperature gradient between warm sea surface temperature and cold land surface temperature and conversely during the day. Over Java Sea, Prec is strongly impacted by land breezes from Borneo and Java islands (**?**), explaining why Prec and Flash reach largest values during the early morning. By contrast, NAusSea, ~~Bismark~~ Sea and WSumSea (Figs. **??**b, c and d, respectively) present small amplitude of diurnal cycle. In our analysis, these three study zones are the areas including the most offshore pixels. Java Sea and WSumSea present a similar diurnal cycle of Prec and Flash, with Flash growing phase starting

about 4 h earlier than that of Prec. China Sea also shows a diurnal maximum of Flash shifted by about 4 hours before the diurnal maximum of Prec, but the time of the diurnal minimum of Prec and Flash is similar. Over China Sea and ~~Bismark~~ Bismarck Sea, the diurnal cycle of Flash shows a weak amplitude with maxima reaching only 0.1 ~~-~~ - 0.2 10^{-3} flashes h^{-1}. Furthermore, over the ~~Bismark~~ Sea, while the diurnal minimum in Prec is around 18:00 LT, there are several local minima in Flash (08:00, 14:00 and 18:00 LT). Over NAusSea, the diurnal minimum of Prec is delayed by more than 7 hours compared to the diurnal minimum of Flash.

To summarize, over ~~island~~islands, Flash and Prec convective increasing phases start at the same time and increase similarly but the diurnal maximum of Flash is reached 1–2 hours before the diurnal maximum of Prec. Over seas, the duration of the convective increasing phase and the amplitude of the diurnal cycles are not always similar depending on the area considered. The diurnal cycle of Flash ~~is advanced by 4 hours~~ over Java Sea and West Sumatra Sea ~~and by more than 7 hours over North Australia Sea compared to~~ is 4 hours ahead of the diurnal cycle of Prec, and over North Australia Sea, it is more than 7 hours ahead. China Sea and ~~Bismark~~ Bismarck Sea present the same time of the onset of the Flash and Prec increasing phase. In Section 7, we estimate ΔIWC over the 5 selected island and sea areas from Prec and Flash as a proxy of deep convection.

6 Horizontal distribution of IWC from ERA5 reanalyses

The ERA5 ~~reanalyses provide~~ reanalysis provides hourly IWC at 150 and 100 hPa (IWC^{ERA5}). The diurnal cycle of IWC^{ERA5} over the MariCont ~~from ERA5~~ will be used to calculate ΔIWC~~from ERA5~~ ^{ERA5} in order to ~~assess~~ support the horizontal distribution and the amount of ice injected in the UT and the TL deduced from our model combining ~~MLS ice and TRMM Prec or MLS ice~~ IWC^{MLS} and TRMM-3B42 Prec or IWC^{MLS} and LIS flash. Since IWC^{ERA5} data quality has not yet been fully evaluated, this may impact on the consistency or lack of thereof found in the comparisons between ΔIWC^{ERA5} and both ΔIWC^{Prec} and ΔIWC^{Flash}. Figures **??**a, b, c and d present the daily mean and the hour of the diurnal maxima of IWC^{ERA5} at 150 and 100 hPa. In the UT, the daily mean of IWC^{ERA5} shows a horizontal distribution over the MariCont ~~consistently~~ consistent with that of IWC^{MLS} (Fig. **??**e), except over ~~NewGuinea~~ New Guinea where IWC^{ERA5} (~~reaching~~ exceeding 6.4 mg m^{-3}) is much stronger than IWC^{MLS} ($\sim$ 4.0 mg m^{-3}). The highest amount of IWC^{ERA5} is located over ~~NewGuinea~~ New Guinea mountain chain and in the West coast of North Australia (~~reaching~~ exceeding 6.4 mg m^{-3} in the UT and 1.0 mg m^{-3} in the TL). Over islands in the UT and the TL, the hour of the IWC^{ERA5} diurnal maximum is found between 12:00 LT and 15:00 LT over Sulawesi and New Guinea and between 15:00 LT and 21:00 LT over Sumatra, Borneo and Java, ~~that~~ which is close to the hour of the diurnal maximum of Flash over islands (Fig. **??**). Over sea, in the UT and the TL, the hour of the IWC^{ERA5} diurnal maximum is found between 06:00 LT and 09:00 LT over West Sumatra Sea, Java Sea, North Australia Sea, between 06:00 LT and 12:00 LT over China Sea and between 00:00 LT and 03:00 LT over ~~Bismark~~ Bismarck Sea. There are no significant differences between the hour of the maximum of IWC^{ERA5} in the UT and in the TL.

The diurnal cycles of IWC^{ERA5} at 150 hPa are presented in Figs. **??** and **??** over the selection of islands and seas of the MariCont together with the diurnal cycles of Prec and Flash. Over islands (Fig. **??**), the maximum of the diurnal cycle of IWC^{ERA5} is found between 16:00 LT and 17:00 LT, consistent with the diurnal cycle of Prec and Flash. The ~~duration~~ durations

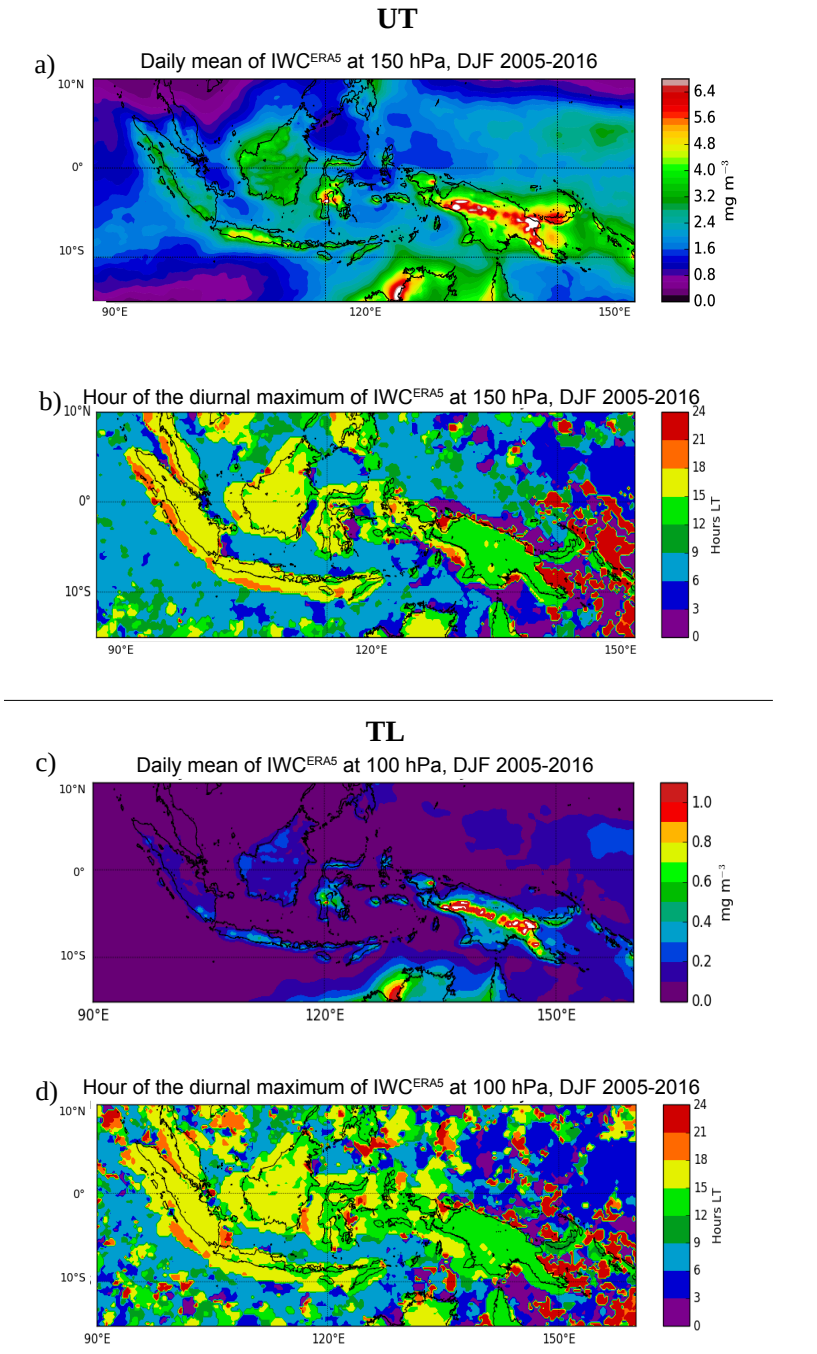

Figure 10. Daily mean of IWC^{ERA5} averaged over the period DJF 2005-2016 at 150 hPa (a) and at 100 hPa (c); Time (hour, local time (LT)) of the diurnal maximum of IWC^{ERA5} at 150 hPa (b) and at 100 hPa (d).

of the increasing phase of the diurnal cycles of Prec, Flash and IWC^{ERA5} are all consistent to each other (6 – 8 h). Over sea (Fig. **??**), the maximum of the diurnal cycle of IWC^{ERA5} is mainly found between 07:00 LT and 10:00 LT over Java Sea and North Australia Sea, ~~consistently~~ consistent with the diurnal cycle of Prec, and a second peak is found around 16:00 LT. Thus, the duration of the increasing phase of the diurnal cycles of IWC^{ERA5} is consistent with the one of Prec over these two sea study zones (∼10 hours), but not with the one of Flash. Over ~~Bismark~~ Bismarck Sea, the diurnal maxima of IWC^{ERA5} are found at 04:00 LT with a second peak later at noon. Over West Sumatra Sea, two diurnal maxima are found at 08:00 LT and 17:00 LT. Over China Sea, the diurnal maximum of IWC^{ERA5} ~~are~~ is found at 16:00 LT with a second peak at 08:00 LT. These differences in the timing of the maximum of the diurnal cycle of Prec, Flash and ~~IWCERA5~~ IWC^{ERA5} observed at small-scale over sea of the MariCont are not well understood. However, these differences do not impact on the calculation of the Δ~~IWCPrec~~IWC^{Prec}, Δ~~IWCFlash~~ IWC^{Flash} or Δ~~IWCERA5. Results are presented Section 7.~~ IWC^{ERA5}, because only the magnitude of the diurnal cycle (max-min) matters for the calculation of ΔIWC.

7 Ice injected over a selection of island and sea areas

7.1 ~~ΔIWC deduced from observations~~

Figure **??** synthesizes ΔIWC deduced from observations and reanalysis in the UT and the TL over the 5 islands and 5 seas of the MariCont studied in the previous section.

7.1 ΔIWC deduced from observations

Eqs. (1-3) are used to calculate ΔIWC from Prec (ΔIWC^{Prec}) and from Flash (ΔIWC^{Flash}). As presented in the previous section, Prec and Flash can be used as two proxies of deep convection, ~~with differences more or less accentuated~~ although differences in their diurnal cycles may be present as a function of the region considered. Thus, the observational ΔIWC range calculated between ΔIWC^{Prec} and ΔIWC^{Flash} provides an upper and lower bound of ΔIWC calculated from observational datasets. In the following, we will consider the relative difference between ΔIWC^{Prec} and ΔIWC^{Flash} as:

$$(\Delta IWC^{Prec} + \Delta IWC^{Flash}) \times 0.5 \quad (4)$$

In the UT (Fig. **??**a), over islands, ΔIWC calculated over Sumatra, Borneo, Sulawesi and New Guinea varies from 4.9 to 6.9 mg m^{-3} ~~whilst~~whereas, over Java, ΔIWC reaches 7.9–8.7 mg m^{-3}. ΔIWC^{Flash} is generally greater than ΔIWC^{Prec} by

~~less than 1.0~~ 0.8 mg m^{-3} (~~((~~ΔIWC^{Flash} with $r^{Prec-Flash}$ ranges from - ~~ΔIWC^{Prec})/ΔIWC^{Flash})×100 ranges from 4 to~~ 6 to - 22% over the study zone) for all the islands, except for Java where ΔIWC^{Prec} is larger than ΔIWC^{Flash} by ~~0.7~~ 0.8 mg m^{-3} (~~-8~~$r^{Prec-Flash}$ = 7.1%). Over sea, ΔIWC varies from 1.2 to 4.4 mg m^{-3}. ΔIWC^{Flash} is greater than ΔIWC^{Prec} by 0.6 to 2.1 mg m^{-3} (~~31-50~~$r^{Prec-Flash}$ = - 35 to - 71%), except for Java Sea, where ΔIWC^{Prec} is greater than ΔIWC^{Flash} by 0.2 mg m^{-3} (~~-7~~$r^{Prec-Flash}$ = 6%). Over North Australia Sea and West Sumatra Sea, ΔIWC^{Flash} ~~is almost~~ are more than twice as large as ~~than~~ ΔIWC^{Prec} (~~53%~~ $r^{Prec-Flash}$ = - 63% and - 71%, respectively).

In the TL (Fig. **??**b), the observational ΔIWC range is found between 0.7 and 1.3 mg m^{-3} over islands and between 0.2 and 0.7 mg m^{-3} over seas. The same conclusions apply to the observational ΔIWC range calculated between ΔIWC^{Prec} and ΔIWC^{Flash} in the TL as in the UT with differences less than 0.4 mg m^{-3}.

To summarize, independently of the proxies used for the calculation of ΔIWC, and at both altitudes, Java island shows the largest injection of ice over the MariCont. Observational ΔIWC over Java island is larger by about 1.0 mg m^{-3} in the UT and about 0.3 mg m^{-3} in the TL than other land study zones. Furthermore, it has been shown that both proxies can be used in our model, with more confidence over land: ΔIWC^{Prec} and ΔIWC^{Flash} are consistent to each other to within ~~4-22% over island and 7-53% over sea~~ $r^{Prec-Flash}$ = - 6 to -22% over islands and $r^{Prec-Flash}$ = +6 to -71% over seas in the UT and the TL. The largest difference over ~~sea~~ seas is probably due to the larger contamination ~~of~~ by stratiform precipitation included in Prec over sea.

7.2 ΔIWC deduced from ~~reanalyses~~reanalysis

ΔIWC from ERA5 (ΔIWC$^{ERA5}_{z_0}$) is calculated in the UT and the TL (z_0 = 150 and 100 hPa, respectively) as the max–min difference in the amplitude of the diurnal cycle. ~~Consistently with the MLS observations, we have degraded the ERA5 vertical resolution~~ We can use the IWC^{ERA5} to assess the impact of the vertical resolution ~~on~~ of the MLS measurements on the observationally-derived ΔIWC ^{ERA5}estimates. According to Wu et al. (2008), ~~IWC^{MLS} estimation~~ estimates of IWC derived from MLS represent spatially-averaged quantities within a volume that can be approximated by a box of ~~~~ 300×7×4 km^3 near the pointing tangent height. In order to compare IWC^{MLS} and IWC^{ERA5}, ~~we degraded~~two steps were taken: 1) the horizontal resolution of ERA5 was degraded from 0.25°×0.25° to 2°×2° (~~~~ 200 km×200 km), and 2) the vertical resolution of ERA5 ~~data by connecting~~ was degraded by convolving the vertical profiles of IWC^{ERA5} with a ~~unitary~~ box function whose width is 5 and 4 km at 100 and 146 hPa, respectively.

~~Consistently with ?, we have fixed δz = 4 and 5 km at z_0 = 146 and 100 hPa, respectively.~~ The ice injected from ERA5 at z_0 = 146 and 100 hPa with degraded vertical resolution ($\langle \Delta IWC^{ERA5}_{z_0} \rangle$) is thus calculated from $\langle IWC^{ERA5}_{z_0} \rangle$. In the following we can consider the difference $r^{ERA5-\langle ERA5 \rangle}$ between ΔIWC^{ERA5} and $\langle \Delta IWC^{ERA5} \rangle$ as:

$$r^{ERA5-\langle ERA5 \rangle} = 100 \times \frac{\Delta IWC^{ERA5} - \langle \Delta IWC^{ERA5} \rangle}{(\Delta IWC^{ERA5} + \langle \Delta IWC^{ERA5} \rangle) \times 0.5} \quad (5)$$

Figure **??** shows ~~ΔIWC^{ERA5}~~ $\Delta IWC^{ERA5}_{z_0}$ and $\langle \Delta IWC^{ERA5}_{z_0} \rangle$ at z_0 = 150 and 100 hPa, over the island and the sea study zones. In the UT (Fig. **??**a), over islands, ΔIWC^{ERA5}_{150} and $\langle \Delta IWC^{ERA5}_{150} \rangle$ calculated over Sumatra and Borneo vary

from 4.9 to 7.0 mg m^{-3} (~~the relative variation calculated as $((\Delta IWC^{ERA5} - \langle \Delta IWC^{ERA5} \rangle)/\Delta IWC^{ERA5}) \times 100$ is 18-19~~ $r^{ERA5-\langle ERA5 \rangle}$ ranges from 20 to 22 %) whilst ΔIWC_{150}^{ERA5} and $\langle \Delta IWC_{150}^{ERA5} \rangle$ over Java, Sulawesi and New Guinea reach 7.5–10.0 mg m^{-3} (~~~19-22 %of variability per study zone~~$r^{ERA5-\langle ERA5 \rangle}$ = 21 to 24 %). Over sea, ΔIWC_{150}^{ERA5} and $\langle \Delta IWC_{150}^{ERA5} \rangle$ vary from 0.35 to 1.1 mg m^{-3} ($r^{ERA5-\langle ERA5 \rangle}$ = 9 ~~– 32 %of variability per study zone~~to 33 %). Over island and sea, ΔIWC_{150}^{ERA5} is greater than $\langle \Delta IWC_{150}^{ERA5} \rangle$. The small differences between ΔIWC_{150}^{ERA5} and $\langle \Delta IWC_{150}^{ERA5} \rangle$ over island and sea in the UT support the fact that the vertical resolution at 150 hPa has a low impact on the estimated ΔIWC.

In the TL, over land, ΔIWC_{100}^{ERA5} and $\langle \Delta IWC_{100}^{ERA5} \rangle$ vary from 0.5 to ~~3.7~~ 3.9 mg m^{-3} (~~~68%of variability per study zone~~$r^{ERA5-\langle ERA5 \rangle}$ = -32 to -138%) with $\langle \Delta IWC_{100}^{ERA5} \rangle$ being larger than ΔIWC_{100}^{ERA5} by less than ~~2.1~~ 2.5 mg m^{-3}. Over sea, ΔIWC_{100}^{ERA5} and $\langle \Delta IWC_{100}^{ERA5} \rangle$ vary from 0.05 to 0.4 mg m^{-3} (~~~71 %of variability per study zone~~$r^{ERA5-\langle ERA5 \rangle}$ = -85 to -139%) with ΔIWC_{100}^{ERA5} lower than $\langle \Delta IWC_{100}^{ERA5} \rangle$ by ~~less than~~ as much as 0.2 mg m^{-3}. The large differences between ΔIWC_{100}^{ERA5} and $\langle \Delta IWC_{100}^{ERA5} \rangle$ over island and sea in the TL support the fact that the vertical resolution at 100 hPa has a high impact on the estimation of ΔIWC.

7.3 Synthesis

The comparison between the observational ΔIWC range and the reanalysis ΔIWC range is presented in Fig. **??**. In the UT, over land, observation and reanalysis ΔIWC ranges ~~overlap (~~agree to within 0.1 to 1.0 mg m^{-3}~~)~~, which highlights the robustness of our model over land, except over Sulawesi and New Guinea, where the observational ~~ΔIWC range~~ and the reanalysis ΔIWC range differ by at least 1.7 and 0.7 mg m^{-3}, respectively~~)~~. Over sea, the observational ΔIWC range is systematically greater than the reanalysis ~~ΔIWC range~~ by ∼ 1.0 – 2.2 mg m^{-3}~~(75 %)~~, showing a systematic ~~positive bias and a too large variability range in our model over sea compared to ERA5. Combining~~ larger estimate derived from observation than derived from reanalysis. The consistency between observational and reanalysis ΔIWC range is calculated as the difference between the minimal value of the largest range minus the maximum value of the lowest range divided by the mean of these two values. In the UT, over land, observational and reanalysis ΔIWC are found consistent to within 0 to 25% while over sea they are inconsistent (to within 62 to 96%) in the UT. In the TL, observational and reanalysis ~~ranges, the total ΔIWC variation range~~ΔIWC ranges are consistent to within 0 to 49% over land and to within 0 to 28% over sea. In the following we will consider r^{Total} as the relative differences between the minimal value of the lower range minus the maximum value of the largest range divided by the mean of these two values. The range between observational and reanalysis ranges is named the total IWC range, and is estimated in the UT between 4.2 and 10.0 mg m^{-3} (~~~ 20 %of variability per study zone~~r^{Total} from 8 to 59%) over land and between 0.3 and 4.4 mg m^{-3} (~~~ 30 %of variability per study zone~~r^{Total} from 104 to 149%) over sea and, in the TL, between ~~0.6 and 3.9~~ 0.5 and 3.7 mg m^{-3} (~~~ 70 %of variability per study zone~~r^{Total} = 85 to 127%) over land, and between 0.1 and 0.7 mg m^{-3} (~~~ 80 %of variability per study zone~~r^{Total} = 142 to 160%) over sea.

~~The amounts~~

Amounts of ice injected ~~in the UT~~ deduced from observations and reanalysis are consistent to each other over ~~MariCont_L, Sumatra, Borneo and Java, with significant differences over Sulawesi, New Guinea (within 1.7 to 0.7 mg m^{-3}, respectively) and all individual offshore study zones (within 0.7 to 2.1 mg m^{-3}). The~~ land in the UT and over land and sea in the TL

(to within 0 to 49%) but inconsistent over sea in the UT (up to 96%). However, the impact of the vertical resolution on the estimation of ΔIWC is much larger in the UT than in the TL (r^{Total} is larger in the TL ~~is certainly non negligible, with larger ΔIWC variability range in the TL (70 – 80 %)~~ than in the UT~~(20 – 30 %)~~). At both levels, observational and reanalyses ΔIWC estimated over land is more than twice as large as ΔIWC estimated over sea. ~~Finally,~~ Java island presents the highest observational and reanalysis ΔIWC range in the UT (between 7.7 and 9.5 mg m^{-3} daily mean, r^{Total} = 21%). However, whatever the level considered, although Java has shown particularly high values in the observational ΔIWC range compared to other study zones, the reanalysis ΔIWC range shows that Sulawesi and ~~NewGuinea~~ New Guinea would also be able to reach similar high values of ΔIWC as Java (assuming that ERA5 IWC data have not yet been evaluated).

8 Discussion on small-scale convective processes impacting ΔIWC over a selection of areas

Our results have shown that, in all the datasets used, Java island and Java Sea are the two areas with the largest amount of ice injected up to the UT and the TL over the MariCont land and sea, respectively. In this section, processes impacting ΔIWC in the different study zones are discussed.

8.1 Java island, Sulawesi and New Guinea

Sulawesi, New Guinea and particularly Java island have been shown as the areas of the largest ΔIWC in the UT and TL. **?** have used high resolution observations and regional climate model simulations to show the three main processes impacting the diurnal cycle of rainfall over the Java island. The main process explaining the rapid and strong peak of Prec during the afternoon over Java (Fig. **??**a) is the sea-breeze convergence around midnight. This convergence caused by sea-breeze phenomenon increases the deep convective activity and impacts on the diurnal cycle of Prec and on the IWC injected up to the TL by amplifying their quantities. The second process is the mountain-valley wind converging toward the mountain peaks, and reinforcing the convergence and the precipitation. The land breeze becomes minor compared to the mountain-valley breeze and this process is amplified with the mountain altitude. As shown in Fig. **??**b, ~~NewGuinea~~ New Guinea has the highest mountain chain of the MariCont. The third process shown by **?** is precipitation that is amplified by the cumulus merging processes which ~~is~~ are processes more important over small islands such as Java (or Sulawesi) than over large islands such as Borneo or Sumatra. Another process is the interaction between sea-breeze and precipitation-driven cold pools that generates lines of strong horizontal moisture convergence (**?**). Thus, IWC is increasing proportionally with Prec consistent with the results from **?** and rapid convergence combined with deep convection transports elevated amounts of IWC at 13:30 LT (Fig. **??**) producing high ΔIWC during the growing phase of the convection (Fig. **??** and Fig. **??**) over Java Island.

8.2 West Sumatra Sea

In section **??**, it has been shown that the West Sumatra Sea is an area with positive anomaly of Prec during the growing phase of the convection but negative anomaly of IWC, which differs from other places. These results suggest that Prec is representative not only of convective precipitation but also of stratiform precipitation. The diurnal cycle of stratiform and

convective precipitations over West Sumatra Sea has been studied by **?** using 3 years of TRMM precipitation radar (PR) datasets, following the ~~2A23Algorithm~~ 2A23 Algorithm (Awaka, 1998). ~~The authors~~ **?** have shown that rainfall over Sumatra is characterized by convective activity with a diurnal maximum between 15:00 LT and 22:00 LT while, over the West Sumatra Sea, the rainfall type is convective and stratiform, with a diurnal maximum during the early morning (as observed in Fig. **??**). Furthermore, their analyses have shown a strong diurnal cycle of 200-hPa wind, humidity and stability, consistent with the PR over ~~Sumatra West~~ West Sumatra Sea and Sumatra Island. Stratiform and convective clouds are both at the origin of heavy rainfall in the tropics (**??**) and in the West Sumatra Sea, but stratiform clouds are mid-altitude clouds in the troposphere and do not transport ice up to the tropopause. Thus, over the West Sumatra Sea, the calculation of ΔIWC estimated from Prec is possibly overestimated because Prec include a non-negligible amount of stratiform precipitation over this area.

8.3 North Australia Sea and seas with nearby islands

The comparisons between Figs. 2c and 6a have shown strong daily mean of Flash (10~~−2~~ $^{-2}$ –10~~−1 flashes day−1~~ $^{-1}$ flashes day^{-1}) but low daily mean of Prec (2.0 – 8.0 mm day~~−1~~$^{-1}$) over the North Australia Sea. Additionally, Fig. 11 shows that the strongest differences between ΔIWC^{Prec} and ΔIWC^{Flash} are found over the North Australia Sea, with ΔIWC^{Flash} greater than ΔIWC^{Prec} by 2.3 mg m~~−3~~ $^{-3}$ in the UT ($r^{Prec-Flash}$ = ~71%) and by 0.4 mg m~~−2~~ $^{-3}$ in the TL (~~53%of variability between ΔIWC^{Flash} and ΔIWC^{Prec}~~ $r^{Prec-Flash}$ = - 75%). These results imply that the variability range in our model is too large ~~and highlight~~ highlighting the difficulty to estimate ΔIWC over this study zone. Furthermore, as for Java Sea or Bismarck Sea, North Australia Sea ~~has the particularity to be surrounding~~ is surrounded by several islands. According to the study from **?**, the cloud size is the largest during the afternoon over the North Australia land, during the night over North Australia coastline and during the early morning over the North Australia sea. These results suggest that deep convective activity moves from the land to the sea during the night. Over the North Australia Sea, it seems that the deep convective clouds are mainly composed ~~by~~ of storms with lightning but ~~precipitationd are weak or do~~ precipitation is weak or does not reach the surface ~~and evaporating before .~~ before evaporating.

9 Conclusions

The present study has combined observations of ice water content (IWC) measured by the Microwave Limb Sounder (MLS), precipitation (Prec) from the algorithm 3B42 of the Tropical Rainfall Measurement Mission (TRMM), the number of flashes (Flash) from the Lightning Imaging Sensor (LIS) on board of TRMM with IWC provided by the ERA5 reanalyses in order to estimate the amount of ice injected (ΔIWC) in the upper troposphere (UT) and the tropopause level (TL) over the MariCont, from the method proposed in a companion paper (**?**). ~~ΔIWC is firstly calculated using the IWC measured by MLS (IWC^{MLS}) in~~ The study is focused on the austral convective season of DJF from 2004 to ~~2017 at the temporal resolution of 2 observations per day and Prec fromTRMM-3B42 during the same period, to obtain a 1-hour resolution diurnal cycle.~~ 2017. In the model used (**?**), Prec is considered as a proxy of deep convection ~~impacting~~ injecting ice (ΔIWC^{Prec}) in the UT and the TL. ΔIWC^{Prec} is firstly calculated by the correlation between the growing phase of the diurnal cycle of Prec from TRMM-3B42 (binned at a

1-hour diurnal cycle) and the value of IWC measured by MLS (IWC^{MLS}, provided at the temporal resolution of 2 observations in local time per day) selected among the growing phase of the diurnal cycle of Prec. While ? have calculated ΔIWC^{Prec} over large convective study zones in the tropics, we show the spatial distribution of ΔIWC^{Prec} ~~into~~ in the UT and the TL at 2° × 2° horizontal resolution over the MariCont, highlighting local areas of strong injection of ice up to 20 mg m^{-3} in the UT and up to 3 mg m^{-3} in the TL. ΔIWC injected in the UT and the TL has also been evaluated by using another proxy of deep convection: Flash measured by TRMM-LIS. Diurnal cycle of Flash has been compared to diurnal cycle of Prec, showing consistencies in 1) the spatial distribution of Flash and Prec over the MariCont (maxima of Prec and Flash located over land and coastline), and 2) their diurnal cycles over land (similar onset and duration of the diurnal cycle increasing phase). Differences have been mainly observed over sea and coastline areas, with the onset of the diurnal cycle increasing phase of Prec delayed by several hours depending on the considered area (from 2 to 7 h) compared to Flash. ΔIWC calculated by using Flash as a proxy of deep convection (ΔIWC^{Flash}) is compared to ΔIWC^{Prec} over five islands and five seas of the MariCont to establish an observational ΔIWC range over each study zone. ΔIWC is also estimated from IWC provided by the ERA5 reanalyses (ΔIWC^{ERA5} and IWC^{ERA5}, respectively) at 150 and 100 hPa over the study zones. We have also degraded the vertical resolution of IWC^{ERA5} to be consistent with that of IWC^{MLS} observations: 4 km at 146 hPa and 5 km at 100 hPa. The ΔIWC ranges calculated from observations and reanalyses were evaluated over the selected study zones (island and sea).

With the study of ΔIWC^{Prec}, results show that the largest amounts of ice injected in the UT and TL per 2° × 2° pixels are related to i) an amplitude of Prec diurnal cycle larger than 0.5 mm h^{-1} ~~, ii) values of IWC measured during the growing phase of the convection larger than 4.5 mg m^{-3} and iii)~~ and ii) a duration of the growing phase of the convection longer than 9 hours. The largest ΔIWC^{Prec} has been found over areas where the convective activity is the deepest. ~~The observational~~ ΔIWC~~range calculated between ΔIWC^{Prec}~~ and ΔIWC^{Flash} ~~has been found to be within 4 – 22~~ depart from -6 to -22 % over land and to ~~within 7 – 53~~ -6 to -71 % over sea. The largest differences between ΔIWC^{Prec} and ΔIWC^{Flash} over sea might be due to the combination of the presence of stratiform precipitation included ~~into~~ in Prec and the very low values of Flash over seas (<10^{-2} flashes day^{-1}). The diurnal cycle of IWC^{ERA5} at 150 hPa is more consistent with that of Prec and Flash over land than over ocean. Finally, ~~the observational~~ ΔIWC ~~range~~ estimated from observations has been shown to be consistent with ~~the reanalysis~~ ΔIWC ~~range to within 23~~ estimated from reanalysis to within 25% over land ~~and to within 30-50 % over sea in the UT~~ in the UT, to within 48 % over land in the TL and to within ~~49 % over land and to within 39~~ 28 % over sea in the TL, but inconsistent to within 96 % over sea in the ~~TL~~UT. Thus, thanks to the combination ~~between~~ of the observational and reanalysis ΔIWC ranges, the total ΔIWC ~~variation~~ range has been found in the UT to be between 4.2 and 10.0 mg m^{-3} ~~(to within 20 % per study zones)~~ over land and between 0.3 and 4.4 mg m^{-3} ~~(to within 30 % per study zones)~~ over sea and, in the TL, between ~~0.6 and 3.9~~ 0.5 and 3.7 mg m^{-3} ~~(to within 70 % per study zones)~~ over land and between 0.1 and 0.7 mg m^{-3} ~~(to within 80% per study zones)~~ over sea. The ~~ΔIWC variation range in the TL is larger than that in the UT highlighting the stronger~~ impact of the vertical resolution ~~in the observations~~ on the estimation of ΔIWC has been found higher in the TL ~~compared to~~ than in the UT.

The study at small scale over islands and seas of the MariCont has shown that ΔIWC from ERA5, Prec and Flash in the UT agree to within ~~0~~ 0.1 – ~~0.6~~ 1.0 mg m^{-3} ~~(8%)~~ over MariCont_L, Sumatra, Borneo and Java with the largest values obtained

over Java ~~. However, while Java~~ Island. Based on observations, the Java Island presents the largest amount of ~~ΔIWC^{Prec} and ΔIWC^{Flash}~~ ice in the UT and the TL (larger by about 1.0 mg m^{-3} in the UT and about 0.3 mg m^{-3} in the TL than other land study zones). Based on the reanalysis, New Guinea and Sulawesi reach similar ranges of ~~values of ice injected with ERA5 thanJava~~ ice injection in the UT and even larger ranges of values ~~as Java~~ in the TL than the Java Island keeping in mind that ERA5 IWC data have not yet been evaluated. Processes related to the strongest amount of ΔIWC injected into the UT and the TL have been identified as the combination of sea-breeze, mountain-valley breeze and merged cumulus, ~~such as over NewGuinea and~~ accentuated over small islands with high topography such as Java or Sulawesi.

Author contributions. IAD analysed the data, formulated the model and the method combining MLS, TRMM and LIS data and took primary responsibility for writing the paper. CD has treated the LIS data, provided the Figures with Flash datasets, gave advices on data processing and contributed to the Prec and Flash comparative analysis. PR strongly contributed to the design of the study, the interpretation of the results and the writing of the paper. PR, FC, PH and TD provided comments on the paper and contributed to its writing.

Acknowledgements. We thank the National Center for Scientific Research (CNRS) and the Excellence Initiative (Idex) of Toulouse, France to fund this study and the project called Turbulence Effects on Active Species in Atmosphere (TEASAO – http://www.legos.obs-mip.fr/projets/axes-transverses-processus/teasao, last access: May 2020, Peter Haynes Chair of Attractivy). We would like to thank the teams that have provided the MLS data (https://disc.gsfc.nasa.gov/datasets?page=1&keywords=ML2IWC_004, last access: ~~June 2019~~May 2020), the TRMM data (https://pmm.nasa.gov/data-access/downloads/trmm), the LIS data (https://ghrc.nsstc.nasa.gov/lightning/data/data_lis_trmm.html, last access: ~~June 2019) ,~~ May 2020) and the ERA5 Reanalysis data (https://cds.climate.copernicus.eu/cdsapp#!/dataset/reanalysis-era5-pressure-levels-monthly tab=form, last access: ~~June 2019), and the NCEP Reanalysis data provided by the NOAA/OAR/ESRL PSD, Boulder, Colorado, USA, (, last access: June 2019).~~ May 2020). We would like to thank both reviewers for their helpful comments and especially Michelle Santee for the many very detailed comments she provided that were invaluable in improving the study.

Main acronyms list

ΔIWC: Amount of ice injected by deep convection up to the study pressure level
ΔIWC^{Prec}: ΔIWC estimated from Prec and from IWC^{MLS}
ΔIWC^{Flash}: ΔIWC estimated from Flash and from IWC^{MLS}
ΔIWC^{ERA5}: ΔIWC estimated from ERA5 reanalysis
$\langle \Delta IWC^{ERA5} \rangle$: ΔIWC^{ERA5} degraded along the vertical at the study pressure level consistently with the MLS vertical resolution of IWC^{MLS}
DJF: December, January, February
Flash: number of Flashes
IWC: Ice water content

IWC^{ERA5}: IWC from ERA5 reanalysis

IWC^{MLS}: IWC measured by MLS

LS: Lower stratosphere

MariCont: Maritime Continent

MariCont_C: Coastlines of the Maritime Continent

MariCont_O: Maritime Continent ocean

MariCont_L: Maritime Continent land

MLS: Microwave Limb Sounder

NAuSea: North Australia Sea

Prec: Precipitation

TTL: Tropical tropopause Layer

UT: Upper troposphere

UTLS: Upper troposphere and lower stratosphere

WSumSea: West Sumatra Sea

WV: Water vapour

References

J. Awaka. Awaka, J.: Algorithm 2A23 —. Rain type classification. In Proc. Symp. on the Precipitation Observation from Non-Sun Synchronous Orbit, pages 215–220, 1998.

Carbone, R. E.Carbone, , Wilson, J. W.Wilson, , Keenan, T. D. Keenan, and and Hacker, J. M.Hacker. : Tropical island convection in the absence of significant topography. part i: Life , part I: life cycle of diurnally forced convection. Monthly weather review, 128(10):3459–3480, 2000.

L.Chappel.

Chappel, L.: Assessing severe thunderstorm potential days and storm types in the tropics. In Presentation at the International Workshop on the Dynamics and Forecasting of Tropical Weather Systems, Darwin, 22-26 January 2001, 2001.

Christian, H. J. , Blakeslee, R. J., Goodman, S. J.: Lightning Imaging Sensor (LIS) for the international space station. In American Institute of Physics Conference Proceedings, Vol. 504, No. 1, pp. 423-428, 2000.

T. Dauhut, J.-P. Dauhut, T. ,Chaboureau, J.Escobar, and P. Mascart. -P. , Escobar, J. and Mascart, P.: Giga-LES of hector the convector Hector the Convector and its two tallest updrafts up to the stratosphere. Journal of the Atmospheric Sciences, 73(12):5041–5060, 2016.

T. Dauhut, Dauhut, T. , Chaboureau, J.-P.Chaboureau, P. Mascart, and T. Lane. , Mascart, P. and Lane, T.: The overshoots that hydrate the stratosphere in the tropics. In EGU General Assembly Conference Abstracts, volume 20, page 9149, 2018.

Dion, I.-A.Dion, P. , Ricaud, P. Haynes, F. Carminati, and T. Dauhut. , Haynes, P. , Carminati, F. and Dauhut, T.: Ice injected into the tropopause by deep convection – part 1: In in the austral convective tropics. Atmospheric Chemistry and Physics, 19(9):6459–6479, 2019.

Duncan, D., Eriksson, P.: An update on global atmospheric ice estimates from observations and reanalyses. In EGU General Assembly Conference Abstracts (Vol. 20, p. 13448), 2018.

S. Fueglistaler, Fueglistaler, S., Dessler, A. E.Dessler, , Dunkerton, T. J.Dunkerton, I. Folkins, Q.Fu, and Folkins, I., Fu, Q. and Mote, P. W.Mote. : Tropical tropopause layer. Reviews of Geophysics, 47(1), 2009a. doi: 10.1029/2008RG000267. URL https://agupubs.onlinelibrary. wiley.com/doi/abs/10.1029/2008RG000267. , 2009a.

Geer, A. J.Geer, F. Baordo, N. Bormann, P. Chambon, , Baordo, F., Bormann, N., Chambon, P., English, S. J. English, M. Kazumori, ... C. Lupu. , Kazumori, M. et al.: The growing impact of satellite observations sensitive to humidity, cloud and precipitation. Quarterly Journal of the Royal Meteorological Society, 143(709), 3189-3206, 2017.

R. Goler, Goler, R., Reeder, M. J.Reeder, , Smith, R. K.Smith, H. Richter, S.Arnup, T.KeenanRichter, P.May, and J. Hacker. H., Arnup, S., Keenan, T., May, P. and Hacker, J.: Low-level convergence lines over North Eastern australia. part i: The Australia. part I: the North Australian cloud line. Monthly weather review, 134(11):3092–3108, 2006.

H. Hatsushika and K. Yamazaki. Interannual Hatsushika, H. and Yamazaki, K.: Inter-annual variations of temperature and vertical motion at the tropical tropopause associated with ENSO. Geophysical research letters, 28(15):2891–2894, 2001.

H. Hersbach. Hersbach, H.:Operational global reanalysis: progress, future directions and synergies with NWP. European Centre for Medium Range Weather Forecasts, 2018.

Houze, R. A. Houze and and Betts, A. K.Betts. : Convection in gate. Reviews of Geophysics, 19(4):541–576, 1981.

Huffman, G. J. Huffman, ,Bolvin, D. T.Bolvin, , Nelkin, E. J.Nelkin, , Wolff, D. B.Wolff, , Adler, R. F.Adler, G. Gu, Y. Hong, , Gu, G., Hong, Y., Bowman, K. P. Bowman, and and Stocker, E. F.Stocker. The TRMM multisatellite : The TRMM multi-satellite precipitation analysis (TMPA): quasi-global, multiyear, combined-sensor precipitation estimates at fine scales. Journal of hydrometeorology, 8(1):38–55, 2007.

Huffman, G. J., Adler, R. F., Bolvin, D. T., Nelkin, E. J.Jensen: The TRMM Multi-satellite Precipitation Analysis (TMPA) in Satellite rainfall applications for surface hydrology. Springer, Dordrecht, 3-22, 2010.

Huffman, G. J., Bolvin, D. T.: Real-time TRMM Multi-satellite Precipitation Analysis data set documentation. Available online: URL https://gpm.nasa.gov/sites/default/files/document_files/3B4XRT_doc_V7_180426.pdf (last access: April 2020).

Jensen, E. J., Ackerman, A. S.Ackerman, , Smith, J. A.Smith (2007). : Can overshooting convection dehydrate the tropical tropopause layer?. Journal of Geophysical Research: Atmospheres, 112(D11), 2007.

C. Liu and Liu, C. and Zipser, E. J.Zipser. : Global distribution of convection penetrating the tropical tropopause. Journal of Geophysical Research: Atmospheres, 110(D23), 2005.

C. Liu and Liu, C. and Zipser, E. J.Zipser. : Diurnal cycles of precipitation, clouds, and lightning in the tropics from 9 years of TRMM observations. Geophys. Res. Lett., 35, L04819, doi:10.1029/2007GL032437, 2008.

Livesey, N. J., Read, W. G., Wagner, P. A., Froidevaux, L., Lambert, A., Manney, G.L., Millan, L.F., Pumphrey, H. C., Santee, M. L., Schwartz, M. J., Wang, S., Fuller, R. A., Jarnot, R. F., Knosp, B. W., Martinez, E. , and Lay, R. R.,: Version 4.2x Level 2 data quality and description doc-umentdocument, Tech. Rep. JPL D-33509 Rev. D, Jet Propulsion Laboratory, available at:http://mls.jpl.nasa.gov (last access: 01 09 2019), 2018.

P. Lopez. Lopez, P.: Direct 4D-Var assimilation of NCEP stage IV radar and gauge precipitation data at ECMWF. Monthly Weather Review, 139(7), 2098-2116, 2011.

Love, B. S.Love, , Matthews, A. J. Matthews, and and Lister, G. M. S.Lister. : The diurnal cycle of precipitation over the maritime continent Maritime Continent in a high-resolution atmospheric model. Quarterly Journal of the Royal Meteorological Society, 137(657):934–947, 2011.

L. Millán, L., Read, W.Read, , Kasai, Y.Kasai, A.Lambert, N. Livesey, , Lambert, A, Livesey, N., Mendrok, J.Mendrok, , Sagawa, H.Sagawa, , Sano, T.Sano, M.Shiotani, and , Shiotani, M. and Wu, D. L.Wu. Smiles : SMILES ice cloud products. Journal of Geophysical Research: Atmospheres, 118(12):6468–6477, 2013.

S. Mori, H. Jun-Ichi, Mori, S., Jun-Ichi, H., Tauhid, Y. I.Tauhid, , Yamanaka, M. D.Yamanaka, N. Okamoto, F.Murata, N.SakuraiOkamoto, H.Hashiguchi, and T. Sribimawati. N., Murata, F., Sakurai, N., Hashiguchi, H. and Sribimawati, T.: Diurnal land–sea rainfall peak migration over Sumatera Sumatra island, Indonesian Maritime Continent, observed by TRMM satellite and intensive rawinsonde radio sonde soundings. Monthly Weather Review, 132(8):2021–2039, 2004.

Nesbitt S. W. Nesbitt and and Zipser, E. J.Zipser. : The diurnal cycle of rainfall and convective inten- sity intensity according to three years of trmm TRMM measurements. Journal of Climate, 16(10):1456–1475, 2003.

Petersen, W. A. Petersen, and and Rutledge, S. A.Rutledge. : Regional variability in tropical convection: Observations observations from TRMM. Journal of Climate, 14(17), 3566-3586, 2001.

M. Pope, C. Jakob, and Pope, M, Jakob, C. and Reeder, M. J.Reeder. : Convective systems of the north australian North Australian monsoon. Journal of Climate, 21(19):5091–5112, 2008.

Qian, J.-H.Qian. : Why precipitation is mostly concentrated over islands in the maritime continentMaritime Continent. Journal of the Atmospheric Sciences, 65(4):1428–1441, 2008.

Ramage, C. S.Ramage. : Role of a tropical "maritime continentMaritime Continent" in the atmospheric circulation. Mon. Wea. Rev, 96(6):365–370, 1968.

Randel, W. J.Randel, F. Wu, H. Voemel, , Wu, F., Voemel, H., Nedoluha, G. E. Nedoluha, and P. Forster. and Forster, P.: Decreases in stratospheric water vapor after 2001: Links links to changes in the tropical tropopause and the brewer-dobson Brewer-Dobson circulation. Journal of Geophysical Re- search: Atmospheres, 111(D12), 2006a.

Randel, W. J. Randel and and Jensen, E.J.Jensen. : Physical processes in the tropical tropopause layer and their roles in a changing climate. Nature Geoscience, 6:169, 2013. doi: 10.1038/ngeo1733. URL https://doi.org/10.1038/ngeo1733. , 2013.

Sherwood, S. C.Sherwood. : A stratospheric "drain" over the maritime continentMaritime Continent. Geophysical research letters, 27(5):677–680, 2000.

A. Stenke and V. Grewe. Stenke A. and Grewe, V.: Simulation of stratospheric water vapor trends: impact on stratospheric ozone chemistry. Atmospheric Chemistry and Physics, 5(5): 1257–1272, 2005.

Stephens G. L. Stephens and and Greenwald, T. J.Greenwald. : The earth's radiation budget and its rela- tion relation to atmospheric hydrology: 2. observations of cloud effects. Journal of Geophysical Research: Atmospheres, 96(D8):15325–15340, 1991.

G. Y. Yang and J. Slingo. The diurnal cycle in the tropics. Monthly Weather Review, 129(4):784–801, 2001. 129<0784:TDCITT>2.0.CO;2. doi: 10.1175/1520-0493(2001) URL https://doi.org/10.1175/1520-0493(2001)129<0784:TDCITT>2.0.CO;2.

Waters, J. W.Waters, L. Froidevaux, , Froidevaux, L., Harwood, R. S.Harwood, , Jarnot, R. F.Jarnot, , Pickett, H. M.Pickett, , Read, W. G. Read, ... and Holden, J. R.Holden (2006). The earth observing system microwave limb sounder : The Earth Observing System Microwave Limb Sounder (EOS MLS) on the Aura satellite. IEEE Transactions on Geoscience and Remote Sensing, 44(5), 1075-1092. , 2006.

Wu, D. L., Jiang, J. H., Read, W. G., Austin, R. T., Davis, C. P., Lambert, A., Stephens, G. L. and Vane, D. G., Waters, J. W.: Validation of the Aura MLS cloud ice water content measurements. Journal of Geophysical Research: Atmospheres, 113, D15, 2008.

Wu, D. L., Austin, R. T., Deng, M. et al. Comparisons of global cloud ice from MLS, CloudSat, and correlative data sets. Journal of Geophysical Research: Atmospheres, 2009, vol. 114, no D8, 2009.

Yang G.-Y. and Slingo, J.: The diurnal cycle in the tropics. Monthly Weather Review, 129(4):784–801, doi: 10.1175/1520-0493(2001), 2001.

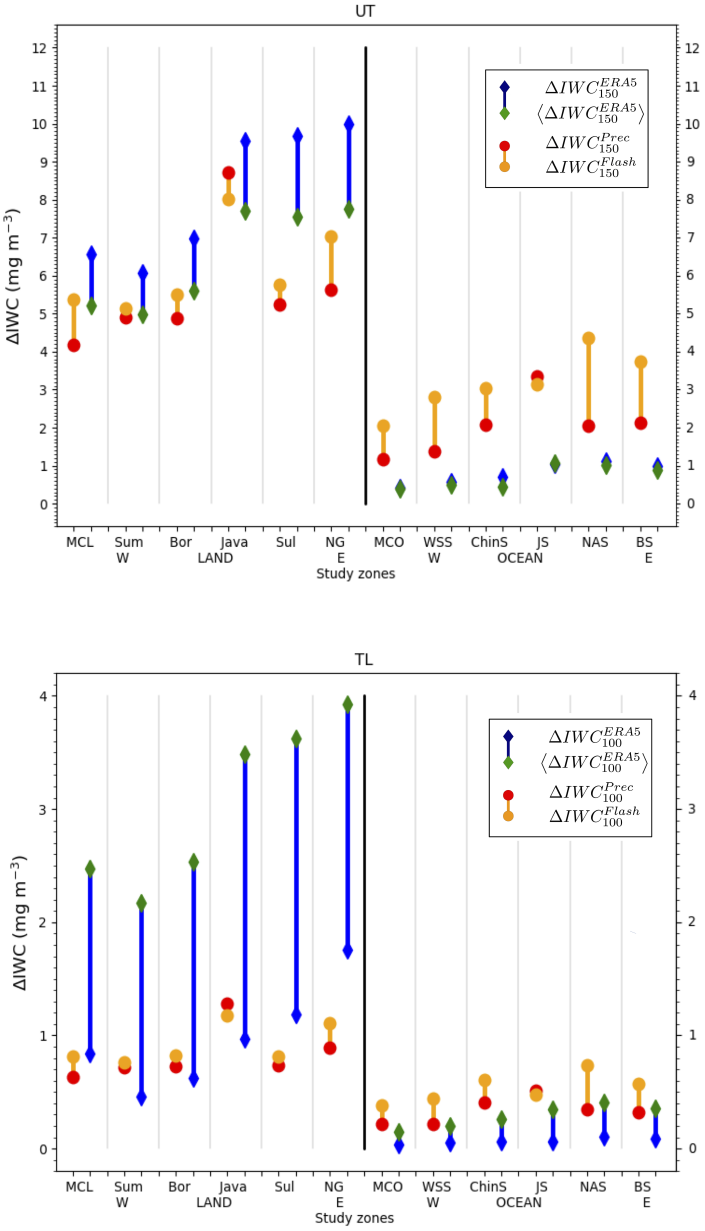

Figure 11. ~~a)~~ Top: ΔIWC (mg m^{-3}) estimated from Prec (red) and Flash (orange) at 146 hPa and ΔIWC estimated from ERA5 at the level 150 hPa and at the level 150 hPa degraded in the vertical, over islands and seas of the MariCont: MariCont_L (MCL) and MariCont_O (MCO); from West (W) to East (E) over land, Sumatra (Sum), Borneo (Bor), Java, Sulawesi (Sul) and New Guinea (NG); and over seas, West Sumatra Sea (WSS), China Sea (ChinS), Java Sea (JS), North Australia Sea (NAS) and ~~Bismark~~ Sea (BS). ~~b),~~ Bottom: Same as ~~a)~~ in top but for 100 hPa.

Ice injected into the tropopause by deep convection – Part 2: Over the Maritime Continent

Dion Iris-Amata[1], Dallet Cyrille[1], Ricaud Philippe[1], Carminati Fabien[2], Dauhut Thibaut[3], and Haynes Peter[4]

[1]CRNM, Meteo-France - CNRS, Toulouse, 31057, France
[2]Met Office, Exeter, Devon, EX1 3PB, UK
[3]Max Planck Institute for Meteorology, Hamburg, Germany
[4]DAMTP, University of Cambridge, Cambridge, CB3 0WA, UK

Correspondence: iris.dion@umr-cnrm.fr

Abstract. The amount of ice injected up to the tropical tropopause layer has a strong radiative impact on climate. In the tropics, the Maritime Continent (MariCont) region presents the largest injection of ice by deep convection into the upper troposphere (UT) and tropopause level (TL) (from results presented in the companion paper Part 1). This study focuses on the MariCont region and aims to assess the processes, the areas and the diurnal amount and duration of ice injected by deep convection over islands and over seas using a 2° × 2° horizontal resolution during the austral convective season of December, January and February. The model presented in the companion paper is used to estimate the amount of ice injected (ΔIWC) up to the TL by combining ice water content (IWC) measured twice a day in local time in tropical UT and TL by the Microwave Limb Sounder (MLS; Version 4.2) ~~,~~ from 2004 to 2017, and precipitation (Prec) measurement from the Tropical Rainfall Measurement Mission (TRMM; Version 007) averaged at high temporal resolution (1 hour). The horizontal distribution of ΔIWC estimated from Prec (ΔIWC^{Prec}) is presented at 2° × 2° horizontal resolution over the MariCont. ΔIWC is also evaluated by using the number of lightning events (Flash) from the TRMM-LIS instrument (Lightning Imaging Sensor, from 2004 to 2015 at 1-h and 0.25° × 0.25° resolutions). ΔIWC^{Prec} and ΔIWC estimated from Flash (ΔIWC^{Flash}) are compared to ΔIWC estimated from the ERA5 reanalyses (ΔIWC^{ERA5}) ~~degrading~~ with the vertical resolution degraded to that of MLS observations ($\langle \Delta IWC^{ERA5} \rangle$). Our study shows that, while the diurnal cycles of Prec and Flash are consistent ~~to~~ with each other in timing and phase over ~~lands and~~ land but different over offshore and coastal areas of the MariCont, the observational ΔIWC range between ΔIWC^{Prec} and ΔIWC^{Flash} ~~is small~~ , interpreted as the uncertainty of our model to estimate the ice injected, is smaller over land (they agree to within ~~4 – 6~~ to - 22 % ~~over land and to within 7 – 53% over ocean~~) than over ocean (to within 6 to - 71 %) in the UT and TL. The ~~reanalysis~~ impact of the vertical resolution on the estimation of ΔIWC ~~range~~ is higher in the TL (difference between ΔIWC^{ERA5} and $\langle \Delta IWC^{ERA5} \rangle$ ~~has been also found to be small in the UT (4 – 29 %) but large in the TL (55 – 78 %), highlighting the stronger impact of the vertical resolution on the TL than in the UT. Combining observational and reanalysis~~ of 32 to 139 %) than in the UT (difference of 9 to 33 %). Considering estimates of ΔIWC ~~ranges, the total~~ from all the methods, ΔIWC ~~range~~ is estimated in the UT between 4.2 and 10.0 mg m^{-3} ~~(20 % of variability per study zone) over land~~ over land, and between 0.3 and 4.4 mg m^{-3} ~~(30% of variability per study zone)~~ over sea, and, in the TL, between ~~0.6 and 3.9~~ 0.5 and 3.7 mg m^{-3} ~~(70% of variability per study zone)~~ over land and between 0.1 and

0.7 mg m^{-3} ~~(80% of variability per study zone)~~ over sea. Finally, ~~from IWC~~ ^{ERA5}based on IWC from MLS and ERA5, Prec and Flash, this study highlights that 1) ΔIWC over land ($\geq$ 4 mg m^{-3}) has been found to be larger than ΔIWC over sea ~~with a limit at 4.0 ($\leq$ 4~~ mg m^{-3}~~in the UT between minimum of ΔIWC estimated over land and maximum of ΔIWC estimated over sea)~~, and 2) small islands with high topography present the ~~strongest amounts of~~ largest ΔIWC such as the Java Island ~~, the area of the largest ΔIWC in the UT~~ (7.7 ~~–~~ to 9.5 mg m^{-3} ~~daily mean~~in the UT).

Copyright statement. TEXT

1 Introduction

In the tropics, water vapour (WV) and ice cirrus clouds near the cold point tropopause (CPT) have a strong radiative effect on climate (**?**) and an indirect impact on stratospheric ozone (**?**). WV and water ice crystals are transported up to the tropopause layer by two main processes: a three-dimensional large-scale slow process (3-m month $^{-1}$), and a ~~small scale~~ small-scale fast convective process (diurnal timescale) (e.g. **??**). Many studies have already shown the impact of convective processes on the hydration of the atmospheric layers from the upper troposphere (UT) to the lower stratosphere (LS) (e.g. **????**). However, the amount of total water (WV and ice) transported by deep convection up to the tropical UT and LS is still not well understood. The vertical distribution of total water in those layers is constrained by thermal conditions of the CPT (**?**). During deep convective events, **?** have shown that air masses transported up to 146 hPa in the UT and up to 100 hPa in the tropopause layer (TL) have ice to total water ratios of more than 50% and 70%, respectively, and that ice in the UT is strongly spatially correlated with the diurnal increases of deep convection, while WV is not. **?** hence focused on the ice phase of total water to estimate the diurnal amount of ice injected into the UT and the TL over convective tropical areas, showing that it is larger over land than over ocean, with maxima over land of the Maritime Continent (MariCont), the region including Indonesian islands. For these reasons, the present study is focusing on the MariCont region in order to better understand small-scale processes impacting the diurnal injection of ice up to the TL.

A method to estimate the amount of ice injected into the UT and up to the TL over convective areas and during convective seasons has been proposed by **?**. This method provides an estimation of the amplitude of the diurnal cycle of ice in those layers using the twice daily in local times Ice Water Content (IWC) measurements from the Microwave Limb Sounder (MLS) instrument and the full diurnal cycle of precipitation (Prec) measured by the Tropical Rainfall Measurement Mission (TRMM) instrument, at one hour resolution. The method first focuses on the increasing phase of the diurnal cycle of Prec (peak to peak from the diurnal Prec minimum to the diurnal Prec maximum) and shows that the increasing phase of Prec is consistent in time and in amplitude with the increasing phase of the diurnal cycle of deep convection, over tropical convective zones and during convective season. The amount of ice (ΔIWC) injected into the UT and the TL is estimated by relating IWC measured by MLS during the growing phase of the deep convection to the increasing phase of the diurnal cycle of Prec. **?** conclude that deep

convection over the MariCont region is the main process impacting the increasing phase of the diurnal cycle of ice in those layers.

The MariCont region is one of the main convective center in the tropics with the wettest troposphere and the coldest and driest tropopause (**???**). **?** have shown that, over the Indonesian area, the phase of the convective activity diurnal cycle drifts from land to coastlines and to offshore areas. Even though those authors have done a comprehensive ~~work around the~~ study of the diurnal cycle of precipitation and convection over the MariCont, the diurnal cycle of ice injected by deep convection up to the TL over this region is still not well understood. **?** have tentatively evaluated the upper tropospheric diurnal cycle of ice from Superconducting Submillimeter-Wave Limb-Emission Sounder (SMILES) measurements over the period 2009-2010 but without differentiating land and sea over the MariCont, which caused their analysis to show little diurnal variation over that region. **?** have 1) highlighted that the MariCont must be considered as two separate areas: the MariCont land (MariCont_L) and the MariCont ocean (MariCont_O), with two distinct diurnal cycles of the Prec and 2) estimated the amount of ice injected in the UT and the TL. Over these two domains, it has also been shown that convective processes are stronger over MariCont_L than over MariCont_O. Consequently, the amount of ice injected in the UT and the TL is greater over MariCont_L than over MariCont_O.

Building upon the results of **?**, the present study aims to improve ~~the methodology of Dion et al. (2019)~~ their methodology by i) studying smaller study zones than in Dion et al. (2019) and by distinguishing island and sea of the MariCont, ii) ~~assessing~~ comparing the sensitivity of our model to different proxies of deep convection and iii) ~~assessing~~ comparing the amount of ice injected in the UT and the TL inferred by our model to that of ERA5 reanalyses. Based on space-borne observations and meteorological reanalyses, ΔIWC is assessed at a horizontal resolution of $2^\circ \times 2^\circ$ over 5 islands (Sumatra, Borneo, Java, Sulawesi and New Guinea) and 5 seas (West Sumatra Sea, Java Sea, China Sea, North Australia Sea, and ~~Bismark~~ Bismarck Sea) of the MariCont during convective season (December, January and February, hereafter DJF) from 2004 to 2017. ΔIWC will be first estimated from Prec measured by TRMM-3B42. A sensitivity study of ΔIWC based on the number of flashes (Flash) detected by the TRMM Lightning Imaging Sensor (TRMM-LIS), an alternative proxy for deep convection as shown by Liu and Zipser (2008), is also proposed. Finally, we will use IWC calculated by the ERA5 reanalyses from 2005 to 2016 to estimate ΔIWC in the UT and the TL over each study zone and compare it to ΔIWC estimated from Prec and Flash.

The observational datasets used in our study are presented in Sect. 2. Method is ~~recalled~~ reviewed in Sect. 3. The amount of ice (ΔIWC) injected up to the TL estimated from Prec is evaluated in Sect. 4. Diurnal cycles of Prec and Flash are compared to each other over different areas of the MariCont in Sect. 5. Results of the estimated ΔIWC injected up to the UT and the TL over five islands and five seas of the MariCont are presented and compared with the ERA5 reanalyses in Sect. 6. Results are discussed in Sect. 7, and conclusions are drawn in Sect. 8. This paper contains many abbreviations and acronyms. To facilitate reading, they are compiled in the Acronyms list.

2 Datasets

This section presents the instruments and the reanalyses used for this study.

2.1 MLS Ice Water Content

The Microwave Limb Sounder (MLS, data processing algorithm version 4.2) instrument on board NASA's Earth Observing System (EOS) Aura platform (**??**) launched in 2004 provides ice water content (IWC^{MLS}, mg m^{-3}) measurements. MLS data processing provides IWC^{MLS} ~~are given~~ at 6 levels in the UTLS (82, 100, 121, 146, 177 and 215 ~~). However, we~~ hPa). Although optimal estimation is used to retrieve almost all other MLS products, a cloud-induced radiance technique is used to derive the IWC^{MLS} (**??**). We have chosen to study only two levels: an upper and a lower level of the TTL. Because the level at 82 hPa does not provide enough significant measurements of IWC to have a good signal-to-noise, we have selected~~2 levels~~: 1) ~~at~~ 100 hPa as the upper level of the TTL (named TL for tropopause level), and 2) ~~at~~ 146 hPa as the lower level of the TTL (named UT for upper ~~tropopshere~~troposphere). MLS follows a sun-synchronous near-polar orbit, completing 233 revolution cycles every 16 days, with daily global coverage every 14 orbits. The instrument ~~is crossing~~ crosses the equator twice a day ~~the equator at fixed time~~at fixed times, measuring IWC^{MLS} at 01:30 local time (LT) and 13:30 LT. The ~~horizontal resolution of IWC^{MLS} measurements is $\sim$ 300 and 7 km along and across the track, respectively. The~~ vertical resolution of IWC^{MLS} is 4 and 5 km at 146 and 100 hPa, respectively. ~~Although optimal estimation is used to retrieve almost all other MLS products, a cloud-induced radiance technique is used to validate the MLS IWC (Wu et al., 2008; Wu et al., 2009).~~ In our study, high horizontal resolution is now possible because we consider 13 years of MLS data, allowing ~~to average~~ the IWC^{MLS} measurements ~~within the~~ to be averaged within bins of horizontal resolution of 2° ×2° ($\sim$ 230 km^2). We select IWC^{MLS} during all austral convective seasons DJF between 2004 and 2017. The IWC measurements were filtered following the recommendations of the MLS team described in **?**. The ~~resolutions~~ resolution of IWC^{MLS} (horizontal along the path, horizontal perpendicular to the path, vertical) measured at 146 and 100 hPa ~~are~~ is 300×7×4 km and 250×7×5 km, respectively. The precision of the measurement is 0.10 mg m^{-3} at 146 hPa and 0.25 to 0.35 mg m^{-3} at 100 hPa. ~~The~~ While the accuracy is 100% for values less than 10 mg m^{-3} at both levels~~and the~~ , it is strongly reduce by averaging on the study period and over the study zones. The valid range is ~~0.02~~0.1-50.0 mg m^{-3} at 146 hPa and ~~0.1~~0.02-50.0 mg m^{-3} at 100 hPa (Wu et al., 2008).

2.2 TRMM-3B42 Precipitation

The Tropical Rainfall Measurement Mission (TRMM) was launched in 1997 and provided measurements of Prec until 2015. TRMM is composed of five instruments, three of them are complementary sensor rainfall suite (PR, TMI, VIRS). TRMM had an almost circular orbit at 350 km altitude ~~height~~ performing a complete revolution in one and a half hour. The 3B42 algorithm product (TRMM-3B42) (version V7) has been created to estimate the precipitation and extend the precipitation product through 2019. TRMM-3B42 is a multi-satellite precipitation analysis~~composing a Global Precipitation Measurement (GPM) Mission. TRMM-3B42 is computed from the various precipitation-relevant satellite passive Microwave (PMW) sensors using GPROF2017 computed at the Precipitation Processing System (PPS) (e.g., GMI, DPR, Ku, Ka, Special Sensor Microwave Imager/Sounder SSMIS, etc.) and including~~ . The analysis merges microwave and infrared space-borne observations and included TRMM measurements from 1997 to 2015 ~~(Huffman et al. , 2007, 2010; and Huffman and Bolvin, 2018).~~ (**???**) . Work is currently underway with NASA funding to develop more appropriate estimators for random error, and to introduce

estimates of bias error (Huffman and Bolvin, 2018). Prec data are provided at a 0.25° × 0.25° (∼ 29.2 km^2) horizontal resolution, extending from 50° S to 50° N (https://pmm.nasa.gov/data-access/downloads/trmm, last access: April 2019). Prec from TRMM-3B42 products ~~depends on input from microwave and IR sensors (?) and~~ does not differentiate between stratiform and convective precipitation. In our study, Prec from TRMM-3B42 is selected over the austral convective seasons (DJF) from 2004 to 2017 and averaged to a horizontal grid of 2° ×2 ° to be compared to IWC^{MLS}. The ~~granule temporal coverage of~~ TRMM-3B42 data ~~is 3 hours, but the temporal resolution of individual measurements is 1 minute. Thus, it is statistically possible to degrade the resolution to 1 hour.~~ have been averaged over a 1-hour interval from 0 to 24 hours. TRMM-3B42 data are provided in Universal Time that we converted into local time (LT). Details of the binning methodology of TRMM-3B42 is provided by Huffman and Bolvin (2018).

2.3 TRMM-LIS number of Flashes

The Lightning Imaging Sensor (LIS) aboard of the TRMM satellite measures several parameters ~~relative~~ related to lightning. According to Christian et al. (2000), LIS used a Real-Time Event Processor (RTEP) that discriminates lightning ~~event~~ events from Earth albedo light. A lightning event corresponds to the detection of a light anomaly on a pixel representing the most fundamental detection of the sensor. After ~~a~~ spatial and temporal processing, the sensor was able to characterize a flash from several detected events. The observation range of the sensor is between 38° N and 38° S. The instrument detects lightning with storm-scale resolution of 3-6 km (3 km at nadir, 6 km at limb) over a large region (~~550-550~~ 550×550 km) of the Earth's surface. The LIS horizontal resolution is provided at 0.25°~~×0.10~~× 0.25°. A significant amount of software filtering has gone into the production of science data to maximize the detection efficiency and confidence level. Thus, each datum is a lightning signal and not noise. Furthermore, the weak lightning signals that occur during the day are hard to detect because of background illumination. A ~~real-tile event processor~~ RTEP removes the background signal to enable the system ~~and~~ to detect weak lightning and ~~achieve a 90%~~ improves the detection efficiency during the day. LIS is thus able to provide the number of flashes (Flash) measured. The TRMM LIS detection efficiency ranges from 69% near noon to 88% at night. The LIS instrument performed measurements between 1 January 1998 and 8 April 2015. To be as consistent as possible to the MLS and TRMM-3B42 period of study, we are using LIS measurements during DJF from 2004 to 2015. ~~The observation range of the sensor is between 38° N and 38° S.~~ As LIS is on the TRMM platform, with an orbit that precesses, Flash from LIS can be averaged to obtain the full 24-h diurnal cycle of Flash over the study period with a 1-h temporal resolution. In our study, Flash measured by LIS is ~~studied~~ binned at 0.25° × 0.25° horizontal resolution to be compared to Prec from TRMM-3B42.

2.4 ERA5 Ice Water Content

The European Centre for Medium-range Weather Forecasts (ECMWF) Reanalysis 5, known as ERA5, replaces the ERA-Interim reanalyses as the fifth generation of the ECMWF reanalysis providing global climate and weather for the past decades (from 1979) (**?**). ERA5 provides hourly estimates for a large number of atmospheric, ocean and land surface quantities and covers the Earth on a 30 km grid with 137 levels from the surface up to a height of 80 km. Reanalyses such as ERA5 provide a physically constrained, continuous, global, and homogeneous representation of the atmosphere through combining a large

number of observations (space-borne, air-borne, and ground-based) with short-range forecasts. Although there is no direct observation of atmospheric ice content in ERA5, the specific cloud ice water content (mass of condensate / mass of moist air) (IWC^{ERA5}) corresponds to the changes in the analysed temperature (and at low levels, humidity) which is mostly driven by the assimilation of temperature-sensitive radiances from satellite instruments (https://cds.climate.copernicus.eu/cdsapp!/dataset/reanalysis-era5-pressure-levels-monthly-means?tab=form, last access: July 2019). IWC^{ERA5} used in our analysis is representative of non-precipitating ice. Precipitating ice, classified as snow water, is also provided by ERA5 but not used in this study in order to focus only on the injected and non-precipitating ice ~~into~~ in the TTL. Furthermore, results from Duncan and Eriksson (2018) have highlighted that ERA5 is able to capture both seasonal and diurnal variability in cloud ice water but the reanalyses exhibit noisier and higher amplitude diurnal variability than borne out by the satellite estimates. The present study uses the IWC^{ERA5} at 100 and 150 hPa averaged over DJF from 2005 to 2016 with one-hour temporal resolution. IWC^{ERA5} is governed by the model microphysics which allows ice supersaturation with respect to ice (100-150% in relative humidity) but not with respect to liquid water. Although microwave radiances at 183 GHz (sensitive to atmospheric scattering induced by ice particles) (Geer et al., 2017) are assimilated, ~~cloud and precipitations are~~ clouds and precipitation are not used as control ~~variable~~ variables in the 4D-Var assimilation system and cannot be adjusted independently in the analysis (Geer et al., 2017). The microwave data have sensitivity to the frozen phase hydrometeors but mainly to larger particles, such as those in the cores of deep convection (Geer et al., 2017), but the sensitivity to cirrus clouds in ERA5 is strongly dependent on microphysical assumptions on the shape and size of the cirrus particles. Indirect feedbacks are also acting on cirrus representation in the model – e.g. changing the intensity of the convection will change the amount of outflow cirrus generated. This is why observations that ~~affects~~ affect the troposphere by changing for example the stability, the humidity, or the synoptic situation can affect the upper level ice cloud indirectly (Geer et al., 2017). IWC^{ERA5} is ~~used to assess~~ compared to the amount of ice injected in the UT and the TL as estimated by the model developed in Dion et al. (2019) and in the present study. IWC^{ERA5} have been degraded along the vertical at 100 and 150 hPa ($\langle \Delta IWC^{ERA5} \rangle$) consistently with the MLS vertical resolution of IWC^{MLS} (5 and 4 km at 100 and 146 hPa, respectively) using ~~an unitary~~ a box function (see section **??**). IWC^{ERA5} and $\langle \Delta IWC^{ERA5} \rangle$ will be both considered in this study. IWC^{ERA5}, initially provided in kg kg^{-1}, has been converted into mg m^{-3} using the temperature provided by ERA5 in order to be compared with ~~MLS IWCobservations~~IWC^{MLS}.

3 Methodology

This section summarizes the method developed by **?** to estimate ΔIWC, the amount of ice injected into the UT and the TL. **?** have presented a model relating Prec (as proxy of deep convection) from TRMM to IWC^{MLS} over tropical convective areas during austral convective season DJF. The IWC^{MLS} value measured by MLS during the growing phase of the convection (at ~~x~~ x = 01:30 LT or 13:30 LT) is compared to the Prec value at the same time ~~x~~ x in order to define the correlation coefficient (C) between Prec and IWC^{MLS}, as follows:

$$C = \frac{IWC_x^{MLS}}{Prec_x} \quad (1)$$

The diurnal cycle of IWC estimated ($IWC^{est}(t)$) can be calculated by using C applied to the diurnal cycle of Prec (~~Prec(t))~~$Prec(t)$), where t is the time, as follows:

$$IWC^{est}(t) = Prec(t) \times C \tag{2}$$

The amount of IWC injected up to the UT or the TL (ΔIWC^{Prec}) is defined by the difference between the maximum of IWC^{est} (IWC$^{est}_{max}$) and its minimum (IWC$^{est}_{min}$).

$$\Delta IWC^{Prec} = C \times (Prec_{max} - Prec_{min}) = IWC^{est}_{max} - IWC^{est}_{min} \tag{3}$$

where $Prec_{max}$ and $Prec_{min}$ are the diurnal maximum and minimum of Prec, respectively. Figure **??** illustrates the relationship between the diurnal cycle of Prec and the two MLS measurements at 01:30 ~~LT~~ and 13:30 LT. The growing phase of the convection is defined as the period of increase in precipitation from $Prec_{min}$ to $Prec_{max}$. The amplitude of the diurnal cycle is defined by the difference between $Prec_{max}$ and $Prec_{min}$. In Fig. 1, because the growing phase of the convection illustrated is happening during the afternoon, only the MLS measurement at 13:30 LT is used in the calculation of ΔIWC. IWC at 01:30 LT is not used in that case.

4 Horizontal distribution of ΔIWC estimated from Prec over the MariCont

4.1 Prec from ~~TRMM~~ TRMM-3B42 related to IWC from MLS

In order to identify the main areas of injection of ice in the TL over the MariCont, Figure **??** presents different parameters associated to this area: a) the name of the main islands and seas over the MariCont, b) the elevation (http://www.soda-pro.com/web-services/altitude/srtm-in-a-tile, last access: June 2019), c) the daily mean of Prec at 0.25° × 0.25° horizontal resolution, d) the hour of the diurnal maxima of Prec at 0.25° × 0.25° horizontal resolution, and e) the daily mean ($I\bar{W}C = (IWC_{01:30} + IWC_{13:30}) \times 0.5$) of IWC^{MLS} at 146 hPa at 2° × 2° horizontal resolution. Several points need to be highlighted. Daily means of Prec over land and coastal parts are higher than over oceans (Fig. **??**c). Areas where the daily mean of Prec is maximum are usually surrounding the highest elevation over land (e.g. over ~~NewGuinea~~) and near coastal areas (North West of Borneo in the China Sea and ~~South of~~ southern Sumatra in the Java Sea) (Fig. **??**b and c). The times of the maxima of Prec are over land during the evening (18:00-00:00 LT), over coast during the night-morning (00:00-06:00 TL) and over sea during the morning-noon and even evening depending ~~of~~ on the sea considered (09:00-12:00 LT and 15:00-00:00 LT). These differences ~~could illustrate~~ may be related to the impact of the land/sea breeze ~~within the~~ over the course of 24 hours. The sea breeze during the day favours the land convection at the end of the day when land ~~temperature surface~~ surface temperature is higher than oceanic ~~temperature surface~~ surface temperature. During the night, the coastline sea surface temperature ~~becomes larger than~~ rises above the land surface temperature, and the land breeze ~~favours systematically the convection development over coast~~systematically favours the development of convection over coasts. These observations are consistent

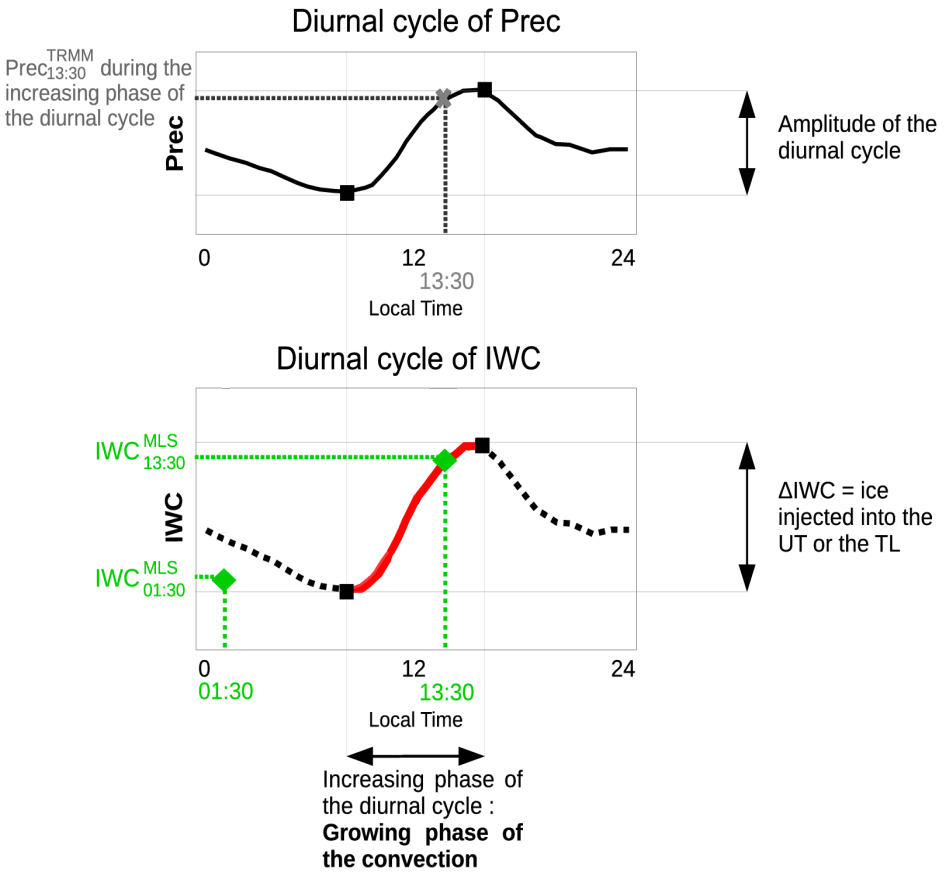

Figure 1. Illustration of the model ~~used~~ developed in **?** to estimate the amount of ice (ΔIWC) injected into the UT or the TL. Diurnal cycle of a proxy of deep convection (Prec) (a), diurnal cycle of ice water content (IWC) estimated from diurnal cycle of the proxy of deep convection (b). In red line, the increasing phase of the diurnal cycle. In black dashed line, the decreasing phase of the diurnal cycle. The green diamonds are the two IWC^{MLS} measurements from MLS. Grey thick cross represents the measurement of Prec during the growing phase of the convection ($Prec_x$), used in the model. Maximum and minimum of the diurnal cycles are represented by black squares. Amplitude of the diurnal cycle is defined by the differences between the maximum and the minimum of the cycle.

215 with results presented ~~in ?, explaining~~ by **?**, who explained that high precipitation is mainly concentrated over land in the MariCont because of the strong sea-breeze convergence, but also because of the combination with the mountain–valley winds and cumulus merging processes. Amplitudes of the diurnal cycles of Prec over the MariCont will be detailed as a function of island and sea in section **??**. The location of the largest concentration of IWC^{MLS} (3.5 – 5.0 mg m^{-3}, Fig. **??**e) is consistent with that of Prec ($\sim$ 12 – 16 mm day^{-1}) over the West Sumatra Sea, and over the South of Sumatra island. However, over

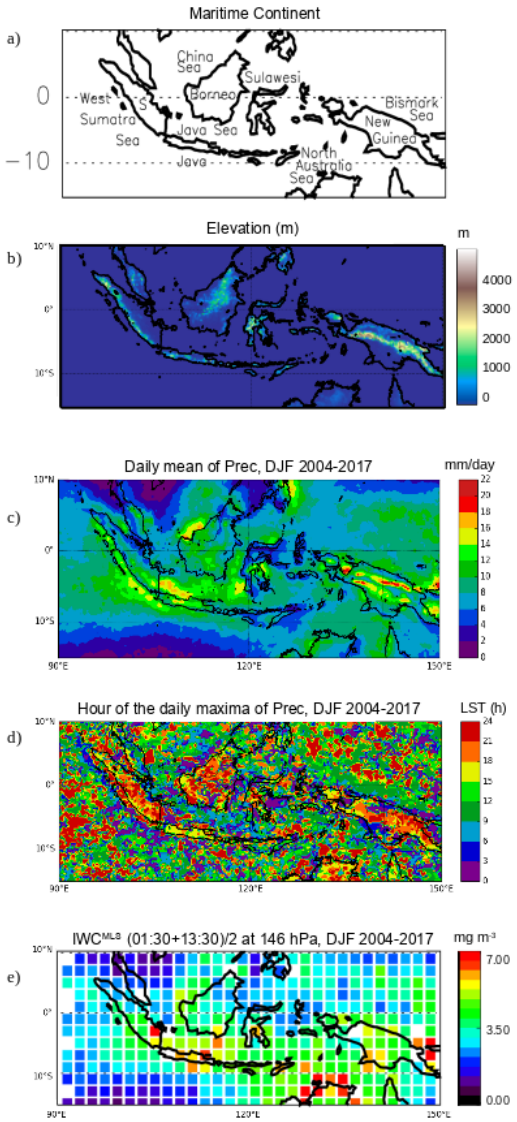

Figure 2. Main islands and seas of the MariCont (S is for Sumatra) (a), elevation from Solar Radiation Data (SoDa) (b); daily mean of Prec ~~measured by~~ obtained from TRMM analysis over the Maritime Continent, averaged over the period of DJF 2004-2017 (c), hour (local solar time (LST)) of the diurnal maxima of Prec over the MariCont (d); daily mean (01:30 LT + 13:30 LT)/2 of IWC^{MLS} at 146 hPa from MLS over the MariCont averaged over the period of DJF 2004-2017 (e). Observations are presented with a horizontal resolution of $0.25^\circ \times 0.25^\circ$ (b, c and d) and $2^\circ \times 2^\circ$ (e).

North Australia seas (including the Timor Sea and the Arafura Sea), we observed large differences between Prec low values (4 – 8 mm day^{-1}) and IWC^{MLS} large concentrations (4 – 7 mg m^{-3}).

4.2 Convective processes compared to IWC measurements

Although TRMM horizontal resolution is 0.25° × 0.25°, we require information at the same resolution as ~~MLS IWC~~IWC^{MLS}. From the diurnal cycle of ~~TRMM Prec measurements~~Prec in TRMM analysis, the duration of the increasing phase of Prec can be known for each 2° × 2° pixel. The duration of the growing phase of the convection can then be defined from Prec over each pixel. Figures ~~??a~~ 3a and b present the anomaly (deviation from the mean) of Prec ~~measured by TRMM–3B42 over the MariCont at 01:30 LT and 13:30 LT, respectively, only over pixels when the convection is in the growing phase. The anomaly of IWC measured by MLS~~ in TRMM-3B42 over the MariCont ~~is shown in Figs. ??c and d, over pixels when the~~ for the pixels where convection is in the growing phase at 01:30 LT and 13:30 LT, respectively. ~~Each pixel of Prec at 01:30 LT or 13:30 LT during the~~ Anomalies are calculated relative to the average computed over the entire MariCont region. Thus, red colors signify regions that are experiencing the growing phase of ~~the convection deviates by the average of the all Prec at~~ convection and whose Prec value is greater than the overall MariCont mean at the respective time (01:30 LT or 13:30 LT), whereas blue colors signify those regions where there is little precipitation compared to the overall MariCont mean during the growing phase of ~~the convectionover the whole MariCont~~convection. The gray color denotes pixels for which convection is not ongoing. ~~Some pixels can be presented on both sets of Prec and IWC panels in Figs. 3~~ Pixels can be represented in the panels for both local times when: 1) the onset of the convection is before 01:30 LT and the end is after 13:30 LT, or 2) the onset of the convection is before 13:30 LT and the end is after 01:30 LT. Similar anomalies of IWC^{MLS} over the MariCont are shown in Figs. 3c and d, over pixels when the convection is in the growing phase at 01:30 LT and 13:30 LT, respectively. Note that, ~~whithin~~ within each 2°~~x2°~~ ° × 2° pixel, at least 60 measurements of Prec or IWC^{MLS} at 13:30 LT or 01:30 LT over the period 2004-2017 have been selected for the average.

The Prec anomaly at 01:30 LT and 13:30 LT varies between -0.15 and +0.15 mm h^{-1}. The IWC^{MLS} anomaly at 13:30 LT and 01:30 LT varies between -3 and +3 mg m^{-3}. At 13:30 LT, the growing phase of the convection ~~over land is mainly at 13:30 LT~~is found mainly over land. At 13:30 LT, over land, the strongest Prec and IWC^{MLS} anomalies (+0.15 mm h^{-1} and +2.50 mg m^{-3}, respectively) are found over the Java island, and ~~north of~~ northern Australia for IWC^{MLS}. At 01:30 LT, the growing phase of the convection is found mainly over sea (while the pixels of the land are mostly gray), with maxima of Prec and IWC^{MLS} anomalies over coastlines and seas close to the coasts such as the Java Sea and the ~~Bismark Sea. The IWC anomaly at 13:30 LT and 01:30 LT varies between -3 and +3 mg m^{-3}.~~ Bismarck Sea. Three types of areas can be distinguished from Fig. **??**: i) area where Prec and IWC^{MLS} anomalies have the same sign (positive or negative either at 01:30 LT or 13:30 LT) (e.g. over Java, Borneo, Sumatra, Java Sea and coast of Borneo or the China Sea); ii) area where Prec anomaly is positive and IWC^{MLS} anomaly is negative (e.g. over West Sumatra Sea); and iii) area where Prec anomaly is negative and IWC^{MLS} anomaly is positive (e.g. over the North Australia Sea at 01:30 LT). Convective processes associated to these three types of areas over islands and seas of the MariCont are discussed in Sect. 6.

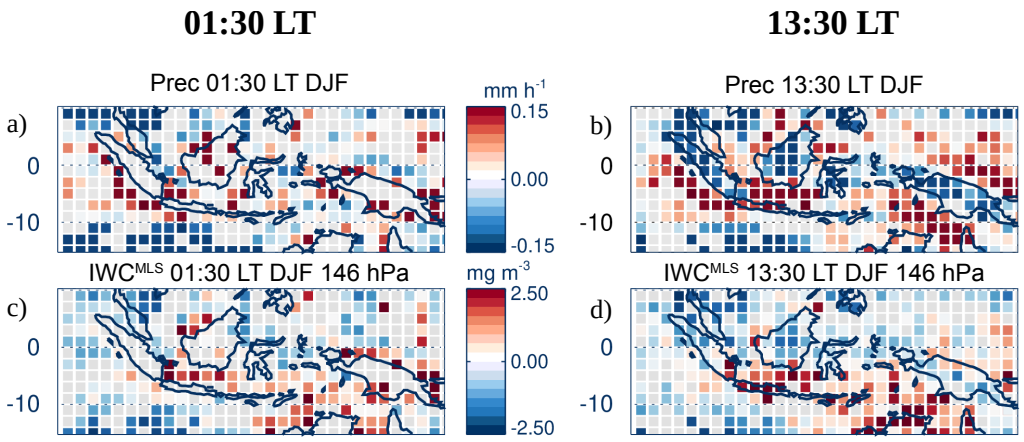

Figure 3. Anomaly (deviation from the mean) of Prec (a-b) and Ice Water Content (IWC^{MLS}) at 146 hPa (c-d), at 01:30 LT (left) and at 13:30 LT (right) over pixels where 01:30 LT and 13:30 LT are during the growing phase of the convection, respectively, averaged over the period of DJF 2004-2017. The gray color denotes pixels for which convection is not ongoing.

4.3 Horizontal distribution of ice injected into the UT and TL estimated from Prec

From the model developed in **?** based on Prec from TRMM–3B42 and IWC from MLS and synthesized in section 2.4, we can calculate the amount of IWC injected (ΔIWC) at 146 hPa (UT, Figure **??**a) and at 100 hPa (TL, Figure **??**b) by deep convection over the MariCont. In the UT, the amount of IWC injected over land is on average larger (> 10 – 20 mg m^{-3}) than over seas (< ~~10~~ 15 mg m^{-3}). ~~South of~~ Southern Sumatra, Sulawesi, ~~North of~~ northern New Guinea and ~~North of~~ northern Australia present the largest amounts of ΔIWC over land (15 – 20 mg m^{-3}). Java Sea, China Sea and ~~Bismark~~ Bismarck Sea present the largest amounts of ΔIWC over seas (7 – 15 mg m^{-3}). West Sumatra Sea and North Australia Sea present low values of ΔIWC (< 2 mg m^{-3}). We can note that the anomalies of Prec and IWC during the growing phase over North Australia Sea at 13:30 LT are positive (> 0.2 ~~mg m^{-3}~~ mm h^{-1}, Fig. **??**~~a and~~ b and > 2.5 mg m^{-3}, Fig. **??**~~c and~~ d, respectively). In the TL, the maxima (up to 3.0 mg m^{-3}) and minima (down to 0.2 – 0.3 mg m^{-3}) of ΔIWC are located within the same pixels as in the UT, although 3 to 6 times lower than in the UT. The decrease of ΔIWC with altitude is larger over land (by a factor 6) than over sea (by a factor 3). We can note that the similar pattern between the two layers ~~come~~ comes from the diurnal cycle of Prec in the calculation of ΔIWC at 146 and 100 hPa. ~~Only the measured value of IWC^{MLS} at 146 and 100 hPa can explain the observed différences in~~ The differences in the magnitudes of the ΔIWC values at ~~these~~ 100 and 146 hPa arise from the different amounts of IWC measured by MLS at those two levels. ~~Thus~~That is, similar ΔIWC patterns are expected between the two levels because, according to the model developed in Dion et al. (2019), ~~the~~ deep convection is the main process transporting ice into the UT and the TL during the growing phase of the convection. Convective processes associated to land and sea are further discussed in Sect. 6.

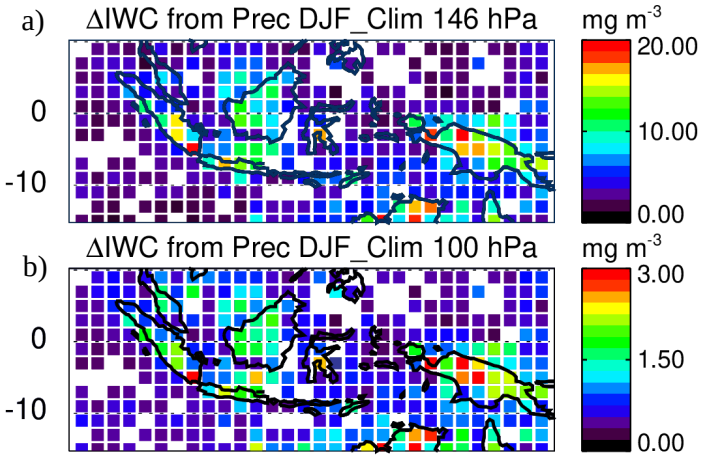

Figure 4. Daily amount of ice injected (ΔIWC) up to the UT (a) and up to the TL (b) estimated from Prec, averaged during DJF 2004-2017.

In order to better understand the impact of deep convection on the strongest ΔIWC injected per pixel up to the TTL, isolated pixels selected in Fig. 4a are presented separately in Figure **??**a and f. This Figure shows the diurnal cycles of Prec in four pixels selected for their large ΔIWC in the UT ($\geq$ 15 mg m^{-3}, Fig. **??**b, c, d, e), and the diurnal cycle of Prec in four pixels selected for their low ΔIWC in the UT (but large enough to observe the diurnal cycles of IWC between 2.0 and 5.0 mg m^{-3}, Fig. **??**g, h, i, j). Pixels with low values of ΔIWC over land (~~Figs~~Fig. **??**g, h and i) present small amplitude of diurnal cycles of Prec ($\sim$ +0.5 mm h^{-1}), with maxima between 15:00 LT and 20:00 LT and minima around 11:00 LT.

The pixel with low value of ΔIWC over sea (Fig. **??**j) presents an almost null amplitude of the diurnal cycle of Prec~~with low value~~, with low values of Prec all day long ($\sim$ 0.25 mm h^{-1}). Pixels with large values of ΔIWC over land (Fig. **??**b, c, d, e) present longer duration of the increasing phase of the diurnal cycle (from $\sim$ 09:00 LT to 20:00 – 00:00 LT) than the increasing phase of Prec diurnal cycle over pixels with low values of ΔIWC (from 10:00 LT to 15:00 – 19:00 LT). More precisely, pixels labeled 1 and 2 over New Guinea (Fig. **??**d and e) and the pixel over ~~South of~~ southern Sumatra (Fig. **??**c) show amplitude of diurnal cycle of Prec reaching 1.0 mm h^{-1}, while the pixel over North Australia (Fig. **??**b) presents lower amplitude of diurnal cycle of Prec (0.5 mm h^{-1}).

~~IWC measured by MLS~~

IWC^{MLS} during the growing phase of deep convection and the diurnal cycle of IWC estimated from Prec are also shown on Fig. **??**. For pixels with large values of ΔIWC, IWC~~observed by MLS~~ ^{MLS} is between 4.5 and 5.7 mg m^{-3} over North Australia~~Sea~~, South Sumatra and New Guinea ~~.~~1. For pixels with low values of ΔIWC, IWC~~observed by MLS~~ ^{MLS} is found between 1.9 and 4.7 mg m^{-3}. To summarize, large values of ΔIWC are observed over land in combination to i) longer growing phase of deep convection (> 9 hours) and/or ii) large diurnal amplitude of Prec (> 0.5 mm h^{-1}). However, as IWC^{MLS} ranges

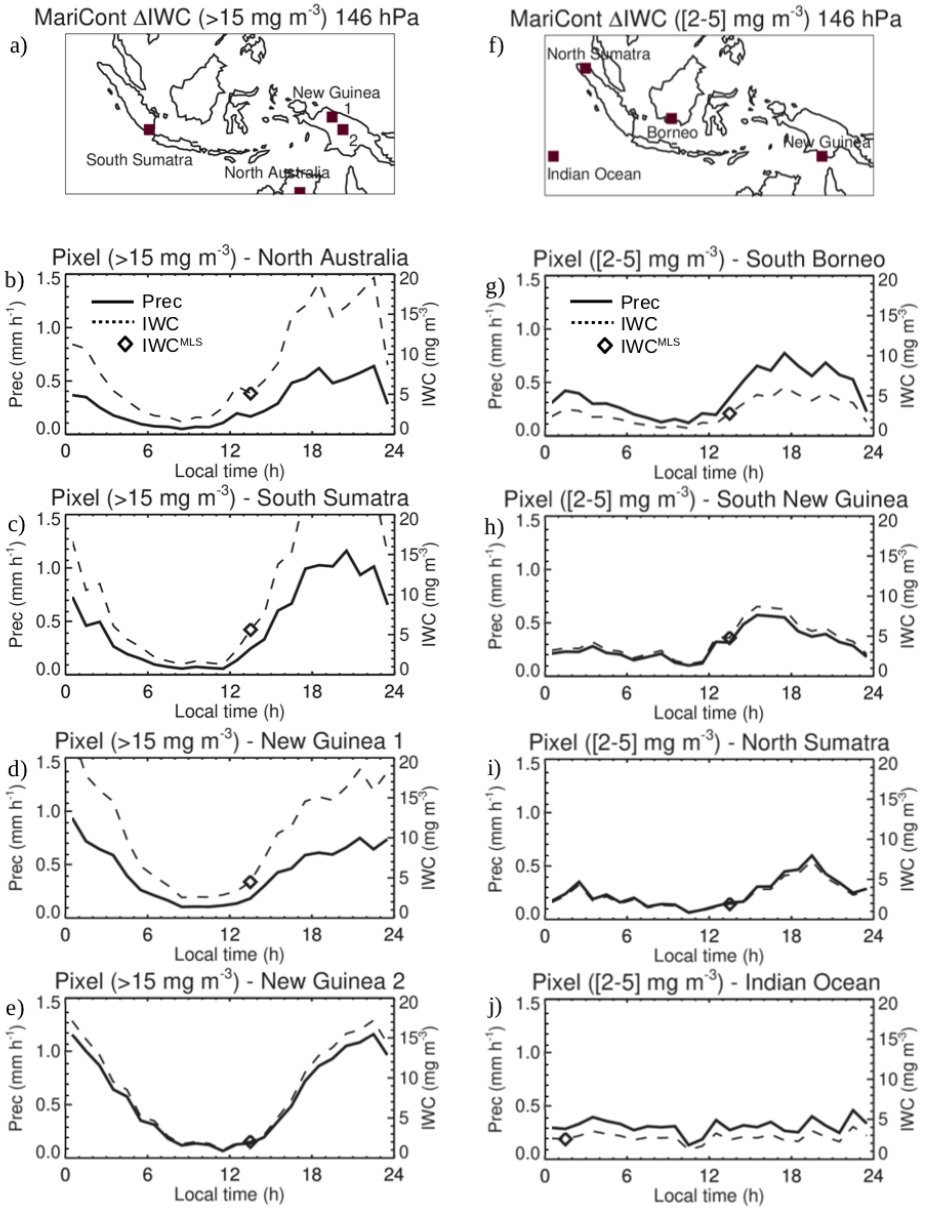

Figure 5. a) and f) Location of 2° × 2° pixels where ΔIWC have been found higher than 15 mg m^{-3} (in Fig. 4) and where ΔIWC have been found between 2 and 5 mg m^{-3} (in Fig. 4), respectively. Diurnal cycle of Prec (solid line): (b, c, d, e) over 4 pixels where ΔIWC have been found higher than 15 mg m^{-3} (in Fig. 4), (g, h, i, j) over 4 pixels where ΔIWC have been found between 2 and 5 mg m^{-3} (in Fig. 4), during DJF 2004-2017. The diamond represents IWC^{MLS} during the increasing phase of the convection. The dashed line is the diurnal cycle of IWC estimated from the diurnal cycle of Prec and from IWC^{MLS}.

overlap for the high and low ΔIWC, no definitive conclusion about the relationship between IWC^{MLS} and ΔIWC can be drawn.

In the next section, we estimate ΔIWC using another proxy of deep convection, namely Flash measurements from LIS.

~~a) and f) location of 2° × 2° pixels where ΔIWC have been found higher than 15 mg m^{-3} (in Fig. 4) and where ΔIWC have been found between 2 and 5 mg m^{-3} (in Fig. 4), respectively. Diurnal cycle of Prec (solid line): (b, c, d, e) over 4 pixels where ΔIWC have been found higher than 15 mg m^{-3} (in Fig. 4), (g, h, i, j) over 4 pixels where ΔIWC have been found between 2 and 5 mg m^{-3} (in Fig. 4), during DJF 2004-2017. The Diamond is IWC^{MLS} measured by MLS during the increasing phase of the convection. The dashed line is the diurnal cycle of IWC estimated from the diurnal cycle of Prec and from IWC^{MLS}.~~

5 Relationship between diurnal cycle of Prec and Flash over MariCont land and sea

Lightning is created ~~into~~ in cumulonimbus clouds when the electric potential energy difference is large between the base and the top of the cloud. Lightning can appear at the advanced stage of the growing phase of the convection and during the mature phase of the convection. For these reasons, in this section, we use Flash measured from LIS during DJF 2004-2015 as another proxy of ~~the~~ deep convection in order to estimate ΔIWC (ΔIWC^{Flash}) and check the consistency with ΔIWC obtained with Prec (ΔIWC^{Prec}).

5.1 Flash distribution over the MariCont

Figure **??**a presents the daily mean of Flash in DJF 2004-2015 at 0.25° × 0.25° horizontal resolution. Over land, Flash can reach a maximum of 10^{-1} flashes day^{-1} per pixel while, over seas, Flash are less frequent ($\sim 10^{-3}$ flashes day^{-1} ~~day~~ per pixel). When compared to the distribution of Prec (Fig. **??**c), maxima of Flash are found over ~~the same~~ similar areas as maxima of Prec (Java, East of Sulawesi coast, Sumatra and ~~North Australialands~~northern Australia). Over Borneo and ~~NewGuinea~~New Guinea, coastlines present more Flash ($\sim 10^{-2}$ flashes day^{-1}) than inland ($\sim 10^{-3}$ flashes day^{-1}). Differences between Flash and Prec distributions are found over North Australia Sea, with relatively large number of Flash (~~~~>10^{-2} flashes day^{-1}) compared to low Prec (4 – 10 mm day^{-1}) (Fig. **??**c), and over ~~NewGuinea~~ several inland areas of New Guinea where the number of Flash is relatively low ($\sim 10^{-2}$~~–~~ 10^{-3} flashes day^{-1}) while Prec is high (~14 – 20 mm day^{-1}). Figure **??**b shows the hour of the Flash maxima. Over land, the maximum of Flash is between 15:00 LT and 19:00 LT, slightly earlier than the maximum of Prec (Fig. **??**d) observed between 16:00 LT and 24:00 LT. Coastal areas present similar hours of maximum of Prec and Flash, i.e between 00:00 LT and 04:00 LT although, over the West Sumatra Coast, diurnal maxima of both Prec and Flash happen 1–4 hours earlier (from 23:00-24:00 LT) than those of other coasts.

5.2 Prec and Flash diurnal cycles over the MariCont

This section compares the diurnal cycle of Flash with the diurnal cycle of Prec in order to assess the potential for Flash to be used as a proxy of deep convection over land and sea of the MariCont. Diurnal cycles of Prec and Flash over the MariCont land, coastline and offshore (MariCont_L, MariCont_C, MariCont_O, respectively) are shown in Figs. **??**a–c, respectively. Within

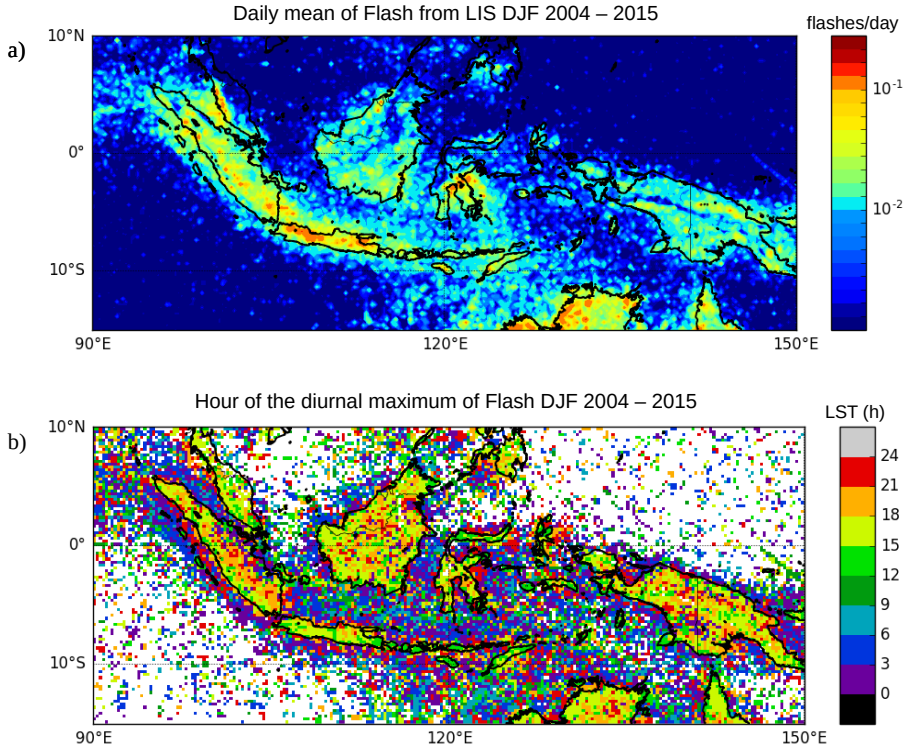

Figure 6. Daily mean of Flash measured by LIS averaged over the period DJF 2004-2015 (a); Hour (local solar time (LST)) of the diurnal maximum of Flash (b).

each 0.25° × 0.25° bin, land/coast/ocean filters were applied from the Solar Radiation Data (SoDa, http://www.soda-pro.com/web-services/altitude/srtm-in-a-tile). MariCont_C is the average of all coastlines defined as 5 pixels extending into the sea from the land limit. This choice of 5 pixels ~~has been taken applying~~ was made after consideration of some sensitivity tests in order to have the best compromise between a high signal-to-noise ratio and a good representation of the coastal region. The MariCont_O is the average of all offshore pixels defined as sea pixels excluding 10 pixels (~~-~~2000 km~~off the land~~) over the sea from the land~~coasts~~, thus coastline pixels are excluded as well as all the coastal influences. MariCont_L is the area of all land pixels. ~~A~~ At the border between the land and the coast areas, a given 0.25°×0.25°pixel can contain information from ~~different origins : land /coastlinesor sea/coastlines~~both land and coastlines. In that case, we can easily discriminate between land and coastlines ~~or sea and coastlines~~ by applying the land/~~ocean/~~coastlines filters. Consequently, this particular pixel will be flagged both as land and coastlines~~or sea and coastlines~~.

Over land, during the growing phase of the convection, Prec and Flash start to increase at the same time (10:00 LT – 12:00 LT) but Flash reaches a maximum earlier (15:00 LT – 16:00 LT) than Prec (17:00 LT – 18:00 LT). This is consistent with the finding of Liu and Zipser (2008) over the whole tropics. Different maximum times could come from the fact that, while the deep convective activity intensity starts to decrease with the number of flashes, Prec is still high during the dissipating stage of

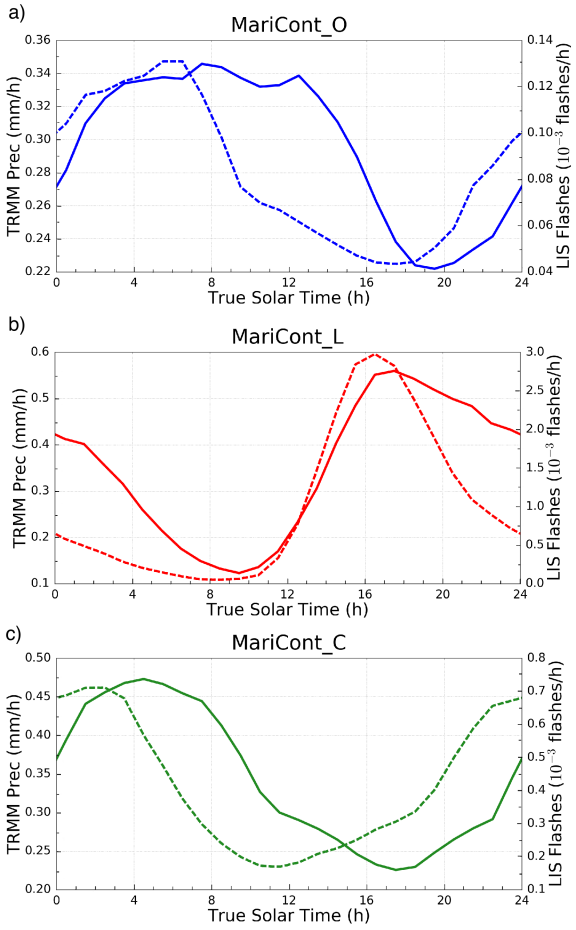

Figure 7. Diurnal cycle of Prec (solid line) and diurnal cycle of Flash (dashed line) over MariCont_L (~~top~~a), MariCont_C (~~middle~~b) and MariCont_O (~~bottom~~c).

the convection and takes longer ~~times~~ to decrease than Flash. Consequently, combining our results with the ones presented in **?**, Flash and Prec can be considered as good proxies of deep convection during the growing phase of the convection over the MariCont_L.

Over coastlines (Fig. **??**~~c~~b), the Prec diurnal cycle is delayed by about +2 to 7 h with respect to the Flash diurnal cycle. Prec minimum is around 18:00 LT while Flash minimum is around 11:30 LT. Maxima of Prec and Flash are found around 04:00 LT and 02:00 LT, respectively. This means that the increasing phase of Flash is 2-3 h longer than that of Prec. These results are consistent with the work of **?** showing a diurnal maximum of precipitation in the early morning between 02:00 LT and 03:00 LT and a diurnal minimum of precipitation ~~around~~ between 11:00 LT and 21:00 LT, over coastal zones of Sumatra. According

to **?** and **?**, coastal zones are areas where precipitation results more from convective activity than from stratiform activity and the amplitude of diurnal maximum of Prec decreases with the distance from the coastline.

Over offshore areas (Fig. **??**~~b~~c), minima of diurnal cycle of Prec and diurnal cycle of Flash are in the late afternoon, between 16:00 LT and 17:00 LT (Flash) and 17:00 LT and 18:00 LT (Prec), whilst maxima of diurnal cycle of Prec and Flash are reached in the early morning, between 06:00 LT and 07:00 LT (Flash) and around 08:00 LT – 09:00 LT (Prec). Results over offshore areas are consistent with diurnal cycle of Flash and Prec calculated by **?** over the whole tropical ocean, showing the increasing phase of the diurnal cycle of Flash starting 1–2 hours before the increasing phase of the diurnal cycle of Prec.

The time of transition from maximum to minimum of Prec is always longer than that of Flash. The period after the maximum of Prec is likely more representative of stratiform rainfall than deep convective rainfall. ~~Consistently~~Consistent with that picture, model results from **?** have shown the suppression of ~~the~~ deep convection over ~~offshore area in West~~ the offshore area west of Sumatra from the early afternoon due to ~~downwelling wavefront highlighted~~ a downwelling wavefront characterized by deep warm anomalies around noon. According to the authors, later in the afternoon, gravity waves are forced by the stratiform heating profile and propagate slowly offshore. They also highlighted that the diurnal cycle of the offshore convection responds strongly to the gravity wave forcing at the horizontal scale of 4 km. To summarize, diurnal cycles of Prec and Flash show that:

i) over land, Flash increases proportionally with Prec during the growing phase of the convection,

ii) over coastlines, Flash increasing phase is ~~advanced by~~ more than 6–7 hours ~~compared to~~ ahead of Prec increasing phase,

iii) over offshore areas, Flash increasing phase is ~~advanced by~~ about 1–2 hours ~~compared to~~ ahead of Prec increasing phase.

In section **??**, we investigate whether this time difference impacts the estimation of ΔIWC over land, coasts, and offshore areas.

5.3 Prec and Flash diurnal cycles and small-scale processes

In this subsection, we study the diurnal cycle of Prec and Flash at $0.25° \times 0.25°$ resolution over areas of deep convective activity over the MariCont. In line with the distribution of large value of Prec (Fig. **??**), IWC^{MLS} (Fig. **??**) and ΔIWC (Fig. **??**), we have selected five islands and five seas over the MariCont. Diurnal cycles of Prec and Flash are presented over land for a) Java, b) Borneo, c) New Guinea, d) Sulawesi and e) Sumatra as shown in Figure **??** and over sea for the a) Java Sea, b) North Australia Sea (NAusSea), c) ~~Bismark~~ Bismarck Sea, d) West Sumatra Sea (WSumSea) and e) China Sea as shown in Figure **??**. Diurnal cycles of IWC from ERA5 (IWC^{ERA5}) are also presented in ~~Fig~~Figs. 8 and 9 and will be discussed in Section 6.

Over land, the amplitude of the diurnal cycle of Prec is the largest over Java (Fig. **??**a), consistent with **?**, with a maximum reaching 1 mm h^{-1}, while, over the other areas, maxima are between 0.4 and 0.6 mm h^{-1}. Furthermore, over Java, the duration of the increasing phase in the diurnal cycle of Prec is ~~6 h~~ 6 h, consistent with that of Flash~~and elsewhere,~~ , whereas elsewhere the duration of the increasing phase is longer in Prec than in Flash by 1–2 h. The particularity of Java is related to the increasing phase of the diurnal cycle of Prec (6 h), ~~that~~ which is faster than over all the other land areas considered in our study (7 – 8 h). The strong and rapid convective growing phase measured over Java might be explained by the fact that the island is narrow with high mountains (up to $\sim$ 2000 m of altitude, as shown in Fig. 2b) reaching the coast. The topography promotes the growth of intense and rapid convective activity. The convection starts around 09:00 LT, rapidly elevating warm air up to the top of

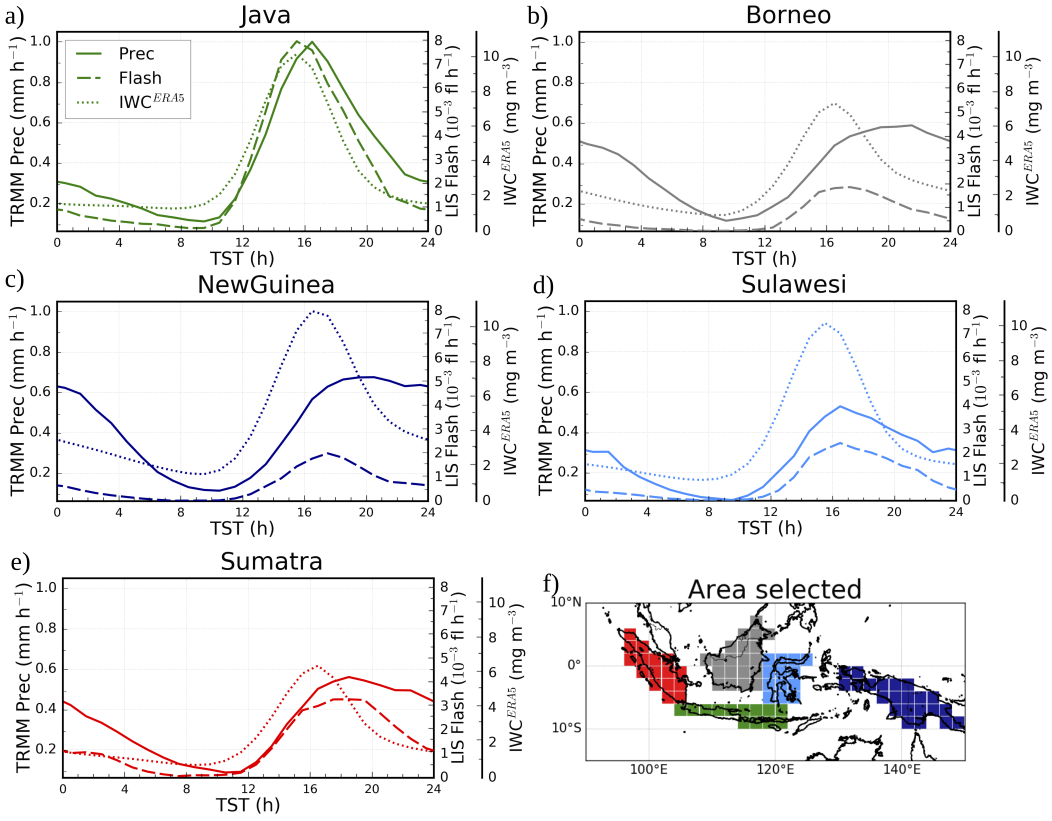

Figure 8. Diurnal cycles of Prec (solid line), Flash (dashed line) and IWC^{ERA5} from ERA5 at 150 hPa (dotted line) over MariCont islands: Java (a), Borneo (b), New Guinea (c), Sulawesi (d) and Sumatra (e) and map of the study zones over land (f).

the mountains. Around 15:00 LT, air masses cooled in altitude are transported to the sea favoring the dissipating stage of the convection. Sulawesi is also a small island with high topography as Java. However, the amplitude of the diurnal cycle of Prec and Flash is not as strong as over Java. Other islands, such as Borneo, New Guinea and Sumatra, have high mountains but also large lowland areas. Mountains promote deep convection at the beginning of the afternoon while lowlands help maintain the convective activity through shallow convection and stratiform rainfall (**??**). Deep and shallow convection are then mixed during the slow dissipating phase of the convection (from $\sim$ 16:00 LT to 08:00 LT). However, because Flash are observed only in deep convective clouds, the decreasing phase of Flash diurnal cycles decreases more rapidly than the decreasing phase of Prec. The diurnal maxima of Prec found separately over the 5 islands of the MariCont (at 0.25° $\times$ 0.25° resolution) are much higher than the diurnal maxima of Prec found over tropical land (South America, South Africa and MariCont_L, at 2° $\times$ 2° resolution) from **?**: $\sim$ 0.6 – 1.0 mm h^{-1} and $\sim$ 0.4 mm h^{-1}, respectively. However, the duration of the increasing phase of the diurnal cycle of Prec is consistent with the one calculated over tropical land by **?**.

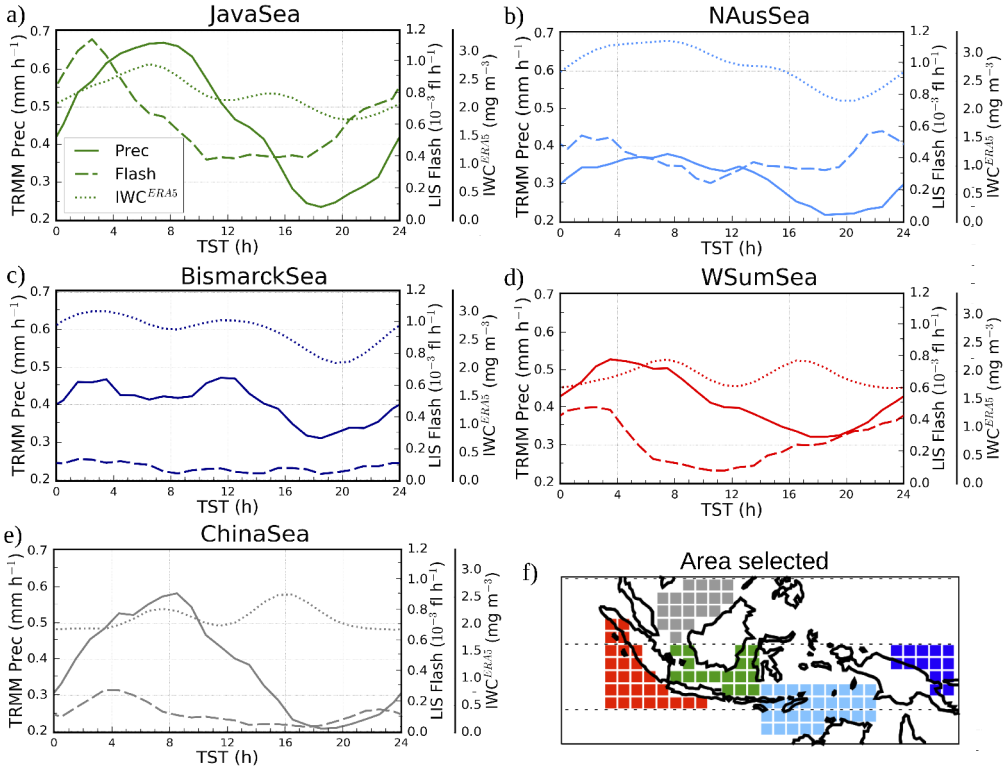

Figure 9. Diurnal cycles of Prec (solid line), Flash (dashed line) and IWC^{ERA5} from ERA5 at 150 hPa (dotted line) over MariCont seas: Java Sea (a), North Australia Sea (NAusSea) (b), ~~Bismark~~ Bismarck Sea (c), West Sumatra Sea (WSumSea) (d), China Sea (e) and map of the study zones over sea (f).

Over sea, the five selected areas (Fig. **??**a–e) show a diurnal cycle of Prec and Flash similar to that of either coastline or offshore areas depending ~~onthe area~~on the region considered. The diurnal cycle of Prec and Flash over Java Sea is similar to the one over coastlines (Fig. **??**~~e~~b). Java Sea (Fig. **??**a), an area mainly surrounded by coasts, shows the largest diurnal maximum of Prec ($\sim$ 0.7 mm h^{-1}) and Flash ($\sim$ 1.1 10^{-3} flashes h^{-1}) with the longest growing phase. In this area, land and sea breezes observed in coastal areas impact the diurnal cycle of the convection (**?**). During the night, land breeze develops from a temperature gradient between warm sea surface temperature and cold land surface temperature and conversely during the day. Over Java Sea, Prec is strongly impacted by land breezes from Borneo and Java islands (**?**), explaining why Prec and Flash reach largest values during the early morning. By contrast, NAusSea, ~~Bismark~~ Sea and WSumSea (Figs. **??**b, c and d, respectively) present small amplitude of diurnal cycle. In our analysis, these three study zones are the areas including the most offshore pixels. Java Sea and WSumSea present a similar diurnal cycle of Prec and Flash, with Flash growing phase starting

about 4 h earlier than that of Prec. China Sea also shows a diurnal maximum of Flash shifted by about 4 hours before the diurnal maximum of Prec, but the time of the diurnal minimum of Prec and Flash is similar. Over China Sea and ~~Bismark~~ Bismarck Sea, the diurnal cycle of Flash shows a weak amplitude with maxima reaching only 0.1 ~~-~~ - 0.2 10^{-3} flashes h^{-1}. Furthermore, over the ~~Bismark~~ Sea, while the diurnal minimum in Prec is around 18:00 LT, there are several local minima in Flash (08:00, 14:00 and 18:00 LT). Over NAusSea, the diurnal minimum of Prec is delayed by more than 7 hours compared to the diurnal minimum of Flash.

To summarize, over ~~island~~islands, Flash and Prec convective increasing phases start at the same time and increase similarly but the diurnal maximum of Flash is reached 1–2 hours before the diurnal maximum of Prec. Over seas, the duration of the convective increasing phase and the amplitude of the diurnal cycles are not always similar depending on the area considered. The diurnal cycle of Flash ~~is advanced by 4 hours~~ over Java Sea and West Sumatra Sea ~~and by more than 7 hours over North Australia Sea compared to~~ is 4 hours ahead of the diurnal cycle of Prec, and over North Australia Sea, it is more than 7 hours ahead. China Sea and ~~Bismark~~ Bismarck Sea present the same time of the onset of the Flash and Prec increasing phase. In Section 7, we estimate ΔIWC over the 5 selected island and sea areas from Prec and Flash as a proxy of deep convection.

6 Horizontal distribution of IWC from ERA5 reanalyses

The ERA5 ~~reanalyses provide~~ reanalysis provides hourly IWC at 150 and 100 hPa (IWC^{ERA5}). The diurnal cycle of IWC^{ERA5} over the MariCont ~~from ERA5~~ will be used to calculate ΔIWC~~from ERA5~~ ^{ERA5} in order to ~~assess~~ support the horizontal distribution and the amount of ice injected in the UT and the TL deduced from our model combining ~~MLS ice and TRMM Prec or MLS ice~~ IWC^{MLS} and TRMM-3B42 Prec or IWC^{MLS} and LIS flash. Since IWC^{ERA5} data quality has not yet been fully evaluated, this may impact on the consistency or lack of thereof found in the comparisons between ΔIWC^{ERA5} and both ΔIWC^{Prec} and ΔIWC^{Flash}. Figures **??**a, b, c and d present the daily mean and the hour of the diurnal maxima of IWC^{ERA5} at 150 and 100 hPa. In the UT, the daily mean of IWC^{ERA5} shows a horizontal distribution over the MariCont ~~consistently~~ consistent with that of IWC^{MLS} (Fig. **??**e), except over ~~NewGuinea~~ New Guinea where IWC^{ERA5} (~~reaching~~ exceeding 6.4 mg m^{-3}) is much stronger than IWC^{MLS} ($\sim$ 4.0 mg m^{-3}). The highest amount of IWC^{ERA5} is located over ~~NewGuinea~~ New Guinea mountain chain and in the West coast of North Australia (~~reaching~~ exceeding 6.4 mg m^{-3} in the UT and 1.0 mg m^{-3} in the TL). Over islands in the UT and the TL, the hour of the IWC^{ERA5} diurnal maximum is found between 12:00 LT and 15:00 LT over Sulawesi and New Guinea and between 15:00 LT and 21:00 LT over Sumatra, Borneo and Java, ~~that~~ which is close to the hour of the diurnal maximum of Flash over islands (Fig. **??**). Over sea, in the UT and the TL, the hour of the IWC^{ERA5} diurnal maximum is found between 06:00 LT and 09:00 LT over West Sumatra Sea, Java Sea, North Australia Sea, between 06:00 LT and 12:00 LT over China Sea and between 00:00 LT and 03:00 LT over ~~Bismark~~ Bismarck Sea. There are no significant differences between the hour of the maximum of IWC^{ERA5} in the UT and in the TL.

The diurnal cycles of IWC^{ERA5} at 150 hPa are presented in Figs. **??** and **??** over the selection of islands and seas of the MariCont together with the diurnal cycles of Prec and Flash. Over islands (Fig. **??**), the maximum of the diurnal cycle of IWC^{ERA5} is found between 16:00 LT and 17:00 LT, consistent with the diurnal cycle of Prec and Flash. The ~~duration~~ durations

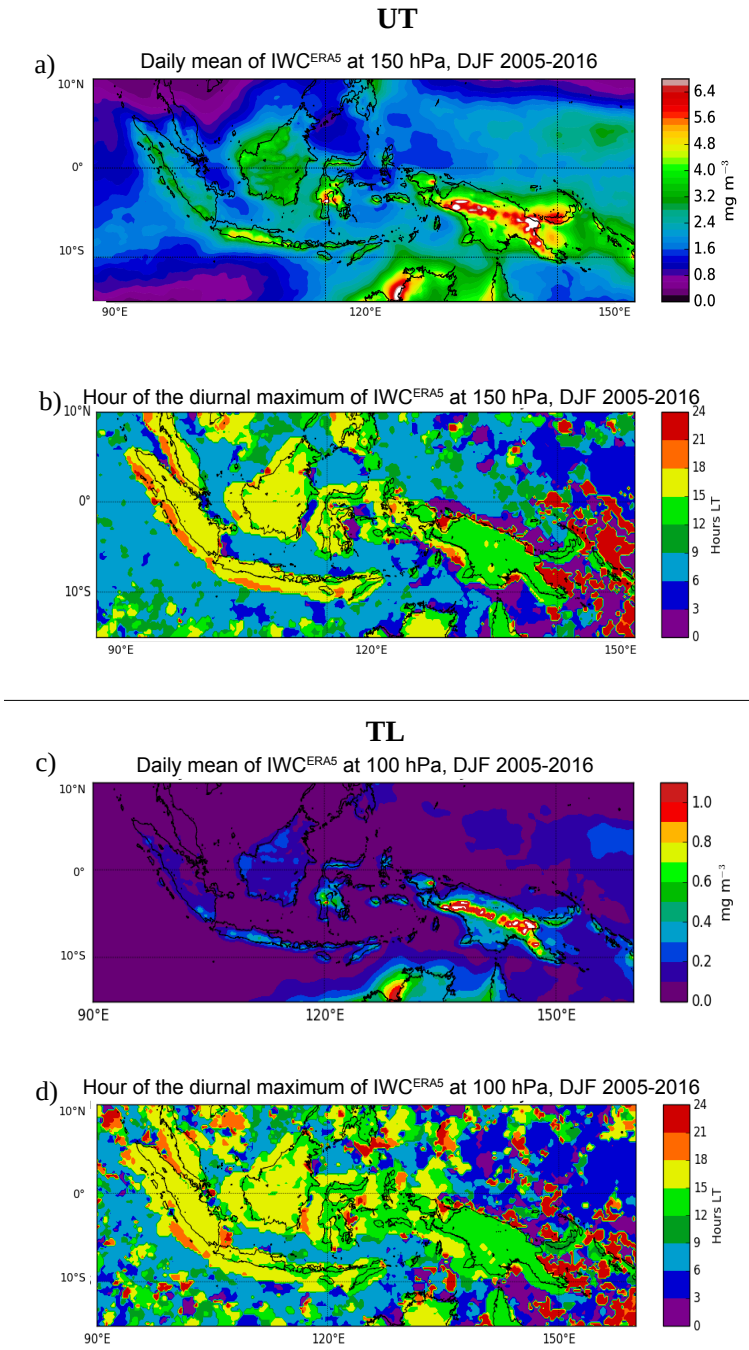

Figure 10. Daily mean of IWC^{ERA5} averaged over the period DJF 2005-2016 at 150 hPa (a) and at 100 hPa (c); Time (hour, local time (LT)) of the diurnal maximum of IWC^{ERA5} at 150 hPa (b) and at 100 hPa (d).

of the increasing phase of the diurnal cycles of Prec, Flash and IWC^{ERA5} are all consistent to each other (6 – 8 h). Over sea (Fig. **??**), the maximum of the diurnal cycle of IWC^{ERA5} is mainly found between 07:00 LT and 10:00 LT over Java Sea and North Australia Sea, ~~consistently~~ consistent with the diurnal cycle of Prec, and a second peak is found around 16:00 LT. Thus, the duration of the increasing phase of the diurnal cycles of IWC^{ERA5} is consistent with the one of Prec over these two sea study zones (∼10 hours), but not with the one of Flash. Over ~~Bismark~~ Bismarck Sea, the diurnal maxima of IWC^{ERA5} are found at 04:00 LT with a second peak later at noon. Over West Sumatra Sea, two diurnal maxima are found at 08:00 LT and 17:00 LT. Over China Sea, the diurnal maximum of IWC^{ERA5} ~~are~~ is found at 16:00 LT with a second peak at 08:00 LT. These differences in the timing of the maximum of the diurnal cycle of Prec, Flash and ~~IWCERA5~~ IWC^{ERA5} observed at small-scale over sea of the MariCont are not well understood. However, these differences do not impact on the calculation of the Δ~~IWCPrec~~IWC^{Prec}, Δ~~IWCFlash~~ IWC^{Flash} or Δ~~IWCERA5. Results are presented Section 7.~~ IWC^{ERA5}, because only the magnitude of the diurnal cycle (max-min) matters for the calculation of ΔIWC.

7 Ice injected over a selection of island and sea areas

7.1 ~~ΔIWC deduced from observations~~

Figure **??** synthesizes ΔIWC deduced from observations and reanalysis in the UT and the TL over the 5 islands and 5 seas of the MariCont studied in the previous section.

7.1 ΔIWC deduced from observations

Eqs. (1-3) are used to calculate ΔIWC from Prec (ΔIWC^{Prec}) and from Flash (ΔIWC^{Flash}). As presented in the previous section, Prec and Flash can be used as two proxies of deep convection, ~~with differences more or less accentuated~~ although differences in their diurnal cycles may be present as a function of the region considered. Thus, the observational ΔIWC range calculated between ΔIWC^{Prec} and ΔIWC^{Flash} provides an upper and lower bound of ΔIWC calculated from observational datasets. In the following, we will consider the relative difference between ΔIWC^{Prec} and ΔIWC^{Flash} as:

$$(\Delta IWC^{Prec} + \Delta IWC^{Flash}) \times 0.5 \quad (4)$$

In the UT (Fig. **??**a), over islands, ΔIWC calculated over Sumatra, Borneo, Sulawesi and New Guinea varies from 4.9 to 6.9 mg m^{-3} ~~whilst~~whereas, over Java, ΔIWC reaches 7.9–8.7 mg m^{-3}. ΔIWC^{Flash} is generally greater than ΔIWC^{Prec} by

~~less than 1.0~~ 0.8 mg m^{-3} ((~~ΔIWC^{Flash}~~ with $r^{Prec-Flash}$ ranges from - ~~ΔIWC^{Prec})/ΔIWC^{Flash})~~×100 ranges from 4 to~~ 6 to - 22% over the study zone) for all the islands, except for Java where ΔIWC^{Prec} is larger than ΔIWC^{Flash} by ~~0.7~~ 0.8 mg m^{-3} (~~-8~~$r^{Prec-Flash}$ = 7.1%). Over sea, ΔIWC varies from 1.2 to 4.4 mg m^{-3}. ΔIWC^{Flash} is greater than ΔIWC^{Prec} by 0.6 to 2.1 mg m^{-3} (~~31-50~~$r^{Prec-Flash}$ = - 35 to - 71%), except for Java Sea, where ΔIWC^{Prec} is greater than ΔIWC^{Flash} by 0.2 mg m^{-3} (~~-7~~$r^{Prec-Flash}$ = 6%). Over North Australia Sea and West Sumatra Sea, ΔIWC^{Flash} ~~is almost~~ are more than twice as large as ~~than~~ ΔIWC^{Prec} (~~53%~~ $r^{Prec-Flash}$ = - 63% and - 71%, respectively).

In the TL (Fig. **??**b), the observational ΔIWC range is found between 0.7 and 1.3 mg m^{-3} over islands and between 0.2 and 0.7 mg m^{-3} over seas. The same conclusions apply to the observational ΔIWC range calculated between ΔIWC^{Prec} and ΔIWC^{Flash} in the TL as in the UT with differences less than 0.4 mg m^{-3}.

To summarize, independently of the proxies used for the calculation of ΔIWC, and at both altitudes, Java island shows the largest injection of ice over the MariCont. Observational ΔIWC over Java island is larger by about 1.0 mg m^{-3} in the UT and about 0.3 mg m^{-3} in the TL than other land study zones. Furthermore, it has been shown that both proxies can be used in our model, with more confidence over land: ΔIWC^{Prec} and ΔIWC^{Flash} are consistent to each other to within ~~4-22% over island and 7-53% over sea~~ $r^{Prec-Flash}$ = - 6 to -22% over islands and $r^{Prec-Flash}$ = +6 to -71% over seas in the UT and the TL. The largest difference over ~~sea~~ seas is probably due to the larger contamination ~~of~~ by stratiform precipitation included in Prec over sea.

7.2 ΔIWC deduced from ~~reanalyses~~reanalysis

ΔIWC from ERA5 (ΔIWC$^{ERA5}_{z_0}$) is calculated in the UT and the TL (z_0 = 150 and 100 hPa, respectively) as the max–min difference in the amplitude of the diurnal cycle. ~~Consistently with the MLS observations, we have degraded the ERA5 vertical resolution~~ We can use the IWC^{ERA5} to assess the impact of the vertical resolution ~~on~~ of the MLS measurements on the observationally-derived ΔIWC ^{ERA5}estimates. According to Wu et al. (2008), ~~IWC^{MLS} estimation~~ estimates of IWC derived from MLS represent spatially-averaged quantities within a volume that can be approximated by a box of ~~~~ 300×7×4 km^3 near the pointing tangent height. In order to compare IWC^{MLS} and IWC^{ERA5}, ~~we degraded~~two steps were taken: 1) the horizontal resolution of ERA5 was degraded from 0.25°×0.25° to 2°×2° (~~~~ 200 km×200 km), and 2) the vertical resolution of ERA5 ~~data by connecting~~ was degraded by convolving the vertical profiles of IWC^{ERA5} with a ~~unitary~~ box function whose width is 5 and 4 km at 100 and 146 hPa, respectively.

~~Consistently with ?, we have fixed δz = 4 and 5 km at z_0 = 146 and 100 hPa, respectively.~~ The ice injected from ERA5 at z_0 = 146 and 100 hPa with degraded vertical resolution ($\langle \Delta IWC^{ERA5}_{z_0} \rangle$) is thus calculated from $\langle IWC^{ERA5}_{z_0} \rangle$. In the following we can consider the difference $r^{ERA5-\langle ERA5 \rangle}$ between ΔIWC^{ERA5} and $\langle \Delta IWC^{ERA5} \rangle$ as:

$$r^{ERA5-\langle ERA5 \rangle} = 100 \times \frac{\Delta IWC^{ERA5} - \langle \Delta IWC^{ERA5} \rangle}{(\Delta IWC^{ERA5} + \langle \Delta IWC^{ERA5} \rangle) \times 0.5} \quad (5)$$

Figure **??** shows ~~ΔIWC^{ERA5}~~ $\Delta IWC^{ERA5}_{z_0}$ and $\langle \Delta IWC^{ERA5}_{z_0} \rangle$ at z_0 = 150 and 100 hPa, over the island and the sea study zones. In the UT (Fig. **??**a), over islands, ΔIWC^{ERA5}_{150} and $\langle \Delta IWC^{ERA5}_{150} \rangle$ calculated over Sumatra and Borneo vary

from 4.9 to 7.0 mg m^{-3} (~~the relative variation calculated as $((\Delta IWC^{ERA5} - \langle \Delta IWC^{ERA5} \rangle)/\Delta IWC^{ERA5}) \times 100$ is 18-19~~ $r^{ERA5-\langle ERA5 \rangle}$ ranges from 20 to 22 %) whilst ΔIWC_{150}^{ERA5} and $\langle \Delta IWC_{150}^{ERA5} \rangle$ over Java, Sulawesi and New Guinea reach 7.5–10.0 mg m^{-3} (~~~19-22 %of variability per study zone~~$r^{ERA5-\langle ERA5 \rangle}$ = 21 to 24 %). Over sea, ΔIWC_{150}^{ERA5} and $\langle \Delta IWC_{150}^{ERA5} \rangle$ vary from 0.35 to 1.1 mg m^{-3} ($r^{ERA5-\langle ERA5 \rangle}$ = 9 ~~– 32 %of variability per study zone~~to 33 %). Over island and sea, ΔIWC_{150}^{ERA5} is greater than $\langle \Delta IWC_{150}^{ERA5} \rangle$. The small differences between ΔIWC_{150}^{ERA5} and $\langle \Delta IWC_{150}^{ERA5} \rangle$ over island and sea in the UT support the fact that the vertical resolution at 150 hPa has a low impact on the estimated ΔIWC.

In the TL, over land, ΔIWC_{100}^{ERA5} and $\langle \Delta IWC_{100}^{ERA5} \rangle$ vary from 0.5 to ~~3.7~~ 3.9 mg m^{-3} (~~~68%of variability per study zone~~$r^{ERA5-\langle ERA5 \rangle}$ = -32 to -138%) with $\langle \Delta IWC_{100}^{ERA5} \rangle$ being larger than ΔIWC_{100}^{ERA5} by less than ~~2.1~~ 2.5 mg m^{-3}. Over sea, ΔIWC_{100}^{ERA5} and $\langle \Delta IWC_{100}^{ERA5} \rangle$ vary from 0.05 to 0.4 mg m^{-3} (~~~71 %of variability per study zone~~$r^{ERA5-\langle ERA5 \rangle}$ = -85 to -139%) with ΔIWC_{100}^{ERA5} lower than $\langle \Delta IWC_{100}^{ERA5} \rangle$ by ~~less than~~ as much as 0.2 mg m^{-3}. The large differences between ΔIWC_{100}^{ERA5} and $\langle \Delta IWC_{100}^{ERA5} \rangle$ over island and sea in the TL support the fact that the vertical resolution at 100 hPa has a high impact on the estimation of ΔIWC.

7.3 Synthesis

The comparison between the observational ΔIWC range and the reanalysis ΔIWC range is presented in Fig. **??**. In the UT, over land, observation and reanalysis ΔIWC ranges ~~overlap (~~agree to within 0.1 to 1.0 mg m^{-3}~~)~~, which highlights the robustness of our model over land, except over Sulawesi and New Guinea, where the observational ~~ΔIWC range~~ and the reanalysis ΔIWC range differ by at least 1.7 and 0.7 mg m^{-3}, respectively~~)~~. Over sea, the observational ΔIWC range is systematically greater than the reanalysis ~~ΔIWC range~~ by ∼ 1.0 – 2.2 mg m^{-3}~~(75 %)~~, showing a systematic ~~positive bias and a too large variability range in our model over sea compared to ERA5. Combining~~ larger estimate derived from observation than derived from reanalysis. The consistency between observational and reanalysis ΔIWC range is calculated as the difference between the minimal value of the largest range minus the maximum value of the lowest range divided by the mean of these two values. In the UT, over land, observational and reanalysis ΔIWC are found consistent to within 0 to 25% while over sea they are inconsistent (to within 62 to 96%) in the UT. In the TL, observational and reanalysis ~~ranges, the total ΔIWC variation range~~ΔIWC ranges are consistent to within 0 to 49% over land and to within 0 to 28% over sea. In the following we will consider r^{Total} as the relative differences between the minimal value of the lower range minus the maximum value of the largest range divided by the mean of these two values. The range between observational and reanalysis ranges is named the total IWC range, and is estimated in the UT between 4.2 and 10.0 mg m^{-3} (~~~ 20 %of variability per study zone~~r^{Total} from 8 to 59%) over land and between 0.3 and 4.4 mg m^{-3} (~~~ 30 %of variability per study zone~~r^{Total} from 104 to 149%) over sea and, in the TL, between ~~0.6 and 3.9~~ 0.5 and 3.7 mg m^{-3} (~~~ 70 %of variability per study zone~~r^{Total} = 85 to 127%) over land, and between 0.1 and 0.7 mg m^{-3} (~~~ 80 %of variability per study zone~~r^{Total} = 142 to 160%) over sea.

~~The amounts~~

Amounts of ice injected ~~in the UT~~ deduced from observations and reanalysis are consistent to each other over ~~MariCont_L, Sumatra, Borneo and Java, with significant differences over Sulawesi, New Guinea (within 1.7 to 0.7 mg m^{-3}, respectively) and all individual offshore study zones (within 0.7 to 2.1 mg m^{-3}). The~~ land in the UT and over land and sea in the TL

(to within 0 to 49%) but inconsistent over sea in the UT (up to 96%). However, the impact of the vertical resolution on the estimation of ΔIWC is much larger in the UT than in the TL (r^{Total} is larger in the TL ~~is certainly non negligible, with larger ΔIWC variability range in the TL (70 – 80 %)~~ than in the UT~~(20 – 30 %)~~). At both levels, observational and reanalyses ΔIWC estimated over land is more than twice as large as ΔIWC estimated over sea. ~~Finally,~~ Java island presents the highest observational and reanalysis ΔIWC range in the UT (between 7.7 and 9.5 mg m^{-3} daily mean, r^{Total} = 21%). However, whatever the level considered, although Java has shown particularly high values in the observational ΔIWC range compared to other study zones, the reanalysis ΔIWC range shows that Sulawesi and ~~NewGuinea~~ New Guinea would also be able to reach similar high values of ΔIWC as Java (assuming that ERA5 IWC data have not yet been evaluated).

8 Discussion on small-scale convective processes impacting ΔIWC over a selection of areas

Our results have shown that, in all the datasets used, Java island and Java Sea are the two areas with the largest amount of ice injected up to the UT and the TL over the MariCont land and sea, respectively. In this section, processes impacting ΔIWC in the different study zones are discussed.

8.1 Java island, Sulawesi and New Guinea

Sulawesi, New Guinea and particularly Java island have been shown as the areas of the largest ΔIWC in the UT and TL. **?** have used high resolution observations and regional climate model simulations to show the three main processes impacting the diurnal cycle of rainfall over the Java island. The main process explaining the rapid and strong peak of Prec during the afternoon over Java (Fig. **??**a) is the sea-breeze convergence around midnight. This convergence caused by sea-breeze phenomenon increases the deep convective activity and impacts on the diurnal cycle of Prec and on the IWC injected up to the TL by amplifying their quantities. The second process is the mountain-valley wind converging toward the mountain peaks, and reinforcing the convergence and the precipitation. The land breeze becomes minor compared to the mountain-valley breeze and this process is amplified with the mountain altitude. As shown in Fig. **??**b, ~~NewGuinea~~ New Guinea has the highest mountain chain of the MariCont. The third process shown by **?** is precipitation that is amplified by the cumulus merging processes which ~~is~~ are processes more important over small islands such as Java (or Sulawesi) than over large islands such as Borneo or Sumatra. Another process is the interaction between sea-breeze and precipitation-driven cold pools that generates lines of strong horizontal moisture convergence (**?**). Thus, IWC is increasing proportionally with Prec consistent with the results from **?** and rapid convergence combined with deep convection transports elevated amounts of IWC at 13:30 LT (Fig. **??**) producing high ΔIWC during the growing phase of the convection (Fig. **??** and Fig. **??**) over Java Island.

8.2 West Sumatra Sea

In section **??**, it has been shown that the West Sumatra Sea is an area with positive anomaly of Prec during the growing phase of the convection but negative anomaly of IWC, which differs from other places. These results suggest that Prec is representative not only of convective precipitation but also of stratiform precipitation. The diurnal cycle of stratiform and

convective precipitations over West Sumatra Sea has been studied by **?** using 3 years of TRMM precipitation radar (PR) datasets, following the ~~2A23Algorithm~~ 2A23 Algorithm (Awaka, 1998). ~~The authors~~ **?** have shown that rainfall over Sumatra is characterized by convective activity with a diurnal maximum between 15:00 LT and 22:00 LT while, over the West Sumatra Sea, the rainfall type is convective and stratiform, with a diurnal maximum during the early morning (as observed in Fig. **??**). Furthermore, their analyses have shown a strong diurnal cycle of 200-hPa wind, humidity and stability, consistent with the PR over ~~Sumatra West~~ West Sumatra Sea and Sumatra Island. Stratiform and convective clouds are both at the origin of heavy rainfall in the tropics (**??**) and in the West Sumatra Sea, but stratiform clouds are mid-altitude clouds in the troposphere and do not transport ice up to the tropopause. Thus, over the West Sumatra Sea, the calculation of ΔIWC estimated from Prec is possibly overestimated because Prec include a non-negligible amount of stratiform precipitation over this area.

8.3 North Australia Sea and seas with nearby islands

The comparisons between Figs. 2c and 6a have shown strong daily mean of Flash (10~~−2~~ $^{-2}$ –10~~−1 flashes day−1~~ $^{-1}$ flashes day^{-1}) but low daily mean of Prec (2.0 – 8.0 mm day~~−1~~$^{-1}$) over the North Australia Sea. Additionally, Fig. 11 shows that the strongest differences between ΔIWC^{Prec} and ΔIWC^{Flash} are found over the North Australia Sea, with ΔIWC^{Flash} greater than ΔIWC^{Prec} by 2.3 mg m~~−3~~ $^{-3}$ in the UT ($r^{Prec-Flash}$ = ~71%) and by 0.4 mg m~~−2~~ $^{-3}$ in the TL (~~53%of variability between ΔIWC^{Flash} and ΔIWC^{Prec}~~ $r^{Prec-Flash}$ = - 75%). These results imply that the variability range in our model is too large ~~and highlight~~ highlighting the difficulty to estimate ΔIWC over this study zone. Furthermore, as for Java Sea or Bismarck Sea, North Australia Sea ~~has the particularity to be surrounding~~ is surrounded by several islands. According to the study from **?**, the cloud size is the largest during the afternoon over the North Australia land, during the night over North Australia coastline and during the early morning over the North Australia sea. These results suggest that deep convective activity moves from the land to the sea during the night. Over the North Australia Sea, it seems that the deep convective clouds are mainly composed ~~by~~ of storms with lightning but ~~precipitationd are weak or do~~ precipitation is weak or does not reach the surface ~~and evaporating before .~~ before evaporating.

9 Conclusions

The present study has combined observations of ice water content (IWC) measured by the Microwave Limb Sounder (MLS), precipitation (Prec) from the algorithm 3B42 of the Tropical Rainfall Measurement Mission (TRMM), the number of flashes (Flash) from the Lightning Imaging Sensor (LIS) on board of TRMM with IWC provided by the ERA5 reanalyses in order to estimate the amount of ice injected (ΔIWC) in the upper troposphere (UT) and the tropopause level (TL) over the MariCont, from the method proposed in a companion paper (**?**). ~~ΔIWC is firstly calculated using the IWC measured by MLS (IWC^{MLS}) in~~ The study is focused on the austral convective season of DJF from 2004 to ~~2017 at the temporal resolution of 2 observations per day and Prec fromTRMM-3B42 during the same period, to obtain a 1-hour resolution diurnal cycle.~~ 2017. In the model used (**?**), Prec is considered as a proxy of deep convection ~~impacting~~ injecting ice (ΔIWC^{Prec}) in the UT and the TL. ΔIWC^{Prec} is firstly calculated by the correlation between the growing phase of the diurnal cycle of Prec from TRMM-3B42 (binned at a

1-hour diurnal cycle) and the value of IWC measured by MLS (IWC^{MLS}, provided at the temporal resolution of 2 observations in local time per day) selected among the growing phase of the diurnal cycle of Prec. While ? have calculated ΔIWC^{Prec} over large convective study zones in the tropics, we show the spatial distribution of ΔIWC^{Prec} ~~into~~ in the UT and the TL at 2° × 2° horizontal resolution over the MariCont, highlighting local areas of strong injection of ice up to 20 mg m^{-3} in the UT and up to 3 mg m^{-3} in the TL. ΔIWC injected in the UT and the TL has also been evaluated by using another proxy of deep convection: Flash measured by TRMM-LIS. Diurnal cycle of Flash has been compared to diurnal cycle of Prec, showing consistencies in 1) the spatial distribution of Flash and Prec over the MariCont (maxima of Prec and Flash located over land and coastline), and 2) their diurnal cycles over land (similar onset and duration of the diurnal cycle increasing phase). Differences have been mainly observed over sea and coastline areas, with the onset of the diurnal cycle increasing phase of Prec delayed by several hours depending on the considered area (from 2 to 7 h) compared to Flash. ΔIWC calculated by using Flash as a proxy of deep convection (ΔIWC^{Flash}) is compared to ΔIWC^{Prec} over five islands and five seas of the MariCont to establish an observational ΔIWC range over each study zone. ΔIWC is also estimated from IWC provided by the ERA5 reanalyses (ΔIWC^{ERA5} and IWC^{ERA5}, respectively) at 150 and 100 hPa over the study zones. We have also degraded the vertical resolution of IWC^{ERA5} to be consistent with that of IWC^{MLS} observations: 4 km at 146 hPa and 5 km at 100 hPa. The ΔIWC ranges calculated from observations and reanalyses were evaluated over the selected study zones (island and sea).

With the study of ΔIWC^{Prec}, results show that the largest amounts of ice injected in the UT and TL per 2° × 2° pixels are related to i) an amplitude of Prec diurnal cycle larger than 0.5 mm h^{-1} ~~, ii) values of IWC measured during the growing phase of the convection larger than 4.5 mg m^{-3} and iii)~~ and ii) a duration of the growing phase of the convection longer than 9 hours. The largest ΔIWC^{Prec} has been found over areas where the convective activity is the deepest. ~~The observational~~ ΔIWC~~range calculated between ΔIWC^{Prec}~~ and ΔIWC^{Flash} ~~has been found to be within 4 – 22~~ depart from -6 to -22 % over land and to ~~within 7 – 53~~ -6 to -71 % over sea. The largest differences between ΔIWC^{Prec} and ΔIWC^{Flash} over sea might be due to the combination of the presence of stratiform precipitation included ~~into~~ in Prec and the very low values of Flash over seas (<10^{-2} flashes day^{-1}). The diurnal cycle of IWC^{ERA5} at 150 hPa is more consistent with that of Prec and Flash over land than over ocean. Finally, ~~the observational~~ ΔIWC ~~range~~ estimated from observations has been shown to be consistent with ~~the reanalysis~~ ΔIWC ~~range to within 23~~ estimated from reanalysis to within 25% over land ~~and to within 30-50 % over sea in the UT~~ in the UT, to within 48 % over land in the TL and to within ~~49 % over land and to within 39~~ 28 % over sea in the TL, but inconsistent to within 96 % over sea in the ~~TL~~UT. Thus, thanks to the combination ~~between~~ of the observational and reanalysis ΔIWC ranges, the total ΔIWC ~~variation~~ range has been found in the UT to be between 4.2 and 10.0 mg m^{-3} ~~(to within 20 % per study zones)~~ over land and between 0.3 and 4.4 mg m^{-3} ~~(to within 30 % per study zones)~~ over sea and, in the TL, between ~~0.6 and 3.9~~ 0.5 and 3.7 mg m^{-3} ~~(to within 70 % per study zones)~~ over land and between 0.1 and 0.7 mg m^{-3} ~~(to within 80% per study zones)~~ over sea. The ~~ΔIWC variation range in the TL is larger than that in the UT highlighting the stronger~~ impact of the vertical resolution ~~in the observations~~ on the estimation of ΔIWC has been found higher in the TL ~~compared to~~ than in the UT.

The study at small scale over islands and seas of the MariCont has shown that ΔIWC from ERA5, Prec and Flash in the UT agree to within ~~0~~ 0.1 – ~~0.6~~ 1.0 mg m^{-3} ~~(8%)~~ over MariCont_L, Sumatra, Borneo and Java with the largest values obtained

over Java ~~. However, while Java~~ Island. Based on observations, the Java Island presents the largest amount of ~~ΔIWC^{Prec} and ΔIWC^{Flash}~~ ice in the UT and the TL (larger by about 1.0 mg m^{-3} in the UT and about 0.3 mg m^{-3} in the TL than other land study zones). Based on the reanalysis, New Guinea and Sulawesi reach similar ranges of ~~values of ice injected with ERA5 thanJava~~ ice injection in the UT and even larger ranges of values ~~as Java~~ in the TL than the Java Island keeping in mind that ERA5 IWC data have not yet been evaluated. Processes related to the strongest amount of ΔIWC injected into the UT and the TL have been identified as the combination of sea-breeze, mountain-valley breeze and merged cumulus, ~~such as over NewGuinea and~~ accentuated over small islands with high topography such as Java or Sulawesi.

Author contributions. IAD analysed the data, formulated the model and the method combining MLS, TRMM and LIS data and took primary responsibility for writing the paper. CD has treated the LIS data, provided the Figures with Flash datasets, gave advices on data processing and contributed to the Prec and Flash comparative analysis. PR strongly contributed to the design of the study, the interpretation of the results and the writing of the paper. PR, FC, PH and TD provided comments on the paper and contributed to its writing.

Acknowledgements. We thank the National Center for Scientific Research (CNRS) and the Excellence Initiative (Idex) of Toulouse, France to fund this study and the project called Turbulence Effects on Active Species in Atmosphere (TEASAO – http://www.legos.obs-mip.fr/projets/axes-transverses-processus/teasao, last access: May 2020, Peter Haynes Chair of Attractivy). We would like to thank the teams that have provided the MLS data (https://disc.gsfc.nasa.gov/datasets?page=1&keywords=ML2IWC_004, last access: ~~June 2019~~May 2020), the TRMM data (https://pmm.nasa.gov/data-access/downloads/trmm), the LIS data (https://ghrc.nsstc.nasa.gov/lightning/data/data_lis_trmm.html, last access: ~~June 2019) ,~~ May 2020) and the ERA5 Reanalysis data (https://cds.climate.copernicus.eu/cdsapp#!/dataset/reanalysis-era5-pressure-levels-monthly tab=form, last access: ~~June 2019), and the NCEP Reanalysis data provided by the NOAA/OAR/ESRL PSD, Boulder, Colorado, USA, (, last access: June 2019).~~ May 2020). We would like to thank both reviewers for their helpful comments and especially Michelle Santee for the many very detailed comments she provided that were invaluable in improving the study.

Main acronyms list

ΔIWC: Amount of ice injected by deep convection up to the study pressure level
ΔIWC^{Prec}: ΔIWC estimated from Prec and from IWC^{MLS}
ΔIWC^{Flash}: ΔIWC estimated from Flash and from IWC^{MLS}
ΔIWC^{ERA5}: ΔIWC estimated from ERA5 reanalysis
$\langle \Delta IWC^{ERA5} \rangle$: ΔIWC^{ERA5} degraded along the vertical at the study pressure level consistently with the MLS vertical resolution of IWC^{MLS}
DJF: December, January, February
Flash: number of Flashes
IWC: Ice water content

IWC^{ERA5}: IWC from ERA5 reanalysis

IWC^{MLS}: IWC measured by MLS

LS: Lower stratosphere

MariCont: Maritime Continent

MariCont_C: Coastlines of the Maritime Continent

MariCont_O: Maritime Continent ocean

MariCont_L: Maritime Continent land

MLS: Microwave Limb Sounder

NAuSea: North Australia Sea

Prec: Precipitation

TTL: Tropical tropopause Layer

UT: Upper troposphere

UTLS: Upper troposphere and lower stratosphere

WSumSea: West Sumatra Sea

WV: Water vapour

References

J. Awaka. Awaka, J.: Algorithm 2A23 —. Rain type classification. In Proc. Symp. on the Precipitation Observation from Non-Sun Synchronous Orbit, pages 215–220, 1998.

Carbone, R. E.Carbone, , Wilson, J. W.Wilson, , Keenan, T. D. Keenan, and and Hacker, J. M.Hacker. : Tropical island convection in the absence of significant topography. part i: Life , part I: life cycle of diurnally forced convection. Monthly weather review, 128(10):3459–3480, 2000.

L.Chappel.

Chappel, L.: Assessing severe thunderstorm potential days and storm types in the tropics. In Presentation at the International Workshop on the Dynamics and Forecasting of Tropical Weather Systems, Darwin, 22-26 January 2001, 2001.

Christian, H. J. , Blakeslee, R. J., Goodman, S. J.: Lightning Imaging Sensor (LIS) for the international space station. In American Institute of Physics Conference Proceedings, Vol. 504, No. 1, pp. 423-428, 2000.

T. Dauhut, J.-P. Dauhut, T. ,Chaboureau, J.Escobar, and P. Mascart. -P. , Escobar, J. and Mascart, P.: Giga-LES of hector the convector Hector the Convector and its two tallest updrafts up to the stratosphere. Journal of the Atmospheric Sciences, 73(12):5041–5060, 2016.

T. Dauhut, Dauhut, T. , Chaboureau, J.-P.Chaboureau, P. Mascart, and T. Lane. , Mascart, P. and Lane, T.: The overshoots that hydrate the stratosphere in the tropics. In EGU General Assembly Conference Abstracts, volume 20, page 9149, 2018.

Dion, I.-A.Dion, P. , Ricaud, P. Haynes, F. Carminati, and T. Dauhut. , Haynes, P. , Carminati, F. and Dauhut, T.: Ice injected into the tropopause by deep convection – part 1: In in the austral convective tropics. Atmospheric Chemistry and Physics, 19(9):6459–6479, 2019.

Duncan, D., Eriksson, P.: An update on global atmospheric ice estimates from observations and reanalyses. In EGU General Assembly Conference Abstracts (Vol. 20, p. 13448), 2018.

S. Fueglistaler, Fueglistaler, S., Dessler, A. E.Dessler, , Dunkerton, T. J.Dunkerton, I. Folkins, Q.Fu, and Folkins, I., Fu, Q. and Mote, P. W.Mote. : Tropical tropopause layer. Reviews of Geophysics, 47(1), 2009a. doi: 10.1029/2008RG000267. URL https://agupubs.onlinelibrary. wiley.com/doi/abs/10.1029/2008RG000267. , 2009a.

Geer, A. J.Geer, F. Baordo, N. Bormann, P. Chambon, , Baordo, F., Bormann, N., Chambon, P., English, S. J. English, M. Kazumori, ... C. Lupu. , Kazumori, M. et al.: The growing impact of satellite observations sensitive to humidity, cloud and precipitation. Quarterly Journal of the Royal Meteorological Society, 143(709), 3189-3206, 2017.

R. Goler, Goler, R., Reeder, M. J.Reeder, , Smith, R. K.Smith, H. Richter, S.Arnup, T.KeenanRichter, P.May, and J. Hacker. H., Arnup, S., Keenan, T., May, P. and Hacker, J.: Low-level convergence lines over North Eastern australia. part i: The Australia. part I: the North Australian cloud line. Monthly weather review, 134(11):3092–3108, 2006.

H. Hatsushika and K. Yamazaki. Interannual Hatsushika, H. and Yamazaki, K.: Inter-annual variations of temperature and vertical motion at the tropical tropopause associated with ENSO. Geophysical research letters, 28(15):2891–2894, 2001.

H. Hersbach. Hersbach, H.:Operational global reanalysis: progress, future directions and synergies with NWP. European Centre for Medium Range Weather Forecasts, 2018.

Houze, R. A. Houze and and Betts, A. K.Betts. : Convection in gate. Reviews of Geophysics, 19(4):541–576, 1981.

Huffman, G. J. Huffman, ,Bolvin, D. T.Bolvin, , Nelkin, E. J.Nelkin, , Wolff, D. B.Wolff, , Adler, R. F.Adler, G. Gu, Y. Hong, , Gu, G., Hong, Y., Bowman, K. P. Bowman, and and Stocker, E. F.Stocker. The TRMM multisatellite : The TRMM multi-satellite precipitation analysis (TMPA): quasi-global, multiyear, combined-sensor precipitation estimates at fine scales. Journal of hydrometeorology, 8(1):38–55, 2007.

Huffman, G. J., Adler, R. F., Bolvin, D. T., Nelkin, E. J.Jensen: The TRMM Multi-satellite Precipitation Analysis (TMPA) in Satellite rainfall applications for surface hydrology. Springer, Dordrecht, 3-22, 2010.

Huffman, G. J., Bolvin, D. T.: Real-time TRMM Multi-satellite Precipitation Analysis data set documentation. Available online: URL https://gpm.nasa.gov/sites/default/files/document_files/3B4XRT_doc_V7_180426.pdf (last access: April 2020).

Jensen, E. J., Ackerman, A. S.Ackerman, , Smith, J. A.Smith (2007). : Can overshooting convection dehydrate the tropical tropopause layer?. Journal of Geophysical Research: Atmospheres, 112(D11), 2007.

C. Liu and Liu, C. and Zipser, E. J.Zipser. : Global distribution of convection penetrating the tropical tropopause. Journal of Geophysical Research: Atmospheres, 110(D23), 2005.

C. Liu and Liu, C. and Zipser, E. J.Zipser. : Diurnal cycles of precipitation, clouds, and lightning in the tropics from 9 years of TRMM observations. Geophys. Res. Lett., 35, L04819, doi:10.1029/2007GL032437, 2008.

Livesey, N. J., Read, W. G., Wagner, P. A., Froidevaux, L., Lambert, A., Manney, G.L., Millan, L.F., Pumphrey, H. C., Santee, M. L., Schwartz, M. J., Wang, S., Fuller, R. A., Jarnot, R. F., Knosp, B. W., Martinez, E. , and Lay, R. R.,: Version 4.2x Level 2 data quality and description doc-umentdocument, Tech. Rep. JPL D-33509 Rev. D, Jet Propulsion Laboratory, available at:http://mls.jpl.nasa.gov (last access: 01 09 2019), 2018.

P. Lopez. Lopez, P.: Direct 4D-Var assimilation of NCEP stage IV radar and gauge precipitation data at ECMWF. Monthly Weather Review, 139(7), 2098-2116, 2011.

Love, B. S.Love, , Matthews, A. J. Matthews, and and Lister, G. M. S.Lister. : The diurnal cycle of precipitation over the maritime continent Maritime Continent in a high-resolution atmospheric model. Quarterly Journal of the Royal Meteorological Society, 137(657):934–947, 2011.

L. Millán, L., Read, W.Read, , Kasai, Y.Kasai, A.Lambert, N. Livesey, , Lambert, A, Livesey, N., Mendrok, J.Mendrok, , Sagawa, H.Sagawa, , Sano, T.Sano, M.Shiotani, and , Shiotani, M. and Wu, D. L.Wu. Smiles : SMILES ice cloud products. Journal of Geophysical Research: Atmospheres, 118(12):6468–6477, 2013.

S. Mori, H. Jun-Ichi, Mori, S., Jun-Ichi, H., Tauhid, Y. I.Tauhid, , Yamanaka, M. D.Yamanaka, N. Okamoto, F.Murata, N.SakuraiOkamoto, H.Hashiguchi, and T. Sribimawati. N., Murata, F., Sakurai, N., Hashiguchi, H. and Sribimawati, T.: Diurnal land–sea rainfall peak migration over Sumatera Sumatra island, Indonesian Maritime Continent, observed by TRMM satellite and intensive rawinsonde radio sonde soundings. Monthly Weather Review, 132(8):2021–2039, 2004.

Nesbitt S. W. Nesbitt and and Zipser, E. J.Zipser. : The diurnal cycle of rainfall and convective inten- sity intensity according to three years of trmm TRMM measurements. Journal of Climate, 16(10):1456–1475, 2003.

Petersen, W. A. Petersen, and and Rutledge, S. A.Rutledge. : Regional variability in tropical convection: Observations observations from TRMM. Journal of Climate, 14(17), 3566-3586, 2001.

M. Pope, C. Jakob, and Pope, M, Jakob, C. and Reeder, M. J.Reeder. : Convective systems of the north australian North Australian monsoon. Journal of Climate, 21(19):5091–5112, 2008.

Qian, J.-H.Qian. : Why precipitation is mostly concentrated over islands in the maritime continentMaritime Continent. Journal of the Atmospheric Sciences, 65(4):1428–1441, 2008.

Ramage, C. S.Ramage. : Role of a tropical "maritime continentMaritime Continent" in the atmospheric circulation. Mon. Wea. Rev, 96(6):365–370, 1968.

Randel, W. J.Randel, F. Wu, H. Voemel, , Wu, F., Voemel, H., Nedoluha, G. E. Nedoluha, and P. Forster. and Forster, P.: Decreases in stratospheric water vapor after 2001: Links links to changes in the tropical tropopause and the brewer-dobson Brewer-Dobson circulation. Journal of Geophysical Re- search: Atmospheres, 111(D12), 2006a.

Randel, W. J. Randel and and Jensen, E.J.Jensen. : Physical processes in the tropical tropopause layer and their roles in a changing climate. Nature Geoscience, 6:169, 2013. doi: 10.1038/ngeo1733. URL https://doi.org/10.1038/ngeo1733. , 2013.

Sherwood, S. C.Sherwood. : A stratospheric "drain" over the maritime continentMaritime Continent. Geophysical research letters, 27(5):677–680, 2000.

A. Stenke and V. Grewe. Stenke A. and Grewe, V.: Simulation of stratospheric water vapor trends: impact on stratospheric ozone chemistry. Atmospheric Chemistry and Physics, 5(5): 1257–1272, 2005.

Stephens G. L. Stephens and and Greenwald, T. J.Greenwald. : The earth's radiation budget and its rela- tion relation to atmospheric hydrology: 2. observations of cloud effects. Journal of Geophysical Research: Atmospheres, 96(D8):15325–15340, 1991.

G. Y. Yang and J. Slingo. The diurnal cycle in the tropics. Monthly Weather Review, 129(4):784–801, 2001. 129<0784:TDCITT>2.0.CO;2. doi: 10.1175/1520-0493(2001) URL https://doi.org/10.1175/1520-0493(2001)129<0784:TDCITT>2.0.CO;2.

Waters, J. W.Waters, L. Froidevaux, , Froidevaux, L., Harwood, R. S.Harwood, , Jarnot, R. F.Jarnot, , Pickett, H. M.Pickett, , Read, W. G. Read, ... and Holden, J. R.Holden (2006). The earth observing system microwave limb sounder : The Earth Observing System Microwave Limb Sounder (EOS MLS) on the Aura satellite. IEEE Transactions on Geoscience and Remote Sensing, 44(5), 1075-1092. , 2006.

Wu, D. L., Jiang, J. H., Read, W. G., Austin, R. T., Davis, C. P., Lambert, A., Stephens, G. L. and Vane, D. G., Waters, J. W.: Validation of the Aura MLS cloud ice water content measurements. Journal of Geophysical Research: Atmospheres, 113, D15, 2008.

Wu, D. L., Austin, R. T., Deng, M. et al. Comparisons of global cloud ice from MLS, CloudSat, and correlative data sets. Journal of Geophysical Research: Atmospheres, 2009, vol. 114, no D8, 2009.

Yang G.-Y. and Slingo, J.: The diurnal cycle in the tropics. Monthly Weather Review, 129(4):784–801, doi: 10.1175/1520-0493(2001), 2001.

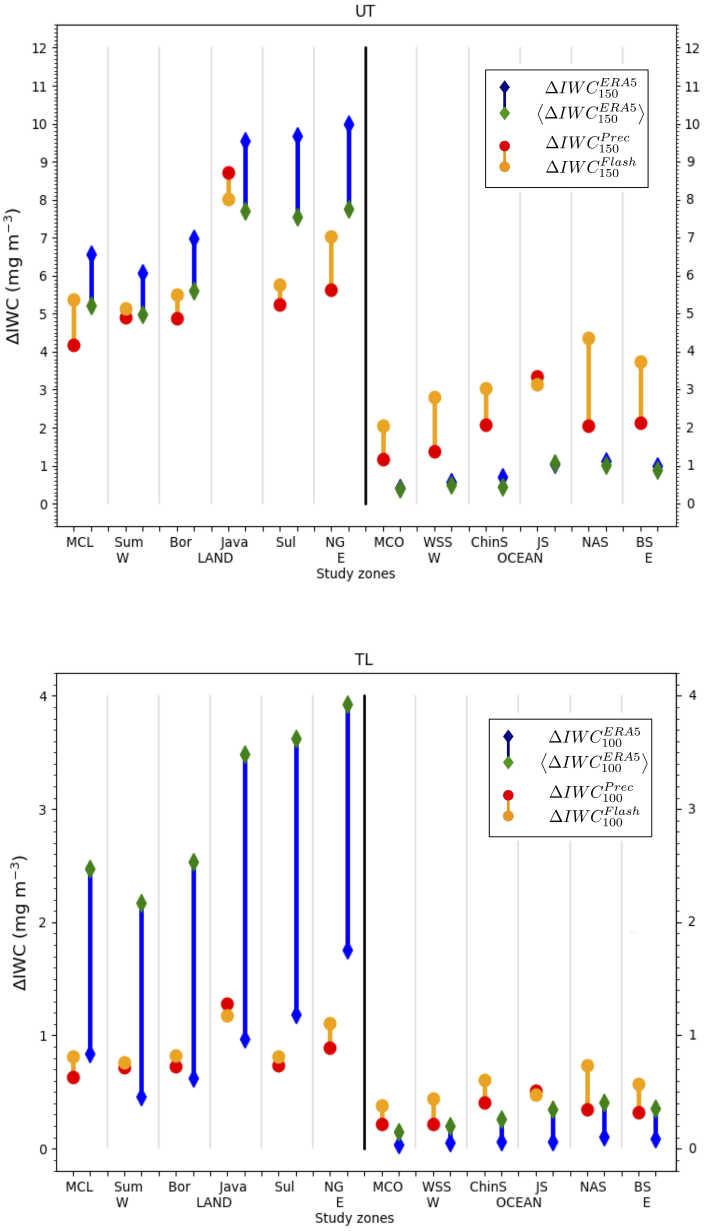

Figure 11. ~~a)~~ Top: ΔIWC (mg m^{-3}) estimated from Prec (red) and Flash (orange) at 146 hPa and ΔIWC estimated from ERA5 at the level 150 hPa and at the level 150 hPa degraded in the vertical, over islands and seas of the MariCont: MariCont_L (MCL) and MariCont_O (MCO); from West (W) to East (E) over land, Sumatra (Sum), Borneo (Bor), Java, Sulawesi (Sul) and New Guinea (NG); and over seas, West Sumatra Sea (WSS), China Sea (ChinS), Java Sea (JS), North Australia Sea (NAS) and ~~Bismark~~ Sea (BS). ~~b),~~ Bottom: Same as ~~a)~~ in top but for 100 hPa.